Western Graduate&PostdoctoralStudies

Western University
Scholarship@Western

Electronic Thesis and Dissertation Repository

January 2013

Topographic Influences on Trends and Cycles in Nutrient Export from Forested Catchments on the Precambrian Shield

Samson G. Mengistu
The University of Western Ontario

Supervisor
Irena Creed
The University of Western Ontario

Graduate Program in Geology

A thesis submitted in partial fulfillment of the requirements for the degree in Doctor of Philosophy

© Samson G. Mengistu 2012

Follow this and additional works at: http://ir.lib.uwo.ca/etd

Part of the Biogeochemistry Commons, Civil and Environmental Engineering Commons, Environmental Monitoring Commons, Geochemistry Commons, Geology Commons, Hydrology Commons, and the Water Resource Management Commons

Recommended Citation
Mengistu, Samson G., "Topographic Influences on Trends and Cycles in Nutrient Export from Forested Catchments on the Precambrian Shield" (2012). *Electronic Thesis and Dissertation Repository.* Paper 1066.

This Dissertation/Thesis is brought to you for free and open access by Scholarship@Western. It has been accepted for inclusion in Electronic Thesis and Dissertation Repository by an authorized administrator of Scholarship@Western. For more information, please contact jpater22@uwo.ca.

Topographic influences on trends and cycles in nutrient export from forested catchments on the Precambrian Shield

(Spine title: Discriminating nutrient export signals from catchments)

(Thesis format: Integrated Article)

by

Samson Girma Mengistu

Geology and Environmental Science

A thesis submitted in partial fulfillment
of the requirements for the degree of
Doctor of Philosophy

The School of Graduate and Postdoctoral Studies
The University of Western Ontario
London, Ontario, Canada

© Samson Girma Mengistu 2012

THE UNIVERSITY OF WESTERN ONTARIO
School of Graduate and Postdoctoral Studies

Certificate Of Examination

Supervisor

Dr. Irena Creed

Supervisory Committee

Dr. Marco Van De Wiel

Dr. Stephen Hicock

Examiners

Dr. Stephen Hicock

Dr. Brian Branfireun

Dr. Katrina Moser

Dr. James Buttle

The thesis by

Samson Girma Mengistu

entitled:

Topographic influences on trends and cycles in nutrient export from forested catchments on the Precambrian Shield

is accepted in partial fulfillment of the
requirements for the degree of
Doctor of Philosophy

Date

Chair of the Thesis Examination Board

Abstract and Keywords

Abstract: This dissertation explored topographic controls on spatial and temporal patterns in water yield and nutrient (carbon, nitrogen and phosphorus) export from forested headwater catchments in the Turkey Lakes Watershed in central Ontario, where other factors contributing to differences in water yield and nutrient export, including climate, geology, forest, and soils, are relatively constant. Topographic characteristics, including (a) hydrological flushing potential (expansion of water table into nitrate-N producing areas); (b) hydrological storage potential (area of wetlands, which can alternatively allow water and nutrients to bypass wetlands when storage capacity is filled with water or to trap them when not filled); and (c) hydrological loading potential (differences in precipitation caused by elevation), were considered in deconstructing non-stationary (linear trends) and stationary (oscillating cycles) patterns in water yield and nutrient export data. Topography explained the majority of differences in water yield and nutrient export. For spatial variation, topographic metrics representing hydrologic flushing potential predicted the majority of the spatial variation in nitrate-N export. In contrast, topographic metrics representing hydrologic storage potential explained the majority of the observed spatial variation in dissolved organic carbon, dissolved organic nitrogen and total dissolved phosphorus export. For temporal variation, catchments with low hydrologic loading potential were generally more sensitive to trends and cycles for water and nutrient export. Among these catchments, hydrological storage potential had no significant effect on water export trends, but had a significant effect on water export cycles; namely, the water export range was larger in the catchments with higher hydrological storage potential, even though the water export average was the same as catchments with lower hydrological storage potential. For nutrient export, the non-stationary signals were not consistent among the nutrients, but the amplitude of stationary signals in nutrient export in catchments with high hydrological storage potential compared to those with low hydrological storage potential was higher for organic nutrients and lower for nitrate-nitrogen. Despite many similarities in these headwater catchments, topography influenced the absolute and relative magnitude of hydrological and biogeochemical export from these catchments, which will have implications on the productivity and biodiversity of downstream aquatic systems.

Keywords: forest, catchment, topography, carbon, nitrogen, phosphorus, surface water, stationary, non-stationary, wavelet analysis

Co-Authorship Statement

Three chapters (2, 3, and 4) are manuscripts that will be submitted for publication in peer-reviewed journals. Samson Girma Mengistu, who led the definition of the research problem, formulation of the research design, completion of data analysis, interpretation of results and writing of manuscripts, will be lead author on each manuscript. Irena Creed who suggested the initial research problem, contributed to the formulation of the research design and interpretation of results, provided editorial guidance on the writing, and provided funding for the research activities, will be co-author on all manuscripts. For Chapter 2, Frederick Beall, who directs the catchment monitoring program at the Turkey Lakes watershed, provided access to data and contributed to the interpretation of the results and will also be listed as co-author. For Chapter 3, Reg Kulperger provided statistical feedback during the formulation of the analytical framework for discriminating non-stationary and stationary signals in the time series and for this reason will be listed as co-author. For Chapter 3 and 4, Christopher Quick who completed his Honours Thesis under the supervision of Irena Creed and Samson Girma Mengistu will be listed as co-author on manuscripts from Chapter 3 and 4 for assisting in the compilation of data and implementation of the analytical framework. This thesis and the manuscripts that will be published from it would not have been possible without the leadership of federal government scientists at Environment Canada and Canadian Forest Service responsible for collection of the 30-year monitoring data for the catchments of the Turkey Lakes experimental watershed and for this they are acknowledged.

Dedication

I dedicate this thesis to my parents, my wife and my daughter.

Acknowledgments

First and foremost, my utmost gratitude goes to my supervisor Dr. Irena Creed for giving me the opportunity to pursue my dream in the Catchment Research Facility (CRF) lab. Her invaluable knowledge and guidance has been monumental in helping me grow as a student and an independent researcher. Throughout the course of this desertation, Dr. Creed challenged me to be better, supported me to move forward, and encouraged me to strive for excellence. With these few words, it is simply impossible to thank Dr. Creed enough for her great insight, tremendous encouragement, high level of support and boundless patience.

I would like to express special thanks to my advisory committee members Dr. Marco Van De Waal and Dr. Stephen Hicock for their time, insightful comments and invaluable expertise. Their input impacted my academic growth in innumerable ways. I thank Dr. Reg Kulperger for helping me expand my knowledge of time series statistical analysis and wavelet based time series investigations. His expertise in statistics, invaluable suggestions and comments helped me to design, appraise and write a beneficial article as a part of my thesis (Chapter 2).

Throughout my Ph.D., I worked and interacted with many enthusiastic and hardworking members of CRF lab. I would take this opportunity to thank all past and present members and affiliates of CRF lab for being friendly and positively touching my life in so many ways. Particularly, I thank Tekleab Gala for showing me the way to CRF, Ryan Sorichetti for his enormous field assistance and Eric Enanga for his unreserved willingness to share discussions in the area of biogeochemistry. Lots of thanks also go to Mr. Johnston Miller for his tremendous assistance with editing the chapters and preparing the graphics, Mr. David Aldred for his help in GIS and graphics, and Dr. Kara Webster for her insights and editorial inputs. I appreciate Christopher Quick for his support in editing and data processing and analysis.

I thank members of the Ethiopian Community in London, particularly, Genet Gebregziabhere, Ephrem Gabriel, Meseret Bereket and Petros Aka for making my stay in London comfortable. I am also very grateful to Maribeth Clemens and the entire Clemens family for the true love and care they have extended to me and my family for the last four years. My former classmates and colleagues, particularly Boud Decrop, Balew Admas,

Getachew Adem, Awdenegest Moges, Meron Getachew and Teshome Edae deserve my gratitude for their continued contact and encouragement.

I would love to sincerely express my heartfelt thank-you to my parents (Girma and Abaynesh), my wife (Yenealem) and my daughter (Yadeal) for their consistent love, support, and encouragement. I owe much of my success to my wife and daughter for their infinite patience and never-ending support. To my close relatives (Romanwork, Tamerayehu, Bogalech, Kassahun, Torstein, Henrick, Tizalu, Tigist, Bruhfana, Ashenafi, Addis Miraf, Bethel, Sintayehu, Samrawit, Sosina, Kalkidan, Kedamawi, Kassew, Asrat, Yared, Asmerom, Belay and Haymanot) who have encouraged me over the years as I pursued my dream, I thank all of them for their moral support to accomplish this achievement.

Financial support was provided by the Earth Science Department of University of Western Ontario and through Dr. Creed's NSERC grant. Writing of this thesis would not have been possible if it were not for the use of the Turkey Lakes Watershed data, kindly provided by Dr. Fredrick Beall (Natural Resource Canada, Canadian Forest Service), Mr. Ray Semkin, Dr. Dean Jeffries (Environment Canada, National Water Research Institute) and R. Vet (Environment Canada, Meteorological Service of Canada). I am also very grateful to Dr. Fredrick Beall for providing insightful ideas and field support.

Last but not the least, the one above all of us, the omnipresent God, for giving me the strength and answering my prayers. Thank you so much Dear Lord for making this to happen and allowing my dad to overcome the dreadful time and witness the completion of what he implanted in me to dream from an early age.

Table of Contents

Certificate Of Examination ii
Abstract and Keywords iii
Co-Authorship Statement v
Dedication vi
Acknowledgments vii
Table of Contents ix
List of Tables xi
List of Figures xiv
List of Appendices xviii
List of Abbreviations xix
Chapter 1: Introduction 1
1.1 Problem Statement 1
1.2 Scientific Rationale 1
1.3 Goals 4
1.4 Hypotheses and Questions 5
1.5 Thesis Organization 6
1.6 References 6
Chapter 2: Searching for similarity in topographic controls on carbon, nitrogen and phosphorus export from forested headwater catchments 11
2.1 Introduction 11
2.2 Study Area 14
2.3 Methods 17
2.4 Results 23
2.5 Discussion 32
2.6 Conclusions 37
2.7 References 38
Chapter 3: Russian nesting dolls effect – Using wavelet analysis to reveal non-stationary and nested stationary signals in water yield from catchments in a northern forested landscape 45
3.1 Introduction 45
3.2 Study Area 47
3.3 Methods 55

3.4 Results 64
3.5 Discussion 81
3.6 Conclusions 89
3.7 References 90
Chapter 4: Nutrient export from catchments on forested landscapes reveal complex non-stationary and stationary climate signals 96
4.1 Introduction 96
4.2 Study Area 99
4.3 Methods 101
4.4 Results 110
4.5 Discussion 130
4.6 Conclusions 137
4.7 References 137
Chapter 5: Conclusion 141
5.1 Research Findings 141
5.2 Recommendations for Future Research 144
5.3 Anticipated Significance 146
5.4 References 147
Appendix 1: Evaluatating the role of topography in nutrient export using two windows of investigation 149
Appendix 2: John Wiley and Sons license terms and conditions 153
Curriculum Vitae 160

List of Tables

Table 2.1: Topographic metrics and ratios or topographic metrics among headwater catchments in the Turkey Lakes Watershed (VSA = variable source area; *eff*VSA = effective VSA; NW*eff*VSA = area of *eff*VSA without wetland; d^2*eff*VSA/dTI^2n = rate of *eff*VSA expansion and contraction). 24

Table 2.2: Pearson correlation between average topographic metrics, including ratios between metrics, for 13 catchments in the Turkey Lakes Watershed (VSA = variable source area; *eff*VSA = effective VSA; NW*eff*VSA = area of *eff*VSA without wetland; d^2*eff*VSA/dTI^2n = rate of *eff*VSA expansion and contraction; NS = not significant, all other relationships $p < 0.05$). 25

Table 2.3: Annual water and nutrient export (coefficient of variation) of dissolved organic carbon (DOC), dissolved nitrate (NO_3^--N), dissolved organic nitrogen (DON) and total dissolved phosphorus (TDP) from the Turkey Lakes Watershed for water years (June through May) from 1981 to 2008, except for catchment c31, c33 and c34 where data from 1981 to 1996 were used due to disturbance. 27

Table 2.4: Relationships between topographic metrics and annualized water export from headwater catchments in the Turkey Lakes Watershed (Direction = direction of relationship, r^2 = coefficient of determination, and NS = not significant, all other relationships $p < 0.05$). 30

Table 2.5: Relationships between topographic metrics and annualized nutrient export from headwater catchments in the Turkey Lakes Watershed (Dir. = direction of relationship, r^2 = coefficient of determination, and NS = not significant, all other relationships $p < 0.05$). 31

Table 2.6: The best regression models for predicting average annual nutrient export from headwater catchments in the Turkey Lakes Watershed. All models were significant at $p<0.001$. 33

Table 3.1: Characteristics of catchments in the Turkey Lakes Watershed. 54

Table 3.2: Large-scale climatic oscillations used for cross-coherence analysis. 63

Table 3.3: Global wavelet power spectrum (GWPS) values of water yield generated from Equation 3.6 in catchments c35 (A), c38 (B), c47 (C) and c50 (D). The detrended water yield was used to generate the first signal from the wavelet transform. Water yield used for subsequent signals is the difference between water yield from the previous step and modeled water yield at the step of investigation. The highlighted values indicate the p*eak GWPS values selected as the stationary signal* in each step. See Figures 3.5-3.7 for sample peak selection. 71

Table 3.4: Amount of variation explained by and magnitude of change of non-stationary (linear trends) and stationary (oscillating cycles) signals in yearly water yield export data from catchments c35, c38, c47 and c50 in the Turkey Lakes Watershed. For variation, data reported are R^2 values (with $p < 0.05$; NS indicating not significant

relationships). For magnitude, data reported are rate of change in export (mm/year) for non-stationary signals and amplitude (mm/year) for stationary cycles..... 73

Table 3.5: Pearson Product Moment Correlations between the annual average values of Multivariant El Niño Southern Oscillation (ENSO) Index (MEI), Atlantic Multidecadal Oscillation (AMO), Northern Atlantic Oscillation (NAO), and Pacific Decadal Oscillation (PDO) (* indicates $p<0.05$; *** indicates $p<0.001$). 79

Table 3.6: Correlations between climatic indices and the identified stationary signals for four catchments in the Turkey Lakes Watershed demonstrating the indices that are the most strongly correlated. 80

Table 4.1: Amount of variation and magnitude of change explained by non-stationary (linear) and stationary (periodic) trends in yearly DOC export data from catchments c35, c38, c47 and c50 in the Turkey Lakes Watershed. Data reported are R^2 values ($p < 0.05$; NS indicating not significant relationships), rate of change in export (mm/year) for non-stationary trends and amplitude for stationary cycles. 122

Table 4.2: Amount of variation and magnitude of change explained by non-stationary (linear) and stationary (periodic) trends in yearly DON export data from catchments c35, c38, c47 and c50 in the Turkey Lakes Watershed. Data reported are R^2 values ($p < 0.05$; NS indicating not significant relationships), rate of change in export (mm/year) for non-stationary trends and amplitude for stationary cycles. 123

Table 4.3: Amount of variation and magnitude of change explained by non-stationary (linear) and stationary (periodic) trends in yearly NO_3^--N export data from catchments c35, c38, c47 and c50 in the Turkey Lakes Watershed. Data reported are R^2 values ($p < 0.05$; NS indicating not significant relationships), rate of change in export (mm/year) for non-stationary trends and amplitude for stationary cycles... 124

Table 4.4: Amount of variation and magnitude of change explained by non-stationary (linear) and stationary (periodic) trends in yearly TDP export data from catchments c35, c38, c47 and c50 in the Turkey Lakes Watershed. Data reported are R^2 values ($p < 0.05$; NS indicating not significant relationships), rate of change in export (mm/year) for non-stationary trends and amplitude for stationary cycles. 125

Table 4.5: Observed stationary signals for DOC, DON, NO_3^--N, and TDP in four catchments in the Turkey Lakes Watershed. 126

Table 4.6: Results of Pearson correlation tests between isolated stationary signals (short = 3.4 to 4.8 year cycle; medium = 5.7 to 8.0 or 6.7 to 9.5 year cycle) and climate oscillation indices. Several correlations were not significantly correlated at $p<0.05$, but are presented to show the general relationships among the catchments and the global oscillations. 129

Table A1.1: Relationships between topography related metrics and annualized nutrient export (1981 to 1996 water years) of the 13 headwater catchments in the Turkey Lakes Watershed (Direction = Directions of relationship, R^2 = coefficient of determination, and NS = not significant, all other relationships $p < 0.05$). 150

Table A1.2: Relationships between topography related metrics and annualized nutrient export (1981 to 2008 water years) of the 13 headwater catchments in the Turkey Lakes Watershed (r = correlation, R^2 = coefficient of determination, and NS = not significant, all other relationships $p < 0.05$). 151

Table A1.3: Best regression models for predicting average annual C, N and P export from TLW headwater catchments. Two models, one for each window of investigation, are presented for each parameter. 152

List of Figures

Figure 2.1: Map of the Turkey Lakes Watershed depicting the thirteen experimental catchments (from Creed and Beall, 2009). 15

Figure 2.2: Method used to derive topographic metrics for hydrologic storage potential. Random errors were introduced into the DEM to calculate depressions, this process was repeated iteratively and the probability of depression was calculated, and wetlands were delineated using a 0.3 threshold determined by the minimum difference in area between simulated and observed (ground truthed) wetlands. 18

Figure 2.3: Description of methods used to derive topographic metrics for hydrological flushing potential: (A) VSA is calculated spatially from the TI_n map by starting at the stream and going recursively to lower TIn values until there is a breakpoint where values increase; (B) *eff*VSA is the upper quartile of the TI_n values within the VSA and describes the portion of the VSA where return flow is likely to occur on an annual basis; NW*eff*VSA is calculated spatially as the area of the *eff*VSA outside wetlands; and (C) the rate of change of *eff*VSA is calculated as the second derivative of the polynomial best fit of curve. 20

Figure 2.4: Spatial variation in annual Nitrate-N, dissolved organic carbon (DOC) dissolved organic nitrogen (DON), and total dissolved phosphorus (TDP) in the Turkey Lakes Watershed. 21

Figure 2.5: Average water yield and nutrient export versus No Wetland effective Variable Source Area (NW*eff*VSA) in 13 catchments of the Turkey Lakes Watershed. 29

Figure 3.1: The forest eco-regions of Ontario. 48

Figure 3.2: The Turkey Lakes Watershed. 49

Figure 3.3: Annual hydroclimatic variation in the Turkey Lakes Watershed region. 52

Figure 3.4: Topographic maps and descriptions of the four catchments selected from the Turkey Lakes Watershed for analysis. In c47, there is a buried side-channel, causing loss of groundwater (F. Beall, pers. comm). Catchment c49 is a high-elevation catchment that has similar average water loading (1327mm/yr) and a relatively small wetland (4%) with average discharge of 710 mm/yr, giving a closer approximation to the total discharge expected from c47. 53

Figure 3.5: Flow chart summarizing the analytical steps. 56

Figure 3.6: Time series of the Multivariate El Niño Southern Oscillation (ENSO) Index (MEI), Atlantic Multidecadal Oscillation (AMO), Northern Atlantic Oscillation (NAO), and Pacific Decadal Oscillation (PDO) indices. 62

Figure 3.7: Non-stationary trends in water yield for (A) c35, (B) c47, (C) c38 and (D) c50. 65

Figure 3.8: Stationary trend analysis for the first signal in c35: (A) c35 yearly detrended water yield data, (B) wavelet transform (from Equation 3.6) of c35 water yield data [strong and weak contributions to the power spectrum are indicated by warm (red)

colours and cold (blue) colours, respectively, on a logarithmic scale; the thin solid line represents the cone of influence, the thick solid lines show the 95% significance level], (C) scale selection based on Global Wavelet Power Spectrum [the dotted line at 14 years indicates the cutoff for selecting periods of signals (half the 28-year time series)], (D) modeling the sine function to the detrended water yield data, and (E) Auto-correlation function analysis for the residuals between the observed and modeled water yield. Subsequent steps repeated the same process until fitting scales were no longer statistically significant. 66

Figure 3.9: Stationary trend analysis for the second signal in c35: (A) c35 yearly detrended water yield data, (B) wavelet transform of c35 water yield data, (C) scale selection based on Global Wavelet Power Spectrum (D) modeling the sine function to the detrended water yield data, and (E) Auto-correlation function analysis for the residuals between the observed and modeled water yield. 67

Figure 3.10: Stationary trend analysis for the third signal in c35: (A) yearly detrended water yield data, (B) wavelet transform of c35 water yield data, (C) scale selection based on Global Wavelet Power Spectrum (D) modeling the sine function to the detrended water yield data, and (E) Auto-correlation function analysis for the residuals between the observed and modeled water yield. 68

Figure 3.11: Time series for the observed and modelled yearly water yields over the study time period for the catchments (A) c35, (B) c47, (C) c38, and (D) c50. 70

Figure 3.12: Cross coherence plots using Morlet mother wavelets to generate wavelet power spectra (from Equation 11) show correlations at each period between yearly water yield of c35 and (A) MEI, (B) AMO, (C) NAO, and (D) PDO. The thin solid line represents the cone of influence, the thick contours indicate the 95% significance level, arrows show the relative phase relationship (left arrows for negative correlations and right arrows for positive correlations). Warm colours indicate strong correlations and cool colours indicate weak relationships along a linear scale. 75

Figure 3.13: Cross coherence plots using Morlet mother wavelets to generate wavelet power spectra (from Equation 11) show correlations at each period between yearly water yield of c38 and (A) MEI, (B) AMO, (C) NAO, and (D) PDO. The thin solid line represents the cone of influence, the thick contours indicate the 95% significance level, arrows show the relative phase relationship (left arrows for negative correlations and right arrows for positive correlations). Warm colours indicate strong correlations and cool colours indicate weak relationships along a linear scale. 76

Figure 3.14: Cross coherence plots using Morlet mother wavelets to generate wavelet power spectra (from Equation 11) show correlations at each period between yearly water yield of c47 and (A) MEI, (B) AMO, (C) NAO, and (D) PDO. The thin solid line represents the cone of influence, the thick contours indicate the 95% significance level, arrows show the relative phase relationship (left arrows for negative correlations and right arrows for positive correlations). Warm colours indicate strong correlations and cool colours indicate weak relationships along a linear scale. 77

Figure 3.15: Cross coherence plots using Morlet mother wavelets to generate wavelet power spectra (from Equation 11) show correlations at each period between yearly water yield of c50 and (A) MEI, (B) AMO, (C) NAO, and (D) PDO. The thin solid line represents the cone of influence, the thick contours indicate the 95% significance level, arrows show the relative phase relationship (left arrows for negative correlations and right arrows for positive correlations). Warm colours indicate strong correlations and cool colours indicate weak relationships along a linear scale. 78

Figure 3.16: Regressions between the AMO Index and the mean annual precipitation (A) and temperature values (B) from the Sault Ste. Marie, Michigan weather station during two distinct AMO cycles (1901-1964 and 1964-2010). 82

Figure 3.17: Conceptual model of role of potential water storage on amplitude of stationary signals water yield time series. 86

Figure 4.1: The Turkey Lakes Watershed. 100

Figure 4.2: Nitrogen and sulphur deposition data from 1983 to 2006 (Unpublished data, M. Shaw, Environment Canada). 102

Figure 4.3: Topographic maps and descriptions of the four catchments selected from the Turkey Lakes Watershed for analysis. 103

Figure 4.4: Diagram detailing the analytical framework of detecting non-stationary and stationary trends in nutrient data. 104

Figure 4.5: Spider plots (A) and line plots (B) showing time series of dissolved organic carbon (DOC) export in four catchments in the Turkey Lakes Watershed. 111

Figure 4.6: Spider plots (A) and line plots (B) showing time series of dissolved organic nitrogen (DON) export in four catchments in the Turkey Lakes Watershed. 112

Figure 4.7: Spider plots (A) and line plots (B) showing time series of nitrate (NO_3^--N) export in four catchments in the Turkey Lakes Watershed. 113

Figure 4.8: Spider plots (A) and line plots (B) showing time series of total dissolved phosphorus (TDP) export in four catchments in the Turkey Lakes Watershed. 114

Figure 4.9: Wavelet cross coherence plots using Morlet wavelets showing correlations at each period between yearly DOC yield and MEI, NAO, PDO, and AMO at four catchments in the Turkey Lakes Watershed. The thin solid line represents the cone of influence, the thick contours indicate the 95% significance level, arrows show the relative phase relationship (left arrows for negative correlations and right arrows for positive correlations). Warm colours indicate strong correlations and cool colours indicate weak relationships along a linear scale. 116

Figure 4.10: Wavelet cross coherence plots using Morlet wavelets showing correlations at each period between yearly DON yield and MEI, NAO, PDO, and AMO at four catchments in the Turkey Lakes Watershed. 117

Figure 4.11: Wavelet cross coherence plots using Morlet wavelets showing correlations at each period between yearly NO_3^--N yield and MEI, NAO, PDO, and AMO at four catchments in the Turkey Lakes Watershed. 118

Figure 4.12: Wavelet cross coherence plots using Morlet wavelets showing correlations at each period between yearly TDP yield and MEI, NAO, PDO, and AMO at four catchments in the Turkey Lakes Watershed. 119

Figure 4.13: Final stationary signal models for DOC, NO_3^--N and DON export. 120

Figure 4.14: Final stationary signal models for TDP, NO_3^--N and DON export. 121

List of Appendices

Appendix 1: Evaluatating the role of topography in nutrient export using two windows of investigation 149

Appendix 2: John Wiley and Sons license terms and conditions 153

List of Abbreviations

Digital terrain analysis

a	*Upslope contributing area*
β	Local slope angle
d^2*eff*VSA/dTI_n^2	Rate of *eff*VSA expansion and contraction
DEM	Digital Elevation Model
*Eff*VSA	Effective Variable Source Area
LiDAR	Light Detection and Ranging
NW*eff*VSA	*Eff*VSA without wetland
Pdep	*Probability of depresion*
TI	Topographic Index
TI_n	Normalized Topographic Index
VSA	Variable Source Area
W: *eff*VSA	Ratio of Wetland to *eff*VSA
W: VSA	Ratio of Wetland to VSA

Wavelet analysis

COI	Cone of Influence
GWPS	Global Wavelet Power Spectrum
nSTD	Number of Standard Deviations
SO	Smoothing Operator
WPS	Wavelet Power Spectrum
W_n	Wavelet transform
X_n	Time series
ψ_o	Wavelet function
Δt	Time interval

Global climate oscillation

AMO	*Atlantic Multidecadal Oscillation*
ENSO	El Niño Southern Oscillation
MEI	Multivariate ENSO Index
NAO	*Northern Atlantic Oscillation*
PDO	*Pacific Decadal Oscillation*
SLP	Sea Level Pressure
SOI	Southern Oscillation index
SST	Sea Surface Temperature

Chapter 1: Introduction

1.1 Problem Statement

Despite continued efforts to understand the major controls of nutrient transport on a landscape, complete understanding of such controls remains challenging (Neff *et al.*, 2003; Deng, *et al.*, 2011) given the need to deal with and characterize spatially heterogeneous landscapes and temporally dynamic climate related transport controls (Stieglitz *et al.*, 2003; Christopher *et al.*, 2008). Heterogeneity in landscape characteristics not only makes identification of potential sources and sinks of nutrients on a landscape difficult but also results in complexity in understanding the net effect of interactions between potential sources and sinks of nutrients. Furthermore, climate is temporally dynamic and often contains a complex mixture of non-stationary linear trends and nested stationary signals of a cyclical nature, making the investigation of climatic control on nutrient transport challenging. Therefore, there is need for improved characterization and understanding of spatial and temporal drivers of nutrient transport on a landscape, because such understanding is central to implementing effective water quality protection strategies (Neal and Heathwaite, 2005; Robinson *et al.*, 2005).

1.2 Scientific Rationale

Many hydrological and biogeochemical processes can only be understood at hillslope or small experimental catchment scales (Harris and Heathwaite, 2005; McDonnell *et al.*, 2007). In the last few decades, catchments have been used as important units of investigation in the study of biogeochemical processes and examination of the spatial and temporal controls in nutrient transport. A catchment is an area of land that funnels water and associated sediment and nutrients to the lowest point within its boundary, the catchment outlet. Here, water as well as the associated nutrients and sediment are exported outside of the catchment's boundary to receiving water bodies, integrating the effects of nutrient transport controls such as climate, landscape characteristics and land-use changes (Ocampo *et al.*, 2006a,b; Saunders *et al.*, 2006; Creed and Beall, 2009; Piatek *et al.*, 2009; Mitchell, 2011). Particularly, headwater catchments, being small in

size and having thin soil layers,, steep slopes and low storage, can quickly respond to small environmental changes and easily detect spatial differences in landscape characteristics, and therefore have the potential to serve as sentinels for climate associated temporal changes and/or landscape related spatial heterogeneities. Strahler (1957) classified a headwater catchment as an area of land draining to a first or second-order stream channel, even though, such classification is controversial because the resolution of the scale of map used for the definition of stream channels affects the identification and interpretation of the size of headwater catchments (Gomi et al., 2002).

The deterioration of water quality due to increased nutrient deposition results in high biological productivity (eutrophication), which has numerous environmental, social and economic implications (Prepas *et al.*, 1997; Kangur and Möls, 2008; Simis *et al.*, 2005; Randolph *et al.*, 2008; Dodds *et al.*, 2009). Generally, excessive enrichment of surface water bodies with sediment and nutrients (mainly phosphorus and nitrogen) from agricultural and/or urban runoff has been the most common explanation for water quality deterioration (Karr and Dudley, 1981; Carpenter *et al.*, 1998; Sharpley *et al.*, 2000). Recent studies have observed increased deterioration of surface waters in relatively pristine forested landscapes such as the Algoma Highlands of Central Ontario (Winter *et al.*, 2011). Mostly, the drivers of biogeochemical dynamics and nutrient movement in such pristine forested landscapes are complex and mainly linked to landscape-related spatial and climate-associated temporal controls (Williams *et al.*, 1996; Mattsson *et al.*, 2003; Fisher *et al.*, 2004; Harris and Watmough *et al.*, 2004; Heathwaite, 2005; Creed and Beall, 2009). Located in the Canadian Precambrian Shield, the Algoma Highland region is dominated by non-carbonate bedrock geology with very poor capacity to buffer sulfur and nitrogen deposition in acid rain (Scheider *et al.*, 1979; Shrivastava, 2007). Even though sulfur deposition has declined over the last few years, nitrogen continues to be the predominant acidifying pollutant in the region (Jeffries *et al.*, 1988; Morrison *et al.*, 1992; Jeffries, 1995; Jeffries *et al.*, 2003; Creed and Beall, 2009). As the current trend of north-ward expansion of human development activities intensifies, the surface water quality and consequently the ecosystem integrity of water bodies in such a sensitive region can, therefore, be easily threatened without taking appropriate measures that are

based on scientific understanding of the controls of biogeochemical dynamics and nutrient transport in the region.

This thesis explores the influence of landscape linked spatial and climate related temporal characteristics on hydrological and biogeochemical responses, specifically water yield and nitrate-nitrogen (NO_3^--N), dissolved organic nitrogen (DON), dissolved organic carbon (DOC) and total dissolved phosphorus (TDP), from small headwater catchments in the Turkey Lakes Watershed (TLW) of the Algoma Highlands. These nutrients were chosen due to the important role they play in primary productivity. The spatial controls on water and nutrient export from headwater catchments include physical characteristics such as topography, geology, soil, vegetation and other characteristics that are spatially heterogeneous. Heterogeneity in catchment physical characteristics can translate to spatial differences in nutrient availability and/or mobility to receiving water bodies (Heathwaite and Johnes, 1996; Geyer and Schumann, 2001; Lu *et al.*, 2007; Fraterrigo and Downing, 2008; Creed and Beall, 2009), causing catchments to exhibit differential hydrologic and biogeochemical responses and reveal differential sensitivity to signals of climatic alteration.

Climate has also an effect on regional hydrology, which in turn influences nutrient production and transport, and thus the water quality of receiving surface water bodies (Whitehead *et al.*, 2009). Catchment responses to climate are temporally dynamic and contain an often complex mixture of non-stationary and nested stationary signals. Non-stationary catchment response signals have statistical means and standard deviations that change over time. They are mainly linked to unidirectional climate warming driven by anthropogenic climate change. Stationary catchment response signals have statistical means and standard deviations that do not change over time. They are linked to naturally varying large-scale climatic oscillations, caused by fluctuations either in sea surface temperature (SST) or sea level pressure (SLP) in areas that can be thousands of kilometres away from the site of investigation. By influencing regional climate, climatic oscillations can affect hydrological and biogeochemical processes, which in turn may have water quality and quantity implications (Keener *et al.*, 2010; Kahya, 2011; Niedzielski, 2011). In regions with unidirectional climate change, the effect of climate on

hydrological and biogeochemical processes can be significantly manifested when the stationary components of climate contribute to the positive phase of oscillations.

Previous studies investigating climate control on catchment responses did not discriminate non-stationary and stationary signals of catchment responses. The majority of these studies tried to identify connections between climatic oscillations and stream hydrologic responses (e.g., Bonsal and Shabbar, 2008; Burn, 2008; Whitfield *et al.*, 2010; Assani *et al.*, 2010), but very little work has focused on relating climatic oscillations to catchment nutrient export (Sang *et al.*, 2011). A scientifically sound, analytical approach is needed to discriminate the non-stationary and stationary components of catchment hydrological and biogeochemical responses and decompose the nested stationary response components into signals of various frequencies of interest. The decomposition helps to reveal catchment signals that are masked by the most dominant signal in catchment responses. In addition, the decomposed signals can be independently tested with climatic oscillations of interest.

The TLW has long-term water yield and nutrient export data. The catchments are relatively pristine, preserving the hydrologically and biogeochemically complex landscapes that are necessary to determine a baseline understanding of how the natural systems function, while at the same time allowing comparisons with altered systems (Mattsson *et al.*, 2003). The watershed is located in a region that shows noticeable annual climatic variability and exhibits substantial landscape spatial heterogeneity in terms of topography over a small watershed area of only 10.5 km^2. In addition, the watershed is close to a meteorological station with long-term climatic records. Analysis of the long term climatic record in the region indicates that the TLW has been experiencing a changing climate, with almost a 1°C per decade rise in average temperature and 80 mm per decade decrease in annual precipitation over the past three decades.

1.3 Goals

The goal of this study was to improve our understanding of the temporal and spatial controls on catchment water yield and nutrient export characteristics by (1) presenting simple topographic metrics that represent landscape nutrient sources and sinks, which can be used to track nutrient transport and export to stream networks from catchments in

forested landscapes, and (2) developing a novel analytical framework for decomposing catchment water and nutrient export signals, so that potential for differential sensitivity of catchment responses in yearly water and nutrient export to climatic forcing can be established.

1.4 Hypotheses and Questions

This thesis tests the following hypotheses: (1) topography determines the dominant hydrologic processes that influence nutrient transport on a landscape; (2) catchment yearly water yield and nutrient export responses contain a complex mixture of non-stationary and stationary climate signals, the significance of which is different among catchments with different topographic characteristics; (3) non-stationary trends contribute high rates over time in nutrient export and can obscure the contribution of stationary cycles to nutrient export signal; (4) metabolically more active nitrogen and phosphorus containing nutrients reveal stronger decline in their rates of change compared to metabolically less active carbon containing nutrients; and (5) catchments with higher hydrologic storage and lower hydrologic loading potentials are sensitive to non-stationary climatic trends in their yearly nutrient export, mainly due to the influence these catchment characteristics have on increasing water residence time and therefore nutrient reactivity time. To test these hypotheses, the following three questions were posed:

Question 1: What relationships are there between spatial topographic metrics and nutrient export?

The study investigated the role of the topographic variation prevalent in the TLW region in terms of explaining the observed spatial variation in nutrient export among TLW headwater catchments.

Question 2: Are there differences in the sensitivity of catchment water export behaviour to non-stationary climate change and naturally occurring stationary climate oscillations?

To answer this question, four representative headwater catchments were selected based on a gradient in water loading (precipitation) and water storage in wetlands. An analytical

framework was first developed, and then 28-year time series of water yield were analysed for non-stationary (linear trends) and nested stationary (non-linear oscillations) signals.

Question 3: How are climate forcing and non-stationary and stationary catchment nutrient export signals linked?

The analytical framework used to reveal non-stationary and stationary signals in water yields was used to detect signals in yearly time series of nutrient export [dissolved organic carbon (DOC), dissolved organic nitrogen (DON), nitrate (NO_3^--N), and total dissolved phosphorus (TDP)].

1.5 Thesis Organization

This thesis has been prepared in the integrated article format and consists of three manuscripts related to the three main questions. The introduction (Chapter 1) provides an overview of the research problem, including the question and objectives that form the basis of the thesis. The first manuscript (Chapter 2) investigates spatial controls on catchment carbon, nitrogen and phosphorus export patterns. The second manuscript (Chapter 3) examines the differential sensitivity of four representative TLW catchments to non-stationary and stationary climate signals in their yearly water export responses. A detailed explanation of the analytical framework developed for the analysis is provided in this chapter. The third manuscript (Chapter 4) applies the analytical framework to reveal complex non-stationary and stationary biogeochemical responses in the export of carbon, nitrogen, and phosphorus nutrients, as well as investigating the sensitivity of responses to climatic forcing and change. The last chapter (Chapter 5) summarizes the major conclusions of the work, draws the linkages among the individual chapters, and identifies future research directions.

1.6 References

Assani AA, Landais D, Mesfioui M, Matteau M. 2010. Relationship between the Atlantic Multidecadal Oscillation index and variability of mean annual flows for catchments in the St. Lawrence watershed (Quebec, Canada) during the past century. *Hydrology Research* **41**. DOI: 10.2166/nh.2010.055.

Bonsal B, Shabbar A. 2008. Impacts of Large-Scale Circulation Variability on Low Streamflows over Canada: A Review. *Canadian Water Resources Journal* **33**.

Burn DH. 2008. Climatic influences on streamflow timing in the headwaters of the Mackenzie River Basin. *Journal of Hydrology* **352**. DOI: 10.1016/j.jhydrol.2008.01.019.

Carpenter SR, Caraco NF, Correll DL, Howarth RW, Sharpley AN, Smith VH. 1998. Nonpoint pollution of surface waters with phosphorus and nitrogen. *Ecological Applications* **8**: 559-568.

Chapin FS, Peterson G, Berkes F, Callaghan TV, Angelstam P, Apps M, Beier C, Bergeron Y, Crepin AS, Danell K, Elmqvist T, Folke C, Forbes B, Fresco N, Juday G, Niemela J, Shvidenko A, Whiteman G. 2004. Resilience and vulnerability of northern regions to social and environmental change. *Ambio* **33**. DOI: 10.1639/0044-7447(2004)033[0344:RAVONR]2.0.CO;2.

Christopher SF, Mitchell MJ, McHale MR, Boyer EW, Burns DA, Kendall C. 2008. Factors controlling nitrogen release from two forested catchments with contrasting hydrochemical responses. *Hydrological Processes* **22**: 46-62. DOI: 10.1002/hyp.6632.

Creed IF, Beall FD. 2009. Distributed topographic indicators for predicting nitrogen export from headwater catchments. *Water Resources Research* **45**: W10407. DOI: 10.1029/2008WR007285.

Deng J, Zhou Z, Zhu B, Zheng X, Li C, Wang X, Jian Z. 2011. Modeling nitrogen loading in a small watershed in southwest China using a DNDC model with hydrological enhancements. *Biogeosciences* **8**. DOI: 10.5194/bg-8-2999-2011.

Dodds WK, Bouska WW, Eitzmann JL, Pilger TJ, Pitts KL, Riley AJ, Schloesser JT, Thornbrugh DJ. 2009. Eutrophication of US Freshwaters: Analysis of Potential Economic Damages. *Environmental science & technology* **43**: 12-19. DOI: 10.1021/es801217q.

Fisher S, Sponseller R, Heffernan J. 2004. Horizons in stream biogeochemistry: Flowpaths to progress. *Ecology* **85**: 2369-2379. DOI: 10.1890/03-0244.

Fraterrigo JM, Downing JA 2008. The Influence of Land Use on Lake Nutrients Varies with Watershed Transport Capacity. *Ecosystems* **11**. DOI: 10.1007/s10021-008-9176-6.

Geyer J, Schumann AH. 2001. Large-scale modelling and spatial heterogeneity of landscape characteristics - experience from the Upper Danube River basin. *Soil-Vegetation-Atmosphere Transfer Schemes and Large-Scale Hydrological Models*.

Harris G, Heathwaite A. 2005. Inadmissible evidence: knowledge and prediction in land and riverscapes. *Journal of Hydrology* **304**: 3-19. DOI: 10.1016/j.jhydrol.2004.07.020.

Heathwaite AL, Johnes PJ. 1996. Contribution of nitrogen species and phosphorus fractions to stream water quality in agricultural catchments. *Hydrological Processes* **10**. DOI: 10.1002/(SICI)1099-1085(199607)10:7<971::AID-HYP351>3.0.CO;2-N.

Jeffries DS. 1995. A preliminary assessment of nitrogen-based fresh water acidification in southeastern Canada. *Water Air and Soil Pollution* **85**. DOI: 10.1007/BF00476867.

Jeffries DS, Clair TA, Couture S, Dillon PJ, Dupont J, Keller W, McNicol DK, Turner MA, Vet R, Weeber R. 2003. Assessing the recovery of lakes in southeastern Canada

from the effects of acidic deposition. *Ambio* **32**. DOI: 10.1639/0044-7447(2003)032[0176:ATROLI]2.0.CO;2.

Jeffries D, Kelso J, Morrison I. 1988. Physical, Chemical, and Biological Characteristics of the Turkey Lakes Watershed, Central Ontario, Canada. *Canadian Journal of Fisheries and Aquatic Sciences* **45**: 3-13.

Kahya E. 2011. The Impacts of NAO on the Hydrology of the Eastern Mediterranean. Hydrological, Socioeconomic and Ecological Impacts of the North Atlantic Oscillation in the Mediterranean Region **46**: 57-71. DOI: 10.1007/978-94-007-1372-7_5.

Kangur K, Moels T. 2008. Changes in spatial distribution of phosphorus and nitrogen in the large north-temperate lowland Lake Peipsi (Estonia/Russia). *Hydrobiologia* **599**: 31-39. DOI: 10.1007/s10750-007-9204-0.

Karr JR, Dudley DR. 1981. Ecological Perspective on Water-Quality Goals. *Environmental management* **5**: 55-68.

Keener VW, Feyereisen GW, Lall U, Jones JW, Bosch DD, Lowrance R. 2010. El-Nino/Southern Oscillation (ENSO) influences on monthly NO_3 load and concentration, stream flow and precipitation in the Little River Watershed, Tifton, Georgia (GA). *Journal of Hydrology* **381**: 352-363. DOI: 10.1016/j.jhydrol.2009.12.008.

Kirpotin S, Polishchuk Y, Zakharova E, Shirokova L, Pokrovsky O, Kolmakova M, Dupre B. 2008. One of the possible mechanisms of thermokarst lakes drainage in West-Siberian North. *International Journal of Environmental Studies* **65**. DOI: 10.1080/00207230802525208.

Lu H, Yin C, Wang W, Shan B. 2007. A comparative study of nutrient transfer via surface runoff from two small agricultural catchments in north China. *Environmental Geology* **52**. DOI: 10.1007/s00254-006-0599-0.

Mattsson T, Finer L, Kortelainen P, Sallantaus T. 2003. Brookwater quality and background leaching from unmanaged forested catchments in Finland. *Water Air and Soil Pollution* **147**: 275-297. DOI: 10.1023/A:1024525328220.

McDonnell JJ, Sivapalan M, Vache K, Dunn S, Grant G, Haggerty R, Hinz C, Hooper R, Kirchner J, Roderick ML, Selker J, Weiler M. 2007. Moving beyond heterogeneity and process complexity: A new vision for watershed hydrology. *Water Resources Research* **43**: W07301. DOI: 10.1029/2006WR005467.

Mitchell MJ. 2011. Nitrate dynamics of forested watersheds: spatial and temporal patterns in North America, Europe and Japan. *Journal of Forest Research* **16**. DOI: 10.1007/s10310-011-0278-1.

Morrison IK, Foster NW, Nicolson JA. 1992. Influence of Acid Deposition on Element Cycling in Mature Sugar Maple Forest, Algoma, Canada. *Water Air and Soil Pollution* **61**. DOI: 10.1007/BF00482608.

Neal C, Heathwaite A. 2005. Nutrient mobility within river basins: a European perspective. *Journal of Hydrology* **304**: 477-490. DOI: 10.1016/j.jhydrol.2004.07.045.

Neff J, Chapin F, Vitousek P. 2003. Breaks in the cycle: dissolved organic nitrogen in terrestrial ecosystems. *Frontiers in Ecology and the Environment* **1**: 205-211. DOI: 10.1890/1540-9295(2003)001[0205:BITCDO]2.0.CO;2.

Niedzielski T. 2011. Is There Any Teleconnection Between Surface Hydrology in Poland and El Nino/Southern Oscillation? *Pure and Applied Geophysics* **168**: 871-886. DOI: 10.1007/s00024-010-0171-4.

Ocampo CJ, Oldham CE, Sivapalan M, Turner JV. 2006a. Hydrological versus biogeochemical controls on catchment nitrate export: a test of the flushing mechanism RID A-3538-2008. *Hydrological Processes* **20**: 4269-4286. DOI: 10.1002/hyp.6311.

Ocampo CJ, Sivapalan M, Oldham C. 2006b. Hydrological connectivity of upland-riparian zones in agricultural catchments: Implications for runoff generation and nitrate transport RID A-3538-2008. *Journal of Hydrology* **331**: 643-658. DOI: 10.1016/j.jhydrol.2006.06.010.

Piatek KB, Christopher SF, Mitchell MJ. 2009. Spatial and temporal dynamics of stream chemistry in a forested watershed. *Hydrology and Earth System Sciences* **13**: 423-439.

Prepas EE, Kotak BG, Campbell LM, Evans JC, Hrudey SE, Holmes CFB. 1997. Accumulation and elimination of cyanobacterial hepatotoxins by the freshwater clam Anodonta grandis simpsoniana. *Canadian Journal of Fisheries and Aquatic Sciences* **54**: 41-46.

Randolph K, Wilson J, Tedesco L, Li L, Pascual DL, Soyeux E. 2008. Hyperspectral remote sensing of cyanobacteria in turbid productive water using optically active pigments, chlorophyll a and phycocyanin. *Remote Sensing of Environment* **112**: 4009-4019. DOI: 10.1016/j.rse.2008.06.002.

Robinson T, Leydecker A, Keller A, Melack J. 2005. Steps towards modeling nutrient export in coastal Californian streams with a Mediterranean climate. *Agricultural Water Management **77***: 144-158. DOI: 10.1016/j.agwat.2004.09.024.

Sang Y, Wang D, Wu J, Zhu Q, Wang L. 2011. Wavelet-Based Analysis on the Complexity of Hydrologic Series Data under Multi-Temporal Scales. *Entropy* **13**. DOI: 10.3390/e13010195.

Saunders TJ, McClain ME, Llerena CA. 2006. The biogeochemistry of dissolved nitrogen, phosphorus, and organic carbon along terrestrial-aquatic flowpaths of a montane headwater catchment in the Peruvian Amazon RID A-2475-2009. *Hydrological Processes* **20**: 2549-2562. DOI: 10.1002/hyp.6215.

Scheider WA, Jeffries DS, Dillon PJ. 1979. Effects of Acidic Precipitation on Precambrian Fresh Waters in Southern Ontario Canada. *Journal of Great Lakes Research* **5**.

Sharpley A, Foy B, Withers P. 2000. Practical and innovative measures for the control of agricultural phosphorus losses to water: An overview. *Journal of environmental quality **29***: 1-9.

Shrivastava, AK. 2007. Global Warming. APH Publishing Corp.: New Delhi; 48-53.

Simis SGH, Peters SWM, Gons HJ. 2005. Remote sensing of the cyanobacterial pigment phycocyanin in turbid inland water. *Limnology and Oceanography* **50**: 237-245.

Stieglitz M, Shaman J, McNamara J, Engel V, Shanley J, Kling G. 2003. An approach to understanding hydrologic connectivity on the hillslope and the implications for nutrient transport. *Global Biogeochemical Cycles* **17**: 1105. DOI: 10.1029/2003GB002041.

Vincent V, Pienitz R. 2006. Vulnerability of northern lake ecosystems to climate change. Contribution to Vulnerability of Cryospheric and Socio-Economic Systems, Peter Wall Institute for Advanced Studies (Feb. 26–28, 2006). Available online at: http://www.cryosphere.pwias.ubc.ca/papers/session%206%20-%20pienitz%20and%20vincent.pdf. Accessed on September 20, 2012.

Watmough S, Eimers M, Aherne J, Dillon P. 2004. Climate effects on stream nitrate concentrations at 16 forested catchments in south central Ontario. *Environmental science & technology* **38**: 2383-2388. DOI: 10.1021/es0351261.

Whitehead PG, Wilby RL, Battarbee RW, Kernan M, Wade AJ. 2009. A review of the potential impacts of climate change on surface water quality. *Hydrological Sciences Journal-Journal Des Sciences Hydrologiques* **54**. DOI: 10.1623/hysj.54.1.101.

Whitfield PH, Moore RD, Fleming SW, Zawadzki A. 2010. Pacific Decadal Oscillation and the Hydroclimatology of Western Canada-Review and Prospects. *Canadian Water Resources Journal* **35**.

Williams M, Losleben M, Caine N, Greenland D. 1996. Changes in climate and hydrochemical responses in a high-elevation catchment in the Rocky Mountains, USA. *Limnology and Oceanography* **41**: 939-946.

Winter JG, DeSellas AM, Fletcher R, Heintsch L, Morley A, Nakamoto L, Utsumi K. 2011. Algal blooms in Ontario, Canada: Increases in reports since 1994. *Lake and Reservoir Management* **27**: 107-114. DOI: 10.1080/07438141.2011.557765.

Chapter 2: Searching for similarity in topographic controls on carbon, nitrogen and phosphorus export from forested headwater catchments

Preface

Topography influences hydrological processes that in turn affect biogeochemical export to surface waters on forested landscapes. In this chapter, the difference in long-term average annual dissolved organic carbon (DOC), organic and inorganic nitrogen (NO_3^--N, DON), and phosphorus (TDP) export from catchments with similar climate, geology, and forest type and age are established. This chapter tests the ***hypothesis*** *that topography determines the dominance in hydrologic processes that in turn determines nutrient export. Topographic indicators are designed to represent topographically-regulated hydrological processes that influence nutrient export: (a) hydrological storage potential (i.e., effect of topographic flats/depressions in a catchment, representing wetlands that may either result in increased runoff when the water table in the wetland is near or at the surface, or decreased runoff when the water table in the wetland is well below the surface preventing water contributing to the wetland from being exported to the stream); and (b) hydrological flushing potential (i.e., effect of topographic slopes on potential for variable source area to expand and tap into previously untapped nutrient source areas in the forest floor and surface mineral layers). These topographic indicators are then related to nutrient export, to see if shifting dominance in hydrological processes may explain differences in nutrient export. The* ***significance*** *of this chapter is that it presents simple topographic indicators that can be used to track nutrient sources, sinks, and their transport and export to surface waters from catchments on forest landscapes.*

2.1 Introduction

General rules of nutrient export derived from careful study of gauged catchments are required to make informed predictions about responses in ungauged basins. This is the first step towards calculating cumulative impacts of terrestrial-atmospheric-aquatic linkages in larger basins. Within landscapes where climate, geology, and biology are

similar, topography is the key control on nutrient accumulation, transformation and transport through its fundamental influence on energy and water mass balances (Sommer and Schlichting, 1997). Topographic characteristics, which are measured or mathematically analysed configurations of the landform shape and structure, influence the flow of water on the landscape (Wagener *et al.*, 2007). In turn, hydrologic flow paths influence the transport and transformation of nutrients. Several studies have shown strong associations between topographic properties and nutrient export behavior of carbon (Creed *et al.*, 2003, 2008), nitrogen (Creed and Beall, 2009) and phosphorus (Devito *et al.*, 2000). However, the nature of topographic controls on nutrient dynamics is complex, suggesting that the dominant hydrologic process influencing export may be different for each nutrient.

Topography is important for understanding the aquatic fate of dissolved carbon, nitrogen and phosphorus. For example, following a rain event on landscapes where topography is controlled by bedrock, the groundwater table rises toward the surface and intersects with surface soils that have accumulated nutrients in the intervening dry period. These nutrients are then mobilized and flushed to receiving waters resulting in export of carbon (Hornberger *et al.*, 1994), nitrogen (Creed *et al.*, 1996) or phosphorus (Evans *et al.*, 2000). In these cases topography influences the hydrological flushing through transport of nutrients to surface waters as a function of the size and spatial organization of the variable source area. Topography provides a conduit for nutrient export, initially through slower shallow, subsurface flows and then more rapidly as nutrients reach zones of saturation directly connected to streams. However, there are instances in which the topography may result in nutrients being transformed. For example, wetlands, depressions or flat areas intercept nutrient runoff. The result of this interception may either reduce the amount of nutrient export from catchments (e.g., NO_3^--N, Creed *et al.*, 2009) or increase the supply of nutrients for export [e.g., carbon, phosphorus (Creed *et al.*, 2008) and organic nitrogen (Creed and Beall, 2009)].

Linking hydrologic processes to nutrient cycling requires an understanding of biogeochemical transformations along hillslope flow pathways. Of primary importance is the impact of hillslope water residence time on oxidation – reduction (redox) conditions. Changes in the redox state of dissolved nutrients can result in losses of nutrients to the

atmosphere (e.g., DOC to CO_2 or NO_3 to N_2O) or as storage (e.g., DOC to soil organic carbon or DOC to sorbed DOC). For example, Webster *et al.* (2008a, b) found that topographic controls on soil moisture and the quantity and quality of carbon substrates were important determinants of CO_2 efflux from soils. Transiently wet areas adjacent to wetlands, streams and lakes were a major source of soil CO_2 because of synchronicity in optimal temperature and moisture conditions during the growing season and a large pool of high quality substrate within freshly fallen leaves that accumulated in these depositional areas. In contrast, upland areas had insufficient soil moisture, which limits CO_2 production due to lack of soluble substrate; however, excess water in the wetland areas also limits CO_2 production due to lack of oxygen. Similarly, topography regulates N_2O efflux. During winter (Fairweather, 2007) and snowfree (Casson, 2008) periods of the year, the transiently wet areas adjacent to wetlands and the wetlands themselves were found to be the major source of soil N_2O efflux, and wetlands with redox conditions promoting denitrification processes were a major source of N_2.

Defining general rules that link hydrologic processes to nutrient export requires tools that precisely and accurately detect topographic characteristics within catchments. Digital terrain analysis generates terrain attribures related to hydrological processes that can assist in relating topographic composition and configuration to hydrological and biogeochemical response characteristics (Wagener *et al*., 2007). The potential of digital terrain analysis has been revolutionized by light detection and ranging (LiDAR), an airborne remote sensing technology that measures the distance to surfaces by illuminating the surface with laser beams and then analyzing the backscattered light. LiDAR has been used to produce fine-resolution digital elevation models of surfaces from which subtle topographic features can be detected. From LiDAR digital elevation models, terrain analysis can better define catchment boundaries, represent low order streams, delineate local depressions that form potentially wet areas, and identify ephemeral and permanent streams that connect these features to the stream (c.f., Creed and Sass, 2011). For example, small hydrological features (1st order streams, small wetlands) that were previously not detected, particularly in areas where vegetation is dense or the ground is otherwise shielded from aerial view (Bishop *et al.*, 2008), can now be mapped. Thus, digital terrain analysis can now be used to derive topographic indicators for tracking

hydrological and biogeochemical dynamics across topographically simple to complex landscapes. Such knowledge will assist in generalizing process controls so that they can be applied to ungauged catchments (Tetzlaff *et al.*, 2008).

Creed and Beall (2009) described the conceptual basis of topographic controls on NO_3^--N and DON export in undisturbed headwater catchments on a sugar maple forested landscape. Topography influences (a) hydrological flushing potential (i.e., effect of topographic slopes on potential for variable source area to expand and tap into previously untapped nutrient source areas in the forest floor and surface mineral layers) and (b) hydrological storage potential (i.e., effect of topographic flats/depressions in catchment which represent wetlands that may either result in increased runoff when the water table in the wetland is near or at the surface, or decreased runoff when the water table in the wetland is well below the surface preventing water contributing to the wetland from being exported to the stream). This study builds on Creed and Beall (2009) by exploring similarity in topographic controls on other nutrient species, DOC and TDP, and determining if topographically regulated shifts in hydrological flushing versus storage potentails can explain differences in NO_3^--N, DOC, DON and TDP export among catchments. The potential significance of this study is that it presents simple topographic indicators that can be used to track nutrient sources, sinks, and their transport and export to surface waters from both gauged and ungauged catchments on forest landscapes.

2.2 Study Area

The Turkey Lakes Watershed (TLW) is a 10.5 km^2 experimental watershed on the Algoma Highlands, about 60 km north of Sault Ste. Marie, Ontario (Figure 2.1). This watershed is located in the northern portion of the Great Lakes-St. Lawrence Forest Region, the second largest forest region in Canada, which extends from southeastern Manitoba to the Gaspe Peninsula. Climate is continental with mean annual precipitation and temperature of 1200 mm and 5.0 °C, respectively (Creed and Beall, 2009), and is strongly influenced by the proximity of Lake Superior to the west of the watershed and local orographic effects at locations of high relief. There is typically snowpack from late-November, early December through to late March, early April. Peak stream discharge occurs during snowmelt and again in October to November during autumn storms.

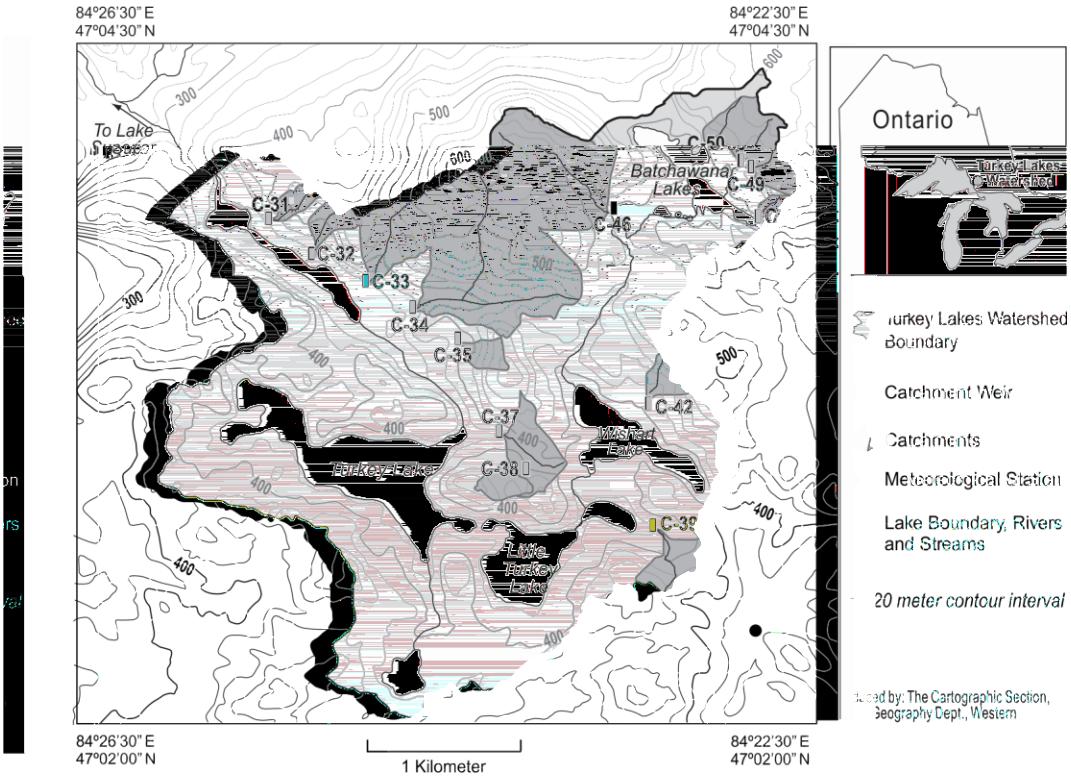


Figure 2.1: Map of the Turkey Lakes Watershed depicting the thirteen experimental catchments (from Creed and Beall, 2009).

Bedrock geology is primarily Precambrian silicate greenstone, except north of the Batchawana Lake area and near the main inflow to Little Turkey Lake, where there are small outcrops of more felsic igneous rock (Semkin and Jeffries, 1983). Surficial geology of upland areas are glacial till with a depth < 1 m and frequent bedrock exposure; lowland areas are glacial till of 1-2 m on average; and bedrock depressions are characterized with deep till reaching up to 71 m in depth (Elliot, 1985). The glacial till is double-layered, comprising sandy loam ablation till overlying a compacted lower silt loam basal till. The upper layer is thin (< 1m) and permeable (10^{-3} cm/sec), whereas the lower layer is thicker with lower permeability (10^{-5} cm/sec) (Johnston and Craig, 1986; Craig and Johnston, 1988). The glacial till has been weathered to present-day loam, sandy loam and silty loam soil textures. The soils on the tills are Orthic Ferro-Humic and Humo-Ferric podzols with dispersed pockets of Ferric Humisols found in bedrock-controlled depressions and adjacent to streams and lakes (Wickware and Cowell, 1985). Forest is comprised of

mature to overmature sugar maple (>90%). Stand density (904 stems ha^{-1}), dominant height (20.5 m), diameter at breast height (15.3 cm), and mean basal area (25.1 m^2 ha^{-1}) are relatively uniform across vegetation types. The sparse understories of upland stands are dominated (>95%) by saplings and seedlings of sugar maple with a depauperate herb flora and a variety of ferns. The wetland understories are composed of the seedlings and saplings of the overstory trees, various ferns, herbs and a mix of feather and sphagnum mosses (Wickware and Cowell, 1985).

The landscape exhibits substantial topographic variability, with gentle to steep hillslopes (11.5° to 20.8° in the experimental catchments) of different curvatures and lengths draining into streams. These hillslopes often drain through topographic flats and/or depressions containing organic-rich mineral or organic soils that are often transiently or permanently saturated. The presence of these topographic flats and depressions influences hydrological flow partitioning and pathways (Lindsay *et al.*, 2004; Lindsay and Creed, 2005) and biogeochemical cycling (Webster *et al.*, 2008a, b).

The TLW has been used as an experimental watershed by the federal government agencies since 1980, initially to study the potential impact of acid rain and climate change in terrestrial and aquatic ecosystems in the Canadian Shield area (Foster, 1985; Jeffries *et al.,* 1988). Since 1980, daily meteorological data (maximum and minimum temperature, precipitation and solar radiation data) around the watershed have continuously been measured at the meteorological station close to the watershed. In addition, since 1981, discharge and various water chemistry parameters have been monitored for 13 gauged headwater catchments within the TLW (Figure 2.1). A harvesting experiment was carried out in 1997 at three of the headwater catchments (c31, c33 and c34) to investigate the hydrological consequences of different forest management alternatives: a diameter limit harvest, shelterwood harvest and a selection harvest. For this study, pre-harvest data from 1981-1997 are used for c31, c33 and c34, while data from 1981-2008 are used for the ten, unharvested catchments.

2.3 Methods

2.3.1 Topographic Indicators

A 5 m Light Detection and Ranging (LiDAR), hydrologically conditioned digital elevation model (DEM) with vertical accuracy of 0.15 m in open canopy and 0.30 m in closed canopy was used to derive topographic metrics. Pits and depressions were filled (Planchon and Darboux, 2002), and the D8 algorithm was used to determine catchment contributing areas and surface drainage networks (O'Callaghan and Mark, 1984; Jenson and Domingue, 1988). Specific contributing area of 2000 m^2 and stream length threshold of 25 grid cells (125 m) were selected because they resulted in drainage networks that matched most closely those observed in the catchments.

Topographic indicators representing hydrological storage mechanisms (i.e., topographic flats/depressions that were assumed to be wetlands) were identified following a stochastic probability approach (Lindsay and Creed, 2005) (Figure 2.2). The approach involved deriving a grid map of the probability of depression (*pdep*) using Monte Carlo simulation where (1) the elevation error term was stochastically drawn from a frequency distribution of elevation error terms with a standard deviation equal to the vertical accuracy of the DEM (i.e., 0.30 m); (2) this error term was added to the DEM; (3) the flats/depressions in this modified DEM were filled and each grid cell modified by the depression filling process identified; (4) a probability of depression occurrence (*pdep*) was calculated by the number of times each grid cell was contained in a depression, with *pdep*s ranging from 0 (area with no probability of being a depression) to 1 (area with 100%

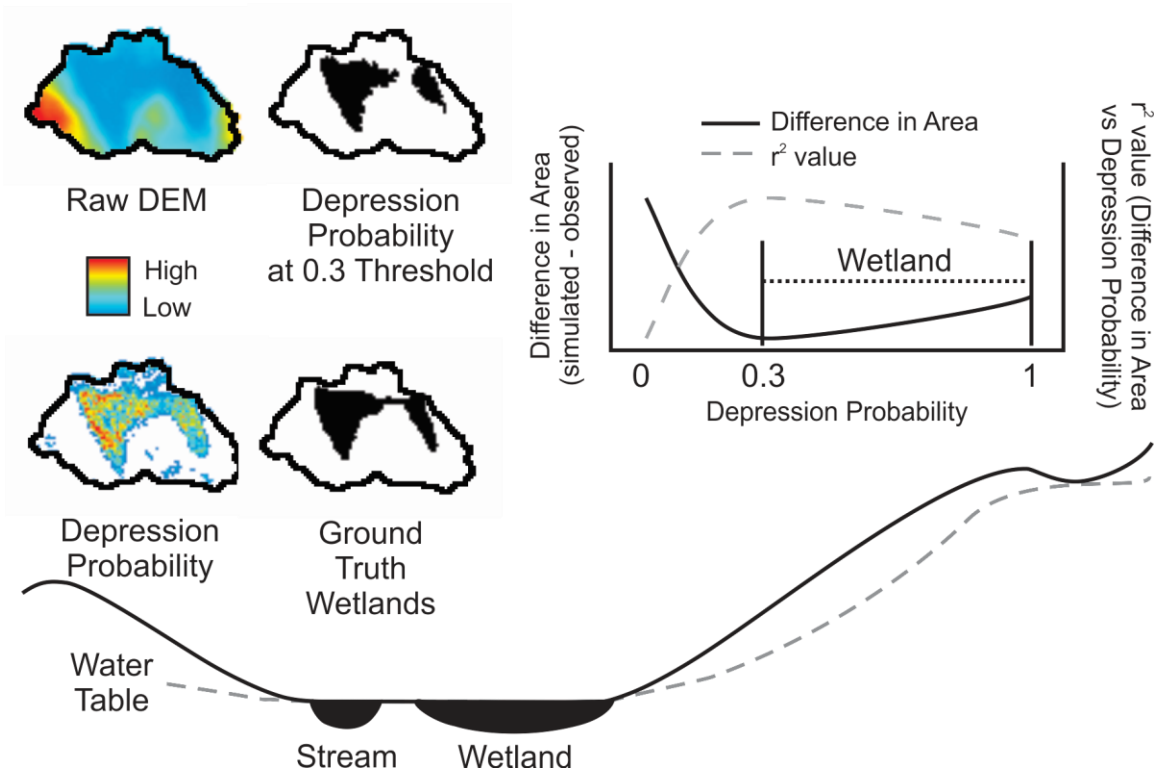


Figure 2.2: Method used to derive topographic metrics for hydrologic storage potential. Random errors were introduced into the DEM to calculate depressions, this process was repeated iteratively and the probability of depression was calculated, and wetlands were delineated using a 0.3 threshold determined by the minimum difference in area between simulated and observed (ground truthed) wetlands.

probability of being a depression). The Monte Carlo simulation was repeated using different elevation error terms until a stable solution occurred, defined by when the RMS difference in *pdep* between two consecutive simulations was < 0.001. Grid cells with *pdep* values greater than a defined critical threshold were identified as topographic depression and/or flat areas (e.g., wetlands). The critical threshold in *pdep* (0.30), above which a depression was defined, was determined by calculating the lowest area difference and highest Kappa statistics between stochastically derived and field surveyed wetlands.

Topographic indicators representing hydrological flushing mechanisms were derived using the following methods (Figure 2.3). Topographic Index (TI) is an indicator of topographically driven soil moisture conditions and was calculated as $\ln(a/\tan\beta)$, where a is upslope contributing area of a given site based on drainage directions calculated using the D-infinity algorithm (Tarboton, 1997) from a specific contributing area and slope gradient maps and β is local slope angle (Beven and Kirkby, 1979). The TI grid map of each catchment was normalized (TI_n) by subtracting catchment average TI values from specific TI for each grid cell. Variable Source Area (VSA) is an indicator of potential hydrological flushing areas were estimated by starting at the stream grid cells, where the TI_n values are the highest, and recursively moving outward from the stream grids to grid cells of lower TI_n value until a point where the TI_n values start to increase again or the catchment boundary is reached (Figure 2.4A). The proportion of VSA where hydrological flushing is likely to occur on an annual basis was referred to as *effective* variable source area (*eff*VSA) and was estimated by grid cells with TI_n values $\geq$ the 75^{th} percentile of the TI_n frequency distribution within the VSA, a percentile that was previously found to provide the best prediction for NO_3^--N export (Creed and Beall, 2009) (Figure 2.4B). A situation was possible where the same pixel can function as both hydrological storage and hydrological flushing (i.e., if topographic flats/depressions occurred within the *eff*VSA). For this reason, both *eff*VSA with and *eff*VSA with no topographic flats/depressions (i.e., no wetlands) (NW*eff*VSA) were derived and considered in the development of models (Figure 2.4C). The potential rate of *eff*VSA expansion and contraction (d^2*eff*VSA/dTI_n^2) was calculated as a second derivative of the best-fit polynomial to the TI_n frequency distribution within the *eff*VSA.

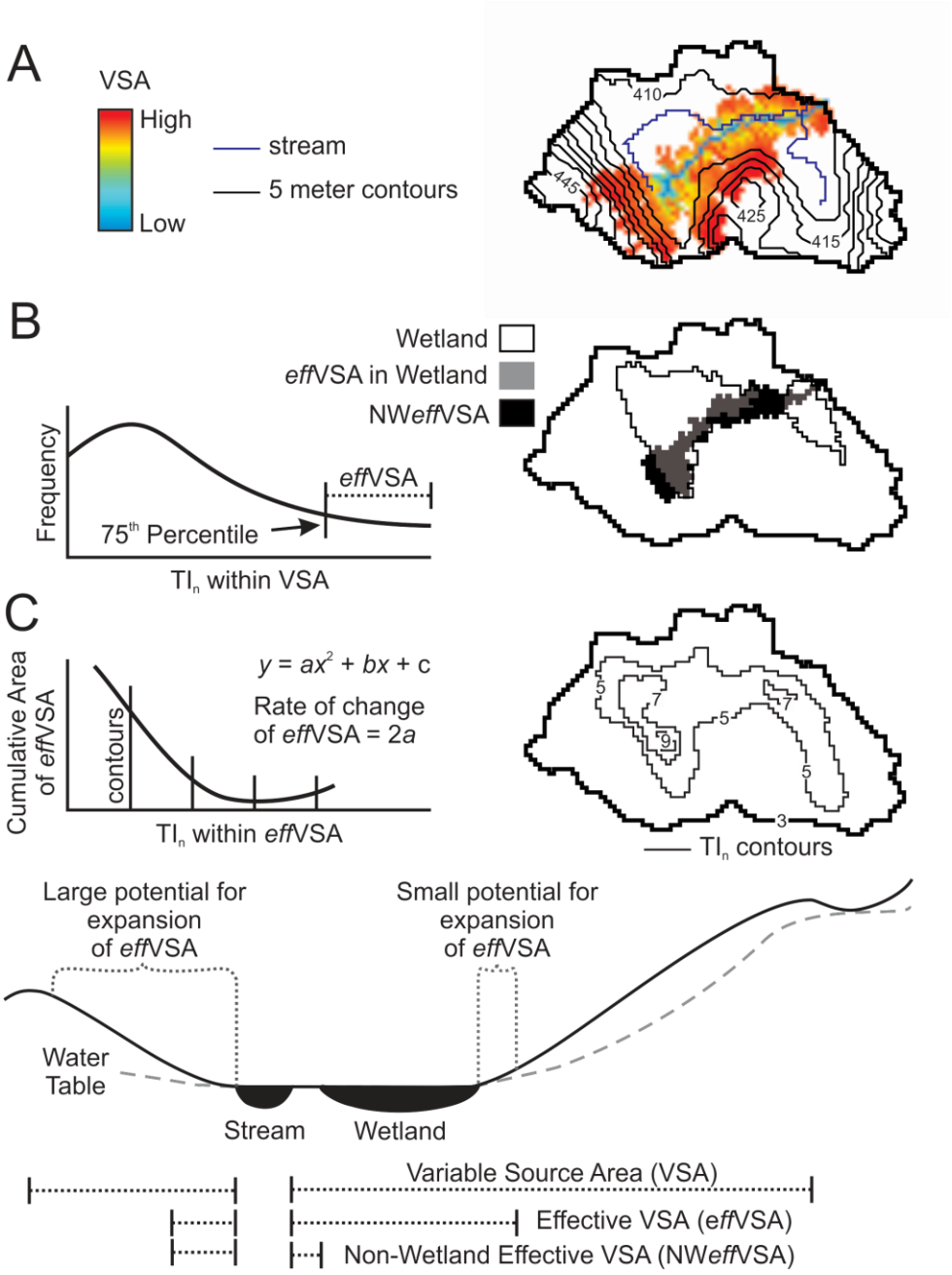


Figure 2.3: Description of methods used to derive topographic metrics for hydrological flushing potential: (A) VSA is calculated spatially from the TI_n map by starting at the stream and going recursively to lower TIn values until there is a breakpoint where values increase; (B) *eff*VSA is the upper quartile of the TI_n values within the VSA and describes the portion of the VSA where return flow is likely to occur on an annual basis; NW*eff*VSA is calculated spatially as the area of the *eff*VSA outside wetlands; and (C) the rate of change of *eff*VSA is calculated as the second derivative of the polynomial best fit of curve.

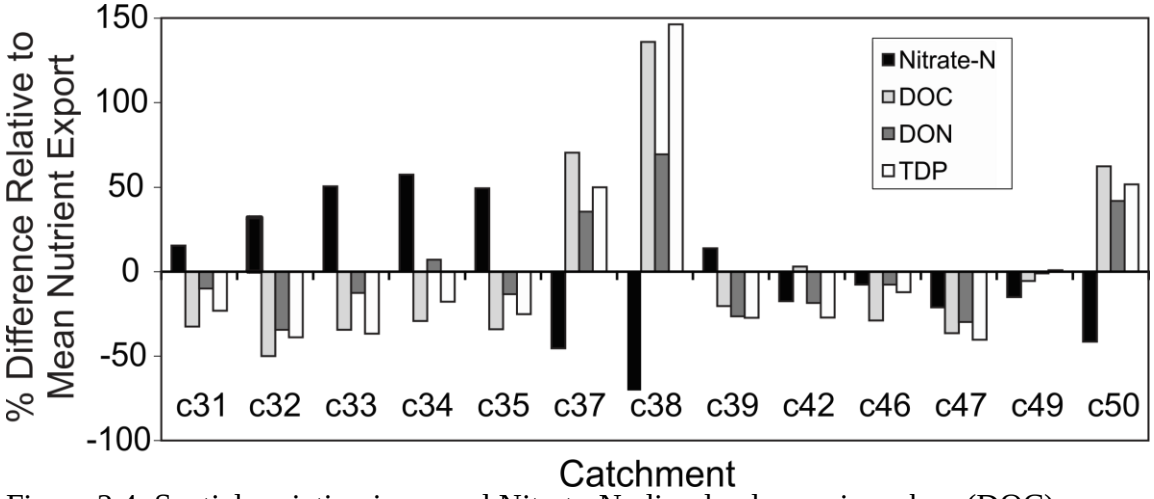


Figure 2.4: Spatial variation in annual Nitrate-N, dissolved organic carbon (DOC) dissolved organic nitrogen (DON), and total dissolved phosphorus (TDP) in the Turkey Lakes Watershed.

Ratios of the topographic metrics were also considered because the relative presence of one metric with respect to another might increase predictive capacity. For example, the ratio of topographic sinks of a nutrient (e.g., proportion of topographic flats/depressions that denitrify NO_3^--N) to topographic sources of a nutrient (e.g., proportion of VSA, *eff*VSA or NW*eff*VSA that are sources of NO_3^--N) were derived to see if they improved the predictive capacity of topographic metrics for NO_3^--N export.

All digital terrain analyses were performed using Terrain Analysis System (TAS) software (Lindsay, 2005).

2.3.2 Solute Export

The concentration of nutrients discharged into the streams were determined from samples collected at mid-day every two weeks during the winter, daily during spring snowmelt, and weekly or every two weeks during the summer and autumn. Samples were collected at the same sampling point, the center of the stream, for each stream. From each sample, particulate matter was removed by filtration through Fisher Q8 (coarse, fast flow) paper filters. Samples were analyzed within 48 h of collection for NH_4^+-N, NO_3^--N, and total dissolved nitrogen (TDN) using sodium nitroprusside, cadmium reduction and cadmium reduction after autoclave digestion methods, respectively, on Technicon Autoanalysers. DON was calculated from TDN minus dissolved inorganic nitrogen (DIN = NH_4^+-N + NO_3^--N). DOC was determined by removing dissolved inorganic carbon (DIC) by purging with N_2 after acidification, converting DOC to DIC by persulfate oxidation catalyzed by UV, then converting the resulting DIC to CO_2 by acidification, which was measured by colorimetry. TDP was analysed on a Technicon Autoanalyser IIC after autoclave digestion using the molybdophosphoric acid colour reaction.

Daily concentrations of nutrients were estimated by interpolating measured values directly before and after the unknown value. Daily fluxes of nutrients were then estimated by the product of the total daily discharge from continuously logged stream stage at V-notch weirs on the catchments and the interpolated daily concentrations of nutrients. Annual nutrient fluxes of nutrients were calculated as the sum of daily flux for the water year (June 1 to May 31) from 1981 to 2008 (except for the three harvested catchments, c31, c33 and c34, where the period was from 1981 to 1996 water years).

2.3.3 Relationships between Topographic Indicators and Nutrient Export

The nature, strength and significance of the relationships between the catchment's topographic indicators and its nutrient export characteristics were evaluated using correlations and linear regressions ($p = 0.05$) using Sigma Plot (Version 11, Systat Software Inc., 2008).

2.4 Results

2.4.1 Topographic Indicators

Topographic indicators of hydrological storage potential (i.e., topographic flats/ depressions) varied substantially (Table 2.1). Catchments c37, c38 and c50 had substantially more wetlands (>10% topographic flats/depressions), whereas c33 and c47 had very few wetlands (<1% topographic flats/depressions). The distribution of wetlands within the catchments varied, with some containing large contiguous wetlands (e.g., c38) and others smaller discontiguous wetlands that cascaded one to the next *via* the surface drainage network (e.g., c50).

Topographic indicators of hydrological flushing varied substantially (Table 2.1). VSA was smallest in c47 (23.62%) and largest in c31 (61.66%). The patterns in *eff*VSA did not follow VSA, reflecting differences in concavity *versus* convexity of the lower hillslopes draining into the stream. The *eff*VSA was smallest in c38 (6.34) and c37 (6.82%), where water moves down steep hillslopes, draining into much more gentle hillslopes before exiting the catchment, and largest in c33 (16.04%), where steep to moderate slopes drain directly to the stream. Topographic flats/depressions that would detain the movement of water from the hillslopes to the stream were prevalent in some of the *eff*VSAs. When these topographic flats/depressions were removed from *eff*VSA, the proportion of area contributing variable source area runoff decreased among all catchments (except c47 where it stayed the same), but the rank order of the NW*eff*VSA in catchments generally remained the same, with c37 (1.73%) and c38 (1.55%) having lowest NW*eff*VSA and c33 having highest NW*eff*VSA (15.75%). These topographic indicators of VSA were correlated with one another (Table 2.2), because they were refinements of the same process. For this reason they were not combined in the models

Table 2.1: Topographic metrics and ratios or topographic metrics among headwater catchments in the Turkey Lakes Watershed (VSA = variable source area; *eff*VSA = effective VSA; NW*eff*VSA = area of *eff*VSA without wetland; d^2*eff*VSA/dTI^2n = rate of *eff*VSA expansion and contraction).

Catchment	Wetlands (%)	VSA (%)	*eff*VSA (%)	NW*eff*VSA (%)	W: VSA	W: N*eff*VSA	d^2*eff*VSA/dTI_n^2
c31	2.88	61.66	13.10	11.33	0.05	0.22	2.00E-06
c32	1.00	54.54	14.32	14.05	0.02	0.07	4.00E-06
c33	0.50	45.13	16.04	15.75	0.01	0.03	2.00E-05
c34	1.12	36.04	9.70	9.22	0.03	0.12	4.00E-05
c35	1.06	36.38	13.18	13.12	0.03	0.08	4.00E-06
c37	15.01	33.63	6.82	1.73	0.45	2.20	1.20E-06
c38	20.54	31.57	6.34	1.55	0.65	3.24	6.00E-07
c39	5.97	47.13	12.96	11.05	0.13	0.46	4.00E-06
c42	8.48	51.84	13.71	10.06	0.16	0.62	4.00E-06
c46	1.35	30.57	9.73	9.08	0.04	0.14	8.00E-06
c47	0.36	23.62	7.58	7.58	0.02	0.05	2.00E-06
c49	3.97	47.27	9.65	8.62	0.08	0.41	2.00E-06
c50	10.03	38.09	7.84	3.72	0.26	1.28	1.00E-06
Average	5.56	41.34	10.84	8.99	0.15	0.69	3.08E-06
Max	20.54	61.66	16.04	15.75	0.01	0.05	4.00E-05
Min	0.36	23.62	7.58	1.55	0.65	3.24	6.00E-07

Table 2.2: Pearson correlation between average topographic metrics, including ratios between metrics, for 13 catchments in the Turkey Lakes Watershed (VSA = variable source area; *eff*VSA = effective VSA; NW*eff*VSA = area of *eff*VSA without wetland; d^2*eff*VSA/dTI^2n = rate of *eff*VSA expansion and contraction; NS = not significant, all other relationships $p < 0.05$).

Topographic Metrics	VSA (%)	*eff*VSA (%)	NW*eff*VSA (%)	W: VSA	W: *eff*VSA	W: NW*eff*VSA	d^2*eff*VSA/dTI_n^2
Wetlands (%)	NS	-0.575	-0.813	0.986	0.978	0.932	NS
VSA (%)		0.707	NS	NS	NS	NS	NS
*eff*VSA (%)			0.929	-0.628	-0.644	-0.629	NS
NW*eff*VSA (%)				-0.828	-0.834	-0.787	NS
W:VSA					0.998	0.977	NS
W:*eff*VSA						0.983	NS
W:NW*eff*VSA							NS

constructed to predict nutrient export. Topographic properties of hillslopes that would affect the rate of potential expansion of *eff*VSA (d^2*eff*VSA/dTI_n^2) varied by orders of magnitude, from high rates of potential expansion in c33 (2×10^{-5}) and c34 (4×10^{-5}) (tapping into relatively high NO_3^--N generating areas that exist on less concave (less flat) hillslopes) to low rates in c38 (6×10^{-7}) (tapping into relatively low NO_3^--N generating areas that exist on more concave (more flat) hillslopes) (Figure 2.2).

A broad range existed in the topographic indicators of hydrological flushing *versus* storage potential among the catchments. Catchments c38, c37 and c50 had the largest proportion of wetlands, but the smallest *eff*VSA and NW*eff*VSA, and the least expandable *eff*VSA (d^2*eff*VSA/dTI_n^2). For example, c38 had the largest wetland (20.54%) but among the smallest VSAs (31.6%), the smallest *eff*VSA (6.3 %) and the smallest NW*eff*VSA (1.55%). In contrast, c33 had among the smallest wetlands (0.5%) but the largest VSA (45.1%), the largest *eff*VSA (16.0%), giving it the largest NW*eff*VSA (15.8%), and one of the most expandable *eff*VSA (d^2*eff*VSA/dTI_n^2). Catchments c33 and c38 represent extremes in terms of topographic indicators of hydrologic flow, and therefore comparisons of these two sites are highlighted in subsequent analyses.

When the ratio of the proportion of topographic flats/depressions (where rising water table leads to inundation) to proportion of VSAs (where rising water table leads to expansion into unsaturated soils) (W:*eff*VSA) was calculated the magnitude of difference among the catchments increased. For example the W:*eff*VSA for c33 was 0.03 (emphasizing the role of *eff*VSA relative to W); whereas, the W:*eff*VSA for c38 was 3.24 (emphasizing role of W to *eff*VSA).

2.4.2 Nutrient Export

Nutrient export from the catchments varied substantially (Table 2.3). Catchments representing lows in inorganic nutrient export tended to be the highest in organic nutrient export, and *vice versa*. For example, catchment NO_3^--N export ranged from a low of 1.02 kg ha^{-1} a^{-1} (c38) to a high of 5.15 kg ha^{-1} a^{-1} (c35). In contrast, catchment organic nutrient export ranged from a low of 13.19 kg ha^{-1} a^{-1} for DOC, 1.02 kg ha^{-1} a^{-1} for DON, and 0.0169 kg ha^{-1} a^{-1} for TDP in catchment c35, to a high of 47.22 kg ha^{-1} a^{-1} for DOC, 2.00 kg ha^{-1} a^{-1} for DON, and 0.0558 kg ha^{-1} a^{-1} for TDP for c38 (Table 2.3).

Table 2.3: Annual water and nutrient export (coefficient of variation) of dissolved organic carbon (DOC), dissolved nitrate (NO_3^--N), dissolved organic nitrogen (DON) and total dissolved phosphorus (TDP) from the Turkey Lakes Watershed for water years (June through May) from 1981 to 2008, except for catchment c31, c33 and c34 where data from 1981 to 1996 were used due to disturbance.

Catchment	Area (ha)	Water (mm a^{-1})	NO_3^--N (kg ha^{-1} a^{-1})	DOC (kg ha^{-1} a^{-1})	DON (kg ha^{-1} a^{-1})	TDP (kg ha^{-1} a^{-1})
c31	4.94	569 (21)	3.98 (26)	13.51 (24)	1.06 (29)	0.0174 (37)
c32	6.5	495 (30)	4.56 (35)	10.00 (25)	0.77 (55)	0.0138 (49)
c33	23.38	531 (19)	5.19 (20)	13.13 (15)	1.03 (28)	0.0143 (48)
c34	68.59	663 (14)	5.43 (19)	14.16 (14)	1.26 (49)	0.0186 (38)
c35	4.02	632 (26)	5.15 (29)	13.19 (29)	1.02 (41)	0.0169 (54)
c37	15.36	633 (21)	1.88 (33)	34.11 (23)	1.60 (26)	0.0340 (25)
c38	6.46	612 (26)	1.02 (43)	47.22 (24)	2.00 (29)	0.0558 (30)
c39	17.25	518 (24)	3.93 (30)	15.92 (24)	0.87 (35)	0.0165 (31)
c42	18.52	457 (22)	2.84 (41)	20.61 (22)	0.96 (33)	0.0165 (26)
c46	43.19	654 (29)	3.18 (36)	14.22 (41)	1.09 (49)	0.0199 (40)
c47	3.43	555 (26)	2.72 (38)	12.72 (32)	0.83 (37)	0.0135 (40)
c49	14.81	710 (29)	2.93 (39)	18.90 (42)	1.16 (34)	0.0228 (31)
c50	9.47	776 (22)	2.02 (40)	32.48 (19)	1.67 (31)	0.0344 (30)
Average	18.1	600	3.45	20.01	1.18	0.0227
Maximum	68.59	776	5.43	47.22	2.00	0.0558
Minimum	3.43	457	1.02	10.01	0.77	0.0135

Catchment differences in nutrient export were also depicted taking the residuals between each catchment and the average across all catchments for each nutrient (Figure 2.4). For example, c35 had 49% higher NO_3^--N export than the average export among catchments, while c38 was 70% lower in NO_3^--N export than the average. The higher elevation catchments (e.g., c42, c46, c47, c49) that had little to no topographic flats/depressions were the exception, showing little difference from average export or slightly lower export than the average export across all catchments (Figure 2.5). NO_3^--N export behaviour was distinct from DOC, DON and TDP export behaviour. For example, c35, which had higher NO_3^--N export, had lower export of organic nutrients. Spatially, c35 exported 14% less DON, 34% less DOC, and 26% less TDP than the average export across all catchments; whereas, c38 exported 69% more DON, 136% more DOC and 146% more TDP than the average export across all catchments (Figure 2.5).

2.4.3 Topographic Indicators vs. Nutrient Export

There were generally no significant correlations between topographic indicators and water export (Table 2.4); the one exception was *eff* VSA *versus* water export, where increase in *eff* VSA led to a decrease in water export (r^2=0.379, $p<0.05$), but an increase in NW*eff*VSA had no significant effect on water export. However, there were significant correlations between topographic indicators and nutrient export (Table 2.5). For example, for NO_3^--N export, the best linear model was the simple indicator of NW*eff*VSA (r^2 = 0.759, $p < 0.001$), while the best multiple linear model was the combination of simple indicators of NW*eff*VSA and d^2*eff*VSA/dTI_n^2 (R^2 = 0.907, $p < 0.001$). Compound indicators, including W:VSA or W:*eff*VSA, did not improve the linear or multiple linear models (Table 2.5). For DOC, DON and TDP export, the best linear model using simple indicators was topographic flats/depressions within the catchment (R^2 = 0.935 for DOC, 0.694 for DON, and 0.821 for TDP). Multiple linear models did not improve performance. However, compound indicators W:VSA or W:*eff*VSA did improve performance. For DOC, DON and TDP export, the best linear model using compound indicators was W:*eff*VSA (R^2 = 0.957 for DOC, 0.783 for DON, and 0.912 for TDP), which resulted in improvements of up to 10% in the explanation of variation in organic nutrient export

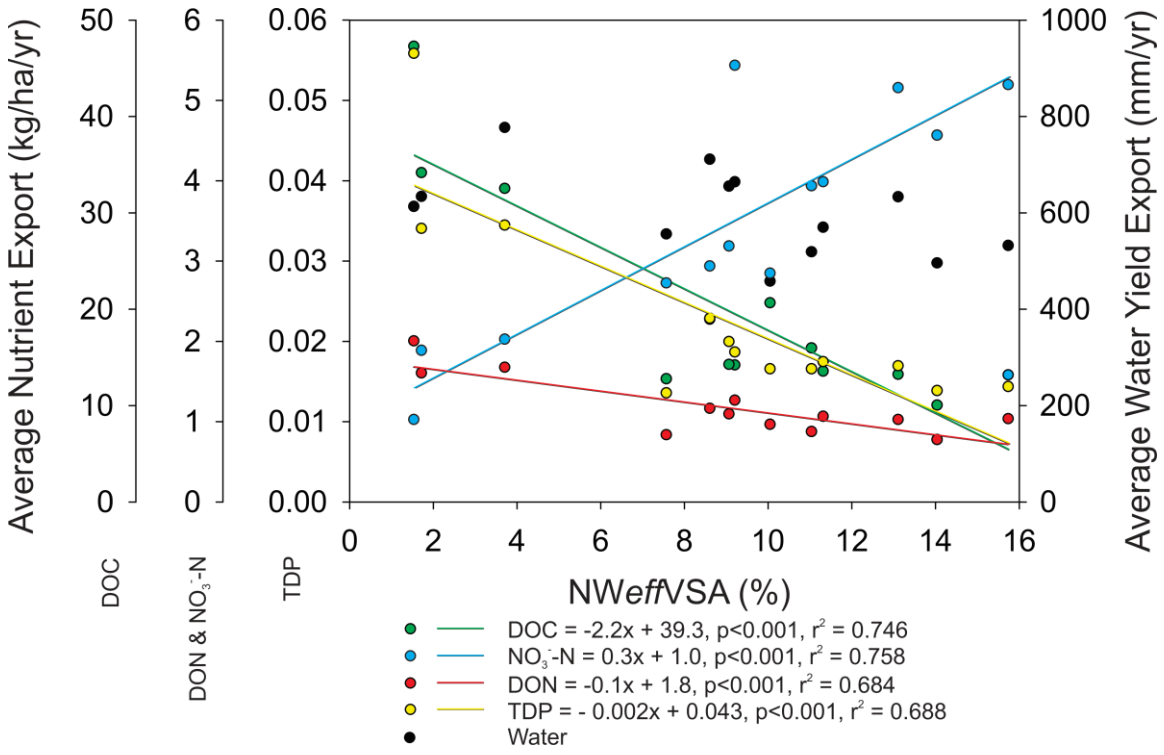


Figure 2.5: Average water yield and nutrient export versus No Wetland effective Variable Source Area (NW*eff*VSA) in 13 catchments of the Turkey Lakes Watershed.

Table 2.4: Relationships between topographic metrics and annualized water export from headwater catchments in the Turkey Lakes Watershed (Direction = direction of relationship, r^2 = coefficient of determination, and NS = not significant, all other relationships $p < 0.05$).

Topographic Metrics	Water	
	Direction	r^2
Wetlands (%)	NS	NS
VSA (%)	NS	NS
*eff*VSA (%)	-	0.379
*NWeff*VSA (%)	NS	NS
d^2*eff*VSA/dTI_n^2	NS	NS
W:VSA	NS	NS
W:*eff*VSA	NS	NS
*NWeff*VSA and d^2*eff*VSA/dTI_n^2	NS	NS

Table 2.5: Relationships between topographic metrics and annualized nutrient export from headwater catchments in the Turkey Lakes Watershed (Dir. = direction of relationship, r^2 = coefficient of determination, and NS = not significant, all other relationships $p < 0.05$).

Topographic Metrics	NO_3^--N		DOC		DON		TDP	
	Dir.	r^2	Dir.	r^2	Dir.	r^2	Dir.	r^2
Wetlands (%)	-	0.646	+	0.935	+	0.694	+	0.821
VSA (%)	NS	NS	NS	NS	NS	NS	NS	NS
*eff*VSA (%)	+	0.561	-	0.456	-	0.489	-	0.484
*NWeff*VSA (%)	+	0.759	-	0.747	-	0.682	-	0.687
d^2*eff*VSA/dTI_n^2	+	0.394	NS	NS	NS	NS	NS	NS
W:VSA	-	0.619	+	0.951	+	0.752	+	0.887
W:*eff*VSA	-	0.618	+	0.957	+	0.783	+	0.912
*NWeff*VSA and d^2*eff*VSA/dTI_n^2	+	0.907	NS	NS	NS	NS	NS	NS

(Table 2.5). Among the organic nutrient exports, model results for DON explained less variation (about 13-17% less) than DOC and TDP (Table 2.6).

2.5 Discussion

Catchment-based water quality monitoring programs are few and far between, and increasingly at risk of being closed due to budget constraints. While perceived as "expensive and wasteful" (Lovett *et al.*, 2007) these long-term monitoring programs are in fact unique and valuable scientific assets, providing insights into spatio-temporal hydrological and biogeochemical dynamics that cannot be gained using other research approaches, such as experimentation or modeling. Importantly, the value and impact of these scientific assets can be increased by developing a "similarity metric" approach in that heterogeneities in environmental factors (e.g., topography, geology and climate) are related to catchment functional responses (Tetzlaff *et al.*, 2008). By developing a metric-based approach we not only capitalize on the unique long-term records these studies provide, but also provide a means to extract general principles that can be used in ungauged basins, thereby increasing efficiencies by removing the need to expand or create new monitoring programs.

Using catchment classification and similarity for predictions in ungauged catchments based on the characterization of appropriate metrics of both temporally variable (e.g., timing of extreme precipitation events, Castellarin *et al.*, 2001) and spatially heterogeneous (e.g., soil and topography, Larsen *et al.*, 1994) catchment properties on runoff responses have a long tradition in hydrology. The strength of this approach has improved with advances in DEM resolution and new digital terrain analysis methods (e.g., Lindsay and Creed, 2005; Creed and Beall, 2009) allowing for precise characterization of the topography used in these metrics. Although considerable effort has been made to apply metrics for defining similarities in hydrologic response (Larsen *et al.*, 1994; Castellarin *et al.*, 2001), little work has been done on developing metrics relevant for predicting nutrient export dynamics, despite various studies relating nutrient export to environmental controls of spatial and temporal nature (Heathwaite and Johnes, 1995; Fraterrigo and Downing, 2008; Andrews *et al.*, 2011).

Table 2.6: The best regression models for predicting average annual nutrient export from headwater catchments in the Turkey Lakes Watershed. All models were significant at $p<0.001$.

Response Variable	r^2	Equation
NO_3^--N (kg N ha^{-1} a^{-1})	0.907	NO_3^--N = 0.978 + (0.235 × *NWeff*VSA) + (50557.598 × d^2*eff*VSA/dTI^2_n)
DOC (kg C ha^{-1} a^{-1})	0.957	DOC = 12.499 + (10.956 × W: *eff*VSA)
DON (kg N ha^{-1} a^{-1})	0.783	DON = 0.954 + (0.326 × W: *eff*VSA)
TDP (kg P ha^{-1} a^{-1})	0.911	TDP = 0.0146 + (0.0117 × W: *eff*VSA)

We examined the effect that topography has on nutrient export from headwater catchments in order to find key metrics that can be applied to prediction in ungauged basins. We found considerable variation in nutrient export at the TLW, despite uniformity in climate, geology, forest type and forest age (Creed *et al.*, 2002). Topographic characteristics were largely responsible for explaining variation in nutrient export among catchments, with topography controlling hydrological processes that influence the production, availability and delivery of nutrients to the downstream surface waters. In particular metrics related to hydrological storage potential (i.e., topographic flats/depressions) and hydrological flushing potential (i.e., NW*eff*VSA and d^2*eff*VSA/dTI_n^2) explained the majority of variation in nutrient export.

Wetlands that form in topographic flats/depressions have been identified as a sink of NO_3^--N and a source of DOC, DON and TDP. Previous studies have shown that wetlands can act as sources (Lee *et al.*, 1975; Sloey *et al.*, 1978), sinks (Peterjohn and Correll, 1984; Kadlec, 1986) and/or transformers of nutrients. Their importance in nutrient export is disproportionate to their area on the landscape. Although wetlands commonly only cover a small proportion of the landscape they are usually positioned so that much of the discharge waters and the associated nutrients pass through them on their way to the receiving water bodies (Devito *et al.*, 1989). The wetland in c38 from our study area was identified as a sink of NO_3^--N, suggesting that NO_3^--N from upland drainage waters that is intercepted in the wetland is transformed and subsequently released *via* denitrification to N_2O and/or N_2 (Creed, Unpubl. Data). Alternatively, NO_3^--N from upland drainage waters that is intercepted in the wetland is retained *via* abiotic immobilization (Davidson *et al.*, 2003) and/or biotic immobilization (Gundersen and Bashkin, 1994; Sirivedhin and Gray, 2005), although we did not quantify the importance of these mechanisms of nitrogen retention.

In contrast, wetlands were a source of DOC, DON and TDP, with the magnitude of nutrient export proportional to wetland area. There are several mechanims to explain this observation. The physical and chemical environment within wetlands affects the solubility, lability and mobility of nutrients. Of particular importance are the organic deposits as a major source of soluble organic by-products (Qualls and Richardson, 2003).

For example, saturation may suppress mineralization of DON to inorganic nitrogen (NH_3^+-N) (Yang and Fan, 2003) leading to organic forms accumulating in wetlands. The wet conditions also have a large impact on the redox state of nutrients (Sorrell and Armstrong, 1994; Reddy and DeLaune, 2008). Low redox potentials may also facilitate abiotic conversion of NO_3^--N to organic forms of nitrogen through the ferrous wheel hypothesis, which involves reduction of Fe (III) hydroxide by organic matter in forest floor to release Fe (II) (Davidson *et al.*, 2003). Low redox potentials may also facilitiate biotic conversion of NO_3^--N to gaseous forms of N_2O and N_2. The potential for alternative fates of nitrogen from uplands passing through wetlands en route to the stream may explain the relatively weak relationship between wetland proportion and DON compared to DOC and TDP.

Uplands and their VSAs (Hewlett and Hibbert, 1967) have been important in predicting nutrient export in many studies (e.g., Govindaraj, 1996; Walter *et al.*, 2000; Marjerison *et al.*, 2011). In this study, despite noticeable variation in VSA proportion among the studied catchments, VSA proportion did not explain the variation of nutrient export among catchments. However, we did find that different derivatives of VSA were important indicators in predicting nutrient export.

For example, the proportion of *eff*VSA, which represents the proportion of frequently flushed area within the VSA, was more effective in predicting NO_3^--N export. The direct relationship observed between *eff*VSA and NO_3^--N export suggested an increased rate of hydrological flushing of NO_3^--N from catchments with larger *eff*VSAs. Aerobic conditions in *eff*VSA surfaces, when not saturated, favor nitrification (oxidation of NH_3^+-N to NO_3^--N), making *eff*VSA a net source of NO_3^--N. Nitrate accumulates in these areas until sufficient precipitation events cause the water table to rise and flush the accumulated NO_3^--N for export to streams (Creed et al. 1996; Creed and Band, 1998). If not absorbed by plants, NO_3^--N, which naturally possesses less affinity for adsorption to mineral soils (Foster *et al.*, 1982; Andrews *et al.*, 2007), can be easily mobilized from *eff*VSA to receiving water bodies.

Furthermore, the proportion of *eff*VSA without topographic flats/depressions (NW*eff*VSA) was even more effective in predicting NO_3^--N export. *Eff*VSA may contain wetlands, and NW*eff*VSA removed the potential effects of wetlands within *eff*VSA.

NW*eff*VSA explained more variation than either of these indicators did on their own. Coupling NW*eff*VSA with potential lateral expansion of *eff*VSA (d^2*eff* VSA/$dTI_n^{\ 2}$) further improved predictions of NO_3^--N export. The size of hydrologically connected portion of VSA (*eff*VSA) varies with season and storm characteristics. Expansion of *eff*VSA in response to climatic forcing can result in larger flushable areas and longer flushing time, causing greater NO_3^--N export (Creed and Band, 1998b). The role of expanding saturated VSA in terms of increasing flushable nutrient concentrations has also been reported for NO_3^--N by Sickman (2001) and Oeung *et al.* (2010) and for DOC by Boyer *et al.* (1995).

It is important to recognize that the VSA and its derivatives are not related to water export (i.e., expansion of rising water table into upland areas does not correspond to an increase in water at the stream). Rather, as VSA increases, the amount of water exported from the catchment decreases as the water enters uplands areas that were previously dry and flushes NO_3^- -N to the stream. Consequently, as VSA increases, water export tends to decrease while NO_3^--N export increases.

The different derivatives of VSA were also significantly related to organic nutrient and TDP export, but negatively correlated, suggesting different controls on their export. Generally catchments with large *eff*VSA proportion contain no to few wetlands whereas those with small *eff*VSA proportion contain substantial wetlands. The inverse relationship between *eff*VSA and DOC, DON and TDP relative to NO_3^--N may be linked to physical processes. For example, the increased adsorption of dissolved organic matter by mineral soils in upland dominated catchments may decrease exports of organic forms of nutrients from these catchments (McDowell and Likens, 1988; Fellman *et al.*, 2009). As *eff*VSA proportion increases, the potential of dissolved organic matter in upland dominated catchments to reach stream networks would decrease because the transport pathways are through mineral-rich soils that strongly adsorb dissolved organic matter (Wallis, 1979, Qualls *et al.,* 2000). Mineral soil adsorption has been well recognized as a primary process responsible for reducing dissolved organic matter export (McDowell and Likens, 1988; Moore *et al.,* 1992; Kalbitz *et al.*, 2000; Moore and Turunen, 2004), while organic soils with little DOC adsorption capacity and the potential to generate soluble carbon compounds are known to be large exporters of DOM (Aitkenhead and McDowell

2000; Aitkenhead-Peterson *et al.*, 2007). For example, due to efficient adsorption by mineral soils, percolation of DOC through subsurface soil can cause a typical decline of DOC concentration by 50-90% (McDowell and Wood, 1984; Neff and Asner, 2001). The inverse relationship between *eff*VSA and DOC, DON and TDP relative to NO_3^--N may also be linked to biological processes. For example, aerobic conditions in *eff*VSA soils of uplands would faciliate microbial organic matter mineralization providing an additional source of NO_3^--N for export while depleting dissolved organic matter reserves faster than what is generated by decomposing detritus (Aiken *et al.*, 2011).

However, wetland proportion was a more important metric than VSA derivatives for predicting DOC, DON and TDP export. We developed new metrics reflecting the relative proportion of wetland area with respect to VSA (W:VSA) and *eff*VSA (W:*eff*VSA). In general, W:VSA and W:*eff*VSA metrics were more effective in predicting export of organic forms of nutrients (DOC, DON, TDP) than wetland proportions (% wetland). While the improvement was marginal in DOC prediction (~2%), it was larger for DON and TDP with W:VSA and W:*eff*VSA, improving predictions by ~6% and 9%, respectively. Catchments with larger wetland area with respect to their VSA and *eff*VSA tend to export more organic nutrients; the sources have a greater influence than the sinks of DOC, DON and TDP.

2.6 Conclusions

We need tools to scale our process-based understanding from experimental catchments to the landscape where policy and managaement decisions are made. Topography is an important determinant of nutrient export through its regulation of hydrological processes that in turn influence formation of nutrient hot spots (sources for export) versus cold spots (sinks for export), transformation of the nutrients to dissolved and/or gaseous forms, and transport to the stream. Specifically, topography exerts an influence on hydrological storage potential (i.e., topographic flats/depressions where wetlands form allowing the accumulation of nutrient-rich organic deposits), and hydrological flushing potential (i.e., topographic controls on the effVSA and its potential for expansion where rising water table allows the prolonged flushing of nutrient-rich near surface/surface soils as rising water table reaches new soils). Topographic characteristics of individual catchments

create different potentials for hydrological storage *versus* flushing which contributes to the substantial variation in nutrient export among catchments, and the relative proportion of one with respect to the other should be considered to improve prediction of nutrient export. Recent developments have revolutionized topographic models of catchments which means that tools can be developed that incorporate topographic indicators representing hydrological and biogeochemical controls on nutrient export behavior of catchments that can be used as a basis for characterizing responses in ungauged catchments.

2.7 References

Aiken GR, Gilmour CC, Krabbenhoft DP, Orem W. 2011. Dissolved Organic Matter in the Florida Everglades: Implications for Ecosystem Restoration. *Critical Reviews in Environmental Science and Technology* **41**: PII 933735105. DOI: 10.1080/10643389.2010.530934.

Aitkenhead JA, McDowell WH. 2000. Soil C:N ratio as a predictor of annual riverine DOC flux at local and global scales. *Global Biogeochemical Cycles* **14**. DOI: 10.1029/1999GB900083.

Aitkenhead-Peterson JA, Smart RP, Aitkenhead MJ, Cresser MS, McDowell WH. 2007. Spatial and temporal variation of dissolved organic carbon export from gauged and ungauged watersheds of Dee Valley, Scotland: Effect of land cover and C:N. *Water Resources Research* **43** : W05442. DOI: 10.1029/2006WR004999.

Andersson J, Nyberg L. 2008. Spatial variation of wetlands and flux of dissolved organic carbon in boreal headwater streams. *Hydrological Processes* **22**: 1965-75. DOI: 10.1002/hyp.6779.

Andrews DM, Lin H, Zhu Q, Jin L, Brantley SL. 2011. Hot Spots and Hot Moments of Dissolved Organic Carbon Export and Soil Organic Carbon Storage in the Shale Hills Catchment. *Vadose Zone Journal* **10**: 943-54. DOI: 10.2136/vzj2010.0149.

Andrews M, Scholefield D, Abberton MT, McKenzie BA, Hodge S, Raven JA. 2007. Use of white clover as an alternative to nitrogen fertiliser for dairy pastures in nitrate vulnerable zones in the UK: productivity, environmental impact and economic considerations. *Annals of Applied Biology* **151**. DOI: 10.1111/j.1744-7348.2007,00137.x.

Anthony W, Hutchinson G, Livingston G. 1995. Chamber Measurement of Soil-Atmosphere Gas-Exchange - Linear Vs Diffusion-Based Flux Models. *Soil Science Society of America Journal* **59**: 1308-10.

Beven K, Kirkby M. 1979. A physically-based variable contributing area model of basin hydrology. *Hydrologic Science Bulletin* **24**: 43-69l.

Bishop K, Buffam I, Erlandsson M, Folster J, Laudon H, Seibert J, Temnerud J. 2008. Aqua Incognita: the unknown headwaters. *Hydrological Processes* **22**. DOI: 10.1002/hyp.7049.

Boyer EW, Hornberger GM, Bencala KE, McKnight DM. 1995. Variation of dissolved organic carbon during snowmelt in soil and stream waters of two headwater catchments, Summit County, Colorado. In Biogeochemistry of Seasonally Snow-Covered Catchments, Tonnessen KA, Williams MW, Transfer M (eds). IAHS Publication no. 228. IAHS Press: Wallingford; 303-312

Castellarin A, Burn DH, Brath A. 2001. Assessing the effectiveness of hydrological similarity measures for flood frequency analysis. *Journal of Hydrology* **241**. DOI: 10.1016/S0022-1694(00)00383-8.

Casson NJ. 2008. Rain induced bursts of denitrification activity account for differences in dissolved nitrogen export from forested catchments. M.Sc. thesis, University of Western Ontario, London, Canada.

Chacon N, Flores S, Gonzalez A. 2006a. Implications of iron solubilization on soil phosphorus release in seasonally flooded forests of the lower Orinoco River, Venezuela. *Soil Biology & Biochemistry* **38**. DOI: 10.1016/j.soilbio.2005.10.018.

Chacon N, Silver WL, Dubinsky EA, Cusack DF. 2006b. Iron reduction and soil phosphorus solubilization in humid tropical forests soils: The roles of labile carbon pools and an electron shuttle compound. *Biogeochemistry* **78**. DOI: 10.1007/s10533-005-2343-3.

Conacher A, Dalrymple J. 1977. The Nine Unit Land-Surface Model - Approach to Pedogeomorphic Research. *Geoderma* **18**: 1-154.

Craig D, Johnston L. 1988. Acidification of Shallow Groundwaters during the Spring Melt Period. *Nordic Hydrology* **19**: 89-98.

Creed IF, Band LE. 1998. Export of nitrogen from catchments within a temperate forest: Evidence for a unifying mechanism regulated by variable source area dynamics. *Water Resources Research* **34**. DOI: 10.1029/98WR01924.

Creed IF, Band LE, Foster NW, Morrison IK, Nicolson JA, Semkin RS, Jeffries DS. 1996. Regulation of nitrate-N release from temperate forests: A test of the N flushing hypothesis. *Water Resources Research* **32**. DOI: 10.1029/96WR02399.

Creed IF, Beall FD. 2009. Distributed topographic indicators for predicting nitrogen export from headwater catchments. *Water Resources Research* **45**: W10407. DOI: 10.1029/2008WR007285.

Creed IF, Beall FD, Clair TA, Dillon PJ, Hesslein RH. 2008. Predicting export of dissolved organic carbon from forested catchments in glaciated landscapes with shallow soils. *Global Biogeochemical Cycles* **22**: GB4024. DOI: 10.1029/2008GB003294.

Creed IF, Sanford SE, Beall FD, Molot LA, Dillon PJ. 2003. Cryptic wetlands: integrating hidden wetlands in regression models of the export of dissolved organic

carbon from forested landscapes. *Hydrological Processes* **17**: 3629-48. DOI: 10.1002/hyp.1357.

Creed IF, CG Trick, LE Band, IK Morrison. 2002. Characterizing the spatial pattern of soil carbon and nitrogen pools in the Turkey Lakes Watershed: A comparison of regression techniques. Water, Air, and Soil Pollution: Focus 2: 81–102.

Davidson EA, Chorover J, Dail DB. 2003. A mechanism of abiotic immobilization of nitrate in forest ecosystems: the ferrous wheel hypothesis. *Global Change Biology* **9**. DOI: 10.1046/j.1365-2486.2003.00592.x.

DeBusk WF, Reddy KR. 1998. Turnover of detrital organic carbon in a nutrient-impacted Everglades marsh. *Soil Science Society of America Journal* **62**.

Del Grosso S, Parton W, Mosier A, Ojima D, Kulmala A, Phongpan S. 2000. General model for N2O and N2 gas emissions from soils due to dentrification. *Global Biogeochemical Cycles* **14**: 1045-60.

Devito KJ, Creed IF, Rothwell RL, Prepas EE. 2000. Landscape controls on phosphorus loading to boreal lakes: implications for the potential impacts of forest harvesting. *Canadian Journal of Fisheries and Aquatic Sciences* **57**. DOI: 10.1139/cjfas-57-10-1977.

Devito K, Dillon P, Lazerte B. 1989. Phosphorus and Nitrogen-Retention in 5 Precambrian Shield Wetlands. *Biogeochemistry* **8**: 185-204.

Elder JF. 1985. Nitrogen and Phosphorus Speciation and Flux in a Large Florida River Wetland System. *Water Resources Research* **21**. DOI: 10.1029/WR021i005p00724.

Elliot H. 1985. Geophysical survey to determine overburden thickness in selected areas within the Turkey Lakes Watershed basin, Algoma District, Ontario. Rep. 85-09, Turkey Lakes Watershed, Algoma, Ontario, Canada.

Evans JE, Prepas EE, Devito KJ, Kotak BG. 2000. Phosphorus dynamics in shallow subsurface waters in an uncut and cut subcatchment of a lake on the Boreal Plain. *Canadian Journal of Fisheries and Aquatic Sciences* **57**. DOI: 10.1139/cjfas-57-S2-60.

Fairweather TA. 2007. Tracking the alternative fates of nitrogen in forested catchments. M.Sc. thesis, University of Western Ontario, London, Canada.

Fellman JB, Hood E, D'Amore DV, Edwards RT, White D. 2009. Seasonal changes in the chemical quality and biodegradability of dissolved organic matter exported from soils to streams in coastal temperate rainforest watersheds. *Biogeochemistry* **95**. DOI: 10.1007/s10533-009-9336-6.

Foster NW. 1985. Acid Precipitation and Soil Solution Chemistry within a Maple Birch Forest in Canada. *Forest Ecology and Management* **12**. DOI: 10.1016/0378-1127(85)90092-1.

Foster SSD, Cripps AC, Smithcarington A. 1982. Nitrate Leaching to Groundwater. *Philosophical Transactions of the Royal Society of London Series B-Biological Sciences* **296**.

Fraterrigo JM, Downing JA. 2008. The Influence of Land Use on Lake Nutrients Varies with Watershed Transport Capacity. *Ecosystems* **11**. DOI: 10.1007/s10021-008-9176-6.

Govindaraju RS. 1996. Modeling overland flow contamination by chemicals mixed in shallow soil horizons under variable source area hydrology. *Water Resources Research* **32**. DOI: 10.1029/95WR03639.

Groffman PM, Altabet MA, Bohlke JK, Butterbach-Bahl K, David MB, Firestone MK, Giblin AE, Kana TM, Nielsen LP, Voytek MA. 2006. Methods for measuring denitrification: Diverse approaches to a difficult problem. *Ecological Applications* **16**. DOI: 10.1890/1051-0761(2006)016[2091:MFMDDA]2.0.CO;2.

Gundersen P, Bashkin VN. 1994. Nitrogen Cycling. In Biogeochemistry of small catchments, Moldan B, Cerny J (Eds). Wiley: New York; 255-284.

Heathwaite AL, Johnes PJ. 1996. Contribution of nitrogen species and phosphorus fractions to stream water quality in agricultural catchments. *Hydrological Processes* **10**. DOI: 10.1002/(SICI)1099-1085(199607)10:7<971::AID-HYP351>3.0.CO;2-N.

Hewlett JD, Hibbert AR. 1967. Factors affecting the response of small watersheds to precipitation in humid areas. In Forest Hydrology, Sopper WE, Lull HW (Eds). Proc. Int. Symp. on Forest Hydrogy, Penn. State Univ., University Park, Pennsylvania; 275-290.

Hornberger GM, Bencala KE, Mcknight DM. 1994. Hydrological Controls on Dissolved Organic-Carbon during Snowmelt in the Snake River Near Montezuma, Colorado. *Biogeochemistry* **25**. DOI: 10.1007/BF00024390.

Jeffries DS, Kelso JRM, Morrison IK. 1988. Physical, Chemical, and Biological Characteristics of the Turkey Lakes Watershed, Central Ontario, Canada. *Canadian Journal of Fisheries and Aquatic Sciences* **45**: 3-13.

Jensons S, Domingue J. 1988. Extracting Topographic Structure from Digital Elevation Data for Geographic Information-System Analysis. *Photogrammetric Engineering and Remote Sensing* **54**: 1593-600.

Johnston L, Craig D. 1986. Turkey Lakes water study: hydrogeological instrumentation and aquifer materials. NHRI unpublished report; contribution No. 87004.

Kadlec JA. 1986. Input Output Nutrient Budgets for Small Diked Marshes. *Canadian Journal of Fisheries and Aquatic Sciences* **43**.

Kalbitz K, Solinger S, Park JH, Michalzik B, Matzner E. 2000. Controls on the dynamics of dissolved organic matter in soils: A review. *Soil Science* **165**. DOI: 10.1097/00010694-200004000-00001.

Kaushal SS, Lewis WM. 2005. Fate and transport of organic nitrogen in minimally disturbed montane streams of Colorado, USA. *Biogeochemistry* **74**. DOI: 10.1007/s10533-004-4723-5.

Kemp GP, Day JW. 1984. Nutrient dynamics in a Louisiana swamp receiving agricultural runoff. In Cypress Swamps, Ewe1 KC, Odum HT (Eds). University Presses of Florida: Gainsville; 286-293.

Lee GF, Bengly E, Amundson R. 1975. Effects of marshes on water quality. In Coupling of Land and Water Systems, Hasler AD (Ed). Springer-Verlag: NY; 105-127

Lindsay J, Creed I. 2005. Removal of artifact depressions from digital elevation models: towards a minimum impact approach. *Hydrological Processes* **19**: 3113-26. DOI: 10.1002/hyp.5835.

Lindsay J, Creed I, Beall F. 2004. Drainage basin morphometrics for depressional landscapes. *Water Resources Research* **40**: W09307. DOI: 10.1029/2004WR003322.

Liptzin D, Silver WL. 2009. Effects of carbon additions on iron reduction and phosphorus availability in a humid tropical forest soil. *Soil Biology & Biochemistry* **41**. DOI: 10.1016/j.soilbio.2009.05.013.

Lovett GM, Burns DA, Driscoll CT, Jenkins JC, Mitchell MJ, Rustad L, Shanley JB, Likens GE, Haeuber R. 2007. Who needs environmental monitoring? *Frontiers in Ecology and the Environment* **5**. DOI: 10.1890/1540-9295(2007)5[253:WNEM]2.0.CO;2.

Marjerison RD, Dahlke H, Easton ZM, Seifert S, Walter MT. 2011. A Phosphorus Index transport factor based on variable source area hydrology for New York State. *Journal of Soil and Water Conservation* **66**. DOI: 10.2489/jswc.66.3.149.

Mcdowell WH, Likens GE. 1988. Origin, Composition, and Flux of Dissolved Organic-Carbon in the Hubbard Brook Valley. *Ecological Monographs* **58**. DOI: 10.2307/2937024.

Mcdowell WH, Wood T. 1984. Podzolization - Soil Processes Control Dissolved Organic-Carbon Concentrations in Stream Water. *Soil Science* **137**. DOI: 10.1097/00010694-198401000-00004.

Moore TR, Desouza W, Koprivnjak JF. 1992. Controls on the Sorption of Dissolved Organic-Carbon by Soils. *Soil Science* **154**. DOI: 10.1097/00010694-199208000-00005.

Moore TR, Turunen J. 2004. Carbon accumulation and storage in mineral subsoil beneath peat. *Soil Science Society of America Journal* **68**.

Neff JC, Asner GP. 2001. Dissolved organic carbon in terrestrial ecosystems: Synthesis and a model. *Ecosystems* **4**. DOI: 10.1007/s100210000058.

Nicolson JA. 1988. Water and Chemical Budgets for Terrestrial Basins at the Turkey Lakes Watershed. *Canadian Journal of Fisheries and Aquatic Sciences* **45**.

Ocallaghan J, Mark D. 1984. The Extraction of Drainage Networks from Digital Elevation Data. *Computer Vision Graphics and Image Processing* **28**: 323-44. DOI: 10.1016/S0734-189X(84)80011-0.

Oeurng C, Sauvage S, Sanchez-Perez J. 2010. Temporal variability of nitrate transport through hydrological response during flood events within a large agricultural catchment in south-west France. *Science of the Total Environment* **409**. DOI: 10.1016/j.scitotenv.2010.09.006.

Peterjohn WT, Correll DL. 1984. Nutrient dynamics in an agricultural watershed - observations on the role of a riparian forest. *Ecology* **65**. DOI: 10.2307/1939127.

Planchon O, Darboux F. 2002. A fast, simple and versatile algorithm to fill the depressions of digital elevation models. *Catena* **46**: 159-76. DOI: 10.1016/S0341-8162(01)00164-3.

Qualls RG, Haines BL, Swank WT, Tyler SW. 2000. Soluble organic and inorganic nutrient fluxes in clearcut and mature deciduous forests. *Soil Science Society of America Journal* **64**.

Qualls RG, Richardson CJ. 2003. Factors controlling concentration, export, and decomposition of dissolved organic nutrients in the Everglades of Florida. *Biogeochemistry* **62**. DOI: 10.1023/A:1021150503664.

Reddy, KR, DeLaune RD. 2008. Biogeochemistry of Wetlands: Science and Applications. CRC Press: Boca Raton, Florida.

Schiff SL, Aravena R, Mewhinney E, Elgood RJ, Warner B, Dillon P, Trumbore S. 1998. Precambrian shield wetlands: Hydrologic control of the sources and export of dissolved organic matter. *Climatic Change* **40**. DOI: 10.1023/A:1005496331593.

Schiff SL, Devito KJ, Elgood RJ, McCrindle PM, Spoelstra J, Dillon P. 2002. Two adjacent forested catchments: Dramatically different NO3- export. *Water Resources Research* **38**: 1292. DOI: 10.1029/2000WR000170.

Semkin RG, Jefferies DS. 1983. Rock chemistry in the Turkey Lakes Watershed. Turkey Lakes Watershed Unpublished Report; No. 83(03): 9.

Sickman, JO. 2001. Comparative analyses of nitrogen biogeochemistry in high-elevation ecosystems. Ph.D. Thesis, University of California, Santa Barbara.

Sirivedhin T, Gray KA. 2006. Factors affecting denitrification rates in experimental wetlands: Field and laboratory studies. *Ecological Engineering* **26**. DOI: 10.1016/j.ecoleng.2005.09.001.

Sloey WE, Spangler FL, Fetter CWJ. 1978. *Management of Fresh Water Wetlands for Nutrient Assimilation*.

Sommer M, Schlichting E. 1997. Archetypes of catenas in respect to matter - A concept for structuring and grouping catenas. *Geoderma* **76**: 1-33. DOI: 10.1016/S0016-7061(96)00095-X.

Sorrell BK, Armstrong W. 1994. On the Difficulties of Measuring Oxygen Release by Root Systems of Wetland Plants. *Journal of Ecology* **82**. DOI: 10.2307/2261396.

Tarboton DG. 1997. A new method for the determination of flow directions and upslope areas in grid digital elevation models. Water Resourc. Res. **33** (2): 309-319. doi:10.1029/96WR03137.

Tetzlaff D, McDonnell JJ, Uhlenbrook S, McGuire KJ, Bogaart PW, Naef F, Baird AJ, Dunn SM, Soulsby C. 2008. Conceptualizing catchment processes: simply too complex? *Hydrological Processes* **22**. DOI: 10.1002/hyp.7069.

Tiedje JM. 1982. Denitrification. *Page AL(Ed). Agronomy: a Series of Monographs, Vol.9.Methods of Soil Analysis, Part 2.Chemical and Microbiological Properties, 2nd Edition.Xxiv+1159p.American Society of Agronomy, Inc.Soil Science Society of America, Inc.Publishers: Madison, (TRUNCATED)* .

Wagener T, Sivapalan M, Troch P, Woods R. 2007. Catchment classification and hydrologic similarity. *Geography Compass* **1**(4): 901-931. DOI: 10.1111/j.1749-8198.2007.00039.x

Wallis PM. 1979. Sources, Transportation, and Utilization of Dissolved Organic Matter in Groundwater and Streams: Scientific Series No. 100. Kananaskis Center for Environmental Research, University of Calgary.

Walter MT, Walter MF, Brooks ES, Steenhuis TS, Boll J, Weiler K. 2000. Hydrologically sensitive areas: Variable source area hydrology implications for water quality risk assessment. *Journal of Soil and Water Conservation* **55**.

Webster KL, Creed IF, Beall FD, Bourbonniere RA. 2011. A topographic template for estimating soil carbon pools in forested catchments. *Geoderma* **160**: 457-67. DOI: 10.1016/j.geoclerma.2010.10.016.

Webster KL, Creed IF, Beall FD, Bourbonniere RA. 2008. Sensitivity of catchment-aggregated estimates of soil carbon dioxide efflux to topography under different climatic conditions. *Journal of Geophysical Research-Biogeosciences* **113**: G03040. DOI: 10.1029/2008JG000707.

Webster KL, Creed IF, Bourbonniere RA, Beall FD. 2008. Controls on the heterogeneity of soil respiration in a tolerant hardwood forest. *Journal of Geophysical Research-Biogeosciences* **113**: G03018. DOI: 10.1029/2008JG000706.

Wickware GM, Cowell DW. 1985. Forest Ecosystem Classification of the Turkey Lake Watershed, Ecol. Classif. Ser. 18, Lands Dir., Environ, Ottawa, Canada.

Wrage N, Velthof G, van Beusichem M, Oenema O. 2001. Role of nitrifier denitrification in the production of nitrous oxide. *Soil Biology & Biochemistry* **33**: 1723-32. DOI: 10.1016/S0038-0717(01)00096-7.

Yang JY, Fan J. 2003. Review of study on mineralization, saturation and cycle of nitrogen in forest ecosystems. *Journal of Forestry Research (Harbin)* **14**.

Yoshinari T, Knowles R. 1976. Acetylene Inhibition of Nitrous-Oxide Reduction by Denitrifying Bacteria. *Biochemical and biophysical research communications* **69**: 705-10. DOI: 10.1016/0006-291X(76)90932-3.

Chapter 3: Russian nesting dolls effect – Using wavelet analysis to reveal non-stationary and nested stationary signals in water yield from catchments in a northern forested landscape[1]

The previous chapter focused on the role of topography on spatial variation in long-term average annual nutrient export, whereas this chapter focuses on the role of topography in influencing temporal variation in annual water yield (as a precursor for examining annual nutrient export). This chapter tests the hypothesis that catchment water yields contain a complex mixture of non-stationary and stationary signals driven by climate that are manifested differently in catchments with different topographic characteristics. A novel analytical framework is introduced to deconstruct time series. Annual time series from catchments with topographic characteristics that represent the range in hydrological flushing potential, hydrological storage potential, and hydrological loading potential are then deconstructed into non-stationary (trend) and stationary (cycle) signals, and then climate drivers are related to these deconstructed signals to determine their contribution to these temporal variation in water yields. The significance of this chapter is that it presents a novel analytical framework for deconstructing export signals, so that potential for differential sensitivity of catchment water yields to climatic forcing can be established.

3.1 Introduction

Understanding climate effects on water resources continue to be a major agenda among hydrologists, ecologists and policy makers. Catchments in various regions have been affected by non-stationary climate warming linked to anthropogenic activities (Arnell, 2004; Christensen *et al.*, 2004; Chen *et al.*, 2006; Pike *et al.*, 2008; Zwiers *et al.*, 2011). Catchments have also been affected by stationary climate patterns, driven by large-scale

[1]A version of this chapter has been published (Mengistu SG, Creed IF, Kulperger RJ, Quick CG. 2012. Russian nesting dolls effect – Using wavelet analysis to reveal non-stationary and nested stationary signals in water yield from catchments on a northern forested landscape, *Hydrological Processes*)

climatic oscillations caused by fluctuations in sea surface temperature or sea level pressure (Keener *et al.,* 2010; Kahya, 2011; Niedzielski, 2011) [e.g., Multivariate El Niño Southern Oscillation (ENSO) Index (MEI), Atlantic Multidecadal Oscillation (AMO), Northern Atlantic Oscillation (NAO), and Pacific Decadal Oscillation (PDO)], although there is some evidence that these oscillations may not be strictly stationary [e.g., ENSO (Gaucherel, 2010)]. Observed temporal variability in water yields may reflect the combined effect of non-stationary climate trends and stationary climate oscillations with multiple periodicities (Zhou *et al*., 2008). There is a critical need to discriminate between non-stationary and stationary signals in changing water yields from these catchments.

Discriminating between non-stationary responses (deterministic responses where the statistical mean and variance change with time, predictably and unpredictably) and stationary responses (stochastic responses where the statistical mean and variance do not change with time) of catchments is an important step to better understanding and predicting the often different responses of catchments and their water yields to climate (Jones *et al.,* 2012). Individual statistical analyses have emerged that enable us to resolve this complexity, including wavelet analysis where decomposition of a time series into a time-frequency space enables not only identification of the dominant wavelets (i.e., periodicities) in the time series, but also estimation of how the dominant wavelets change over time (Torrence and Compo, 1998; Santos and De Morais, 2008). Wavelet cross coherence analysis between the spectra of large-scale climatic oscillations and water yields can be used to identify specific climatic oscillations responsible for stationary signals in the water yield time series. Guiding principles are needed to combine these statistical analyses to discriminate non-stationary from stationary signals in catchment responses to climate.

Small, headwater catchments have great potential to serve as sentinels for climate change because of their ability to respond rapidly to changing environmental conditions including freeze-thaw and flood-drought transitions and trends (Strand *et al.,* 2008). Headwater catchments typically have high topographic positions, collect precipitation from a relatively small area, and have thin soil layers for moisture storage, making their hydrologic regime more sensitive to climate-related changes in environmental conditions compared to the higher order catchments into which they drain (Feminella, 1996; Winter,

2000; Eimers *et al.*, 2004). Furthermore, headwater catchments contribute a large amount of water (Kirby, 1978; Haycock *et al*., 1993) and cover a large spatial extent (Meyer and Wallace, 2001; Sidle *et al.*, 2000; Bishop *et al.,* 2008) of larger catchments, and so have considerable influence on what may happen to higher order catchment water yields. In addition, these headwater catchments serve as sources of sediments, nutrients, and biota to downstream reaches of larger catchment systems (Rabeni and Wallace, 1998; Gomi *et al.*, 2002; Wipfli and Gregovich, 2002; Clarke *et al.*, 2008). Therefore, scientific investigations of the effects of climate-related environmental changes on water, sediment and nutrient export are best made in headwater catchments.

The purpose of this paper is to present an analytical framework for discriminating non-stationary and stationary signals in water yield responses of headwater catchments in a forested landscape where climatic variability is evident, but little is known about its effect on sustainability of water yields. The (null) hypothesis that climate has no significant effect on water yields was tested using a 28-year time series of water yields (the longest available within the region) from headwater catchments. If climate does have an effect, then a corollary to the hypothesis is that stationary signals are more important than non-stationary signals in water yields. Also, if climate does have an effect, then a corollary to the hypothesis is that sensitivity to these signals is greater in catchments that have lower rates of change in water loading and lower water storage capacity. By examining the ability of headwater catchments to respond to both directional climate change and non-directional naturally occurring climatic oscillations, it may be possible to infer what types of catchments may be the most sensitive sentinels of climate change and may see the most extreme impacts of continuing climate warming.

3.2 Study Area

Located on the northern edge of the Great Lakes-St. Lawrence Forest Region in the Algoma Highlands of Central Ontario (Figure 3.1), the Turkey Lakes Watershed (TLW) is about 60 km north of Sault Ste. Marie (47°80’30’’N, 84°82’50’’W; Figure 3.2). In 1980 the TLW was established as a long-term experimental research station by Canadian federal government agencies to investigate the potential effects of acid rain and climate change on terrestrial and aquatic ecosystems (Jeffries *et al.*, 1988). Within the TLW a

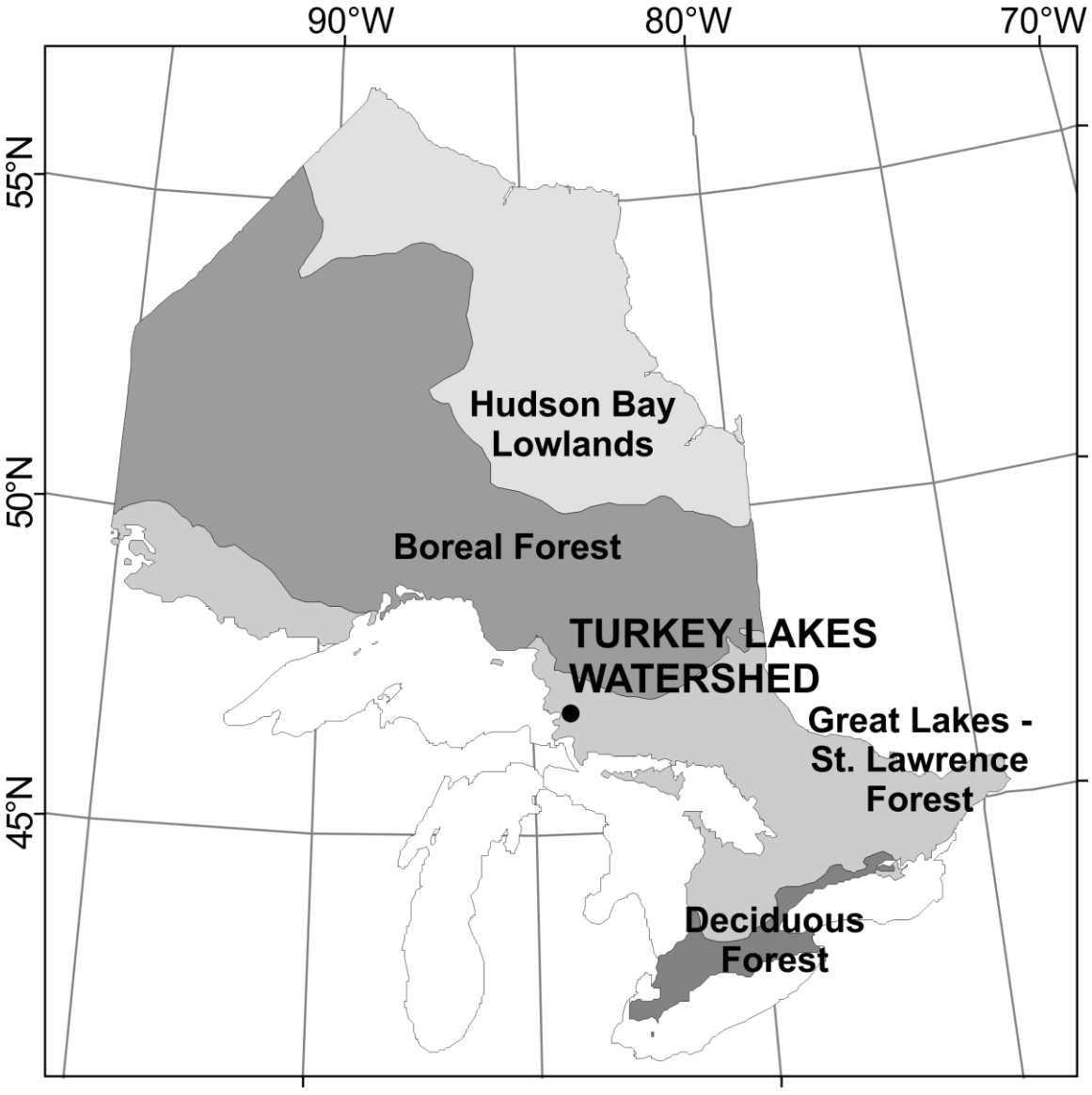


Figure 3.1: The forest eco-regions of Ontario.

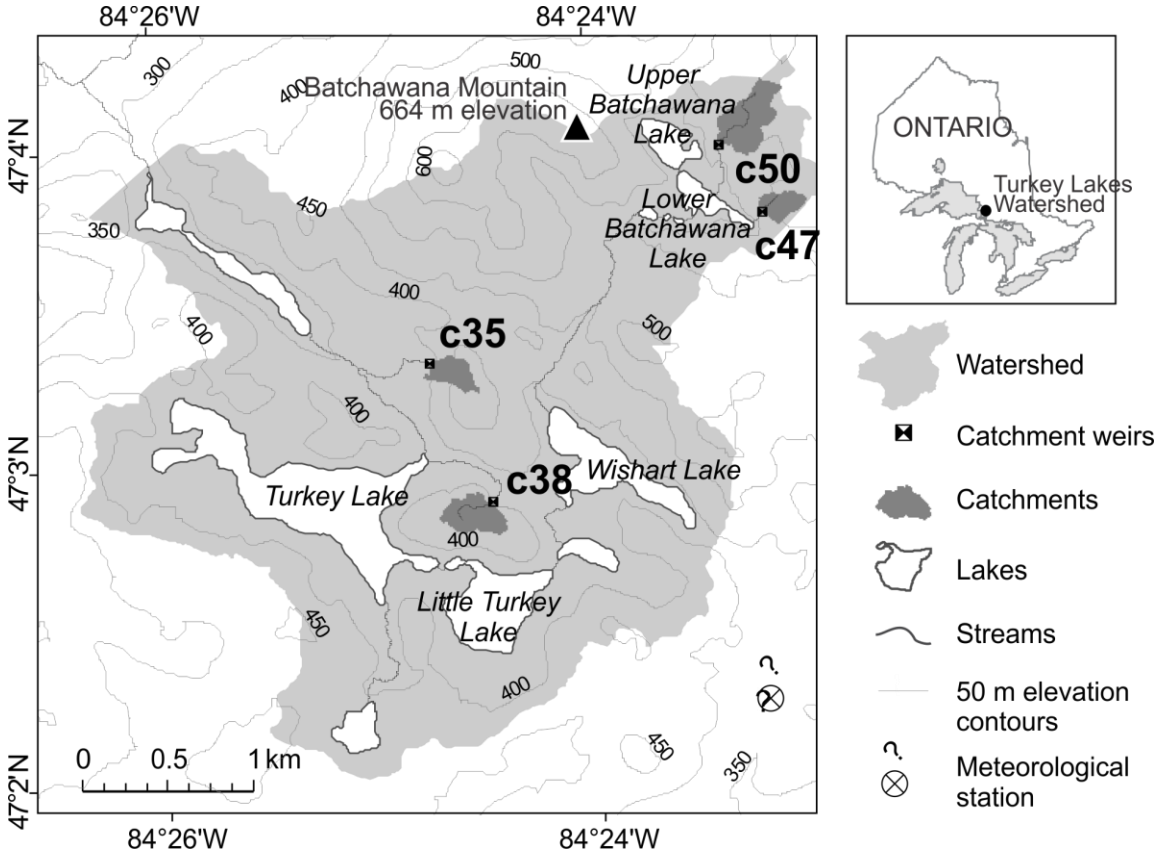


Figure 3.2: The Turkey Lakes Watershed.

series of headwater catchments representing the range of natural geologic and geomorphic variation have been continuously monitored for hydrology and biogeochemistry by Natural Resources Canada-Canadian Forest Service and Environment Canada scientists.

The TLW rests on Precambrian silicate greenstone that is metamorphosed basalt, with small intrusions of felsic igneous rock (Giblin and Leahy, 1977). The overall relief is 400 m, from 644 m above sea level at the summit of Batchawana Mountain to 244 m above sea level at the outlet to the Batchawana River. Overlying the bedrock is a thin and discontinuous till, ranging in depth from <1 m at higher elevations to 1–2 m at lower elevations (Jeffries and Semkin, 1982), although till deposits up to 65 m occasionally occur in bedrock depressions (Elliot, 1985). The podzolic soils that have developed in the tills follow a generalized sequence of thin and undifferentiated near the ridge, gradually thickening, differentiating, and increasing in organic content on topographic benches and toward streams (Nicolson, 1988). Highly humified organic deposits occur in wetlands (Canada Soil Survey Committee, 1978; Cowell and Wickware, 1983).

The watershed is covered by a northern tolerant hardwood forest dominated by sugar maple (*Acer saccharum* Marsh.) (Wickware and Cowell, 1985). There have been no disturbances since the 1950s, except an experimental harvest in 1998 on a portion of the watershed not included in the present study. Average stand density (904 stems ha^{-1}), dominant height (20.5 m), diameter at breast height (15.3 cm) and basal area (25.1 m^2 ha^{-1}) are relatively uniform across the uplands, with stand density increasing and dominant height decreasing in the wetlands (Jeffries *et al*., 1988). White pine (*Pinus strobes* L.), white spruce (*Picea glauca* Moench Voss.), ironwood (*Ostrya virginiana* (Mill.) K. Koch), and yellow birch (*Betula alleghaniensis* Britton) comprise less than 10% of basal area in the uplands. The sparse understory of upland stands is dominated (95%) by saplings and seedlings of sugar maple as well as a variety of herbs and ferns. Wetland stands are mixtures of black ash (*Fraxinus nigra* Marsh.), eastern white cedar (*Thuja occidentalis* L.), red maple (*Acer rubrum* L.), balsam fir (*Abies balsamea* (L.) Mill.), yellow birch, and tamarack (*Larix laricina* (DuRoi) K. Koch.). The understory in the wetlands is composed of the seedlings and saplings of overstory trees and various herbs

and ferns. There has been no to minimal natural or anthropogenic disturbance to the forest cover within these four catchments.

The watershed is influenced by a continental climate with average 28-year annual precipitation of 1200 mm and average annual temperature of 5 °C (Figure 3.3). These headwater catchments are influenced by a snowpack that persists from late November, early December through to late March, early April and peak flows that occur during snowmelt and again during autumn storms. Future climate scenarios for the area predict temperatures increasing by 1.0 to 3.0 °C by 2040 and 2.5 to 4.5 °C by 2070, and precipitation increasing by 0 to 10% by 2040 and 0 to 20% by 2070 (Price *et al*., 2011).

The four selected catchments, c35, c38, c47 and c50, exhibit a gradient in water loading in the form of rain and snow and in water storage in wetlands (percent wetlands by area) (Figure 3.4, Table 3.1). To establish the magnitude of the gradient in water loading, precipitation records from 1981 to 2010 of six TLW precipitation network gauges (namely, the main meteorological recording station outside of the TLW and five precipitation gauges distributed within the TLW) were used to calculate the long term monthly average precipitation for each of station. The long term monthly average precipitations of all the stations were then used to interpolate grid maps of long term monthly average precipitation for the whole TLW regions using Anusplin Version 4.37. The monthly average precipitation layers were added to derive a grid map of long term annual average precipitation for TLW region. For each studied catchments, the long term annual average precipitations were calculated by taking the average of all annual average precipitation grids that fall within the catchment boundaries. Based on an analysis of the precipitation and discharge, the higher elevation catchments had on average approximately 5% more precipitation than the lower elevantion catchments (4.16% in c47 and 5.13 in c50), and on average approximately 20% more discharge (12.34% in c49 (which was used instead of c47 because of a dysfunctional weir in c47 that resulted in significant bypass of water from the weir and therefore an underestimate in discharge, F. Beall, Canadian Forest Service, Pers. Comm.) and 26.80% in c50). The additional 15% in discharge relative to precipitation may be attributed to underestimates in the interpolated precipitation at these specific catchments due to inadequate spatial

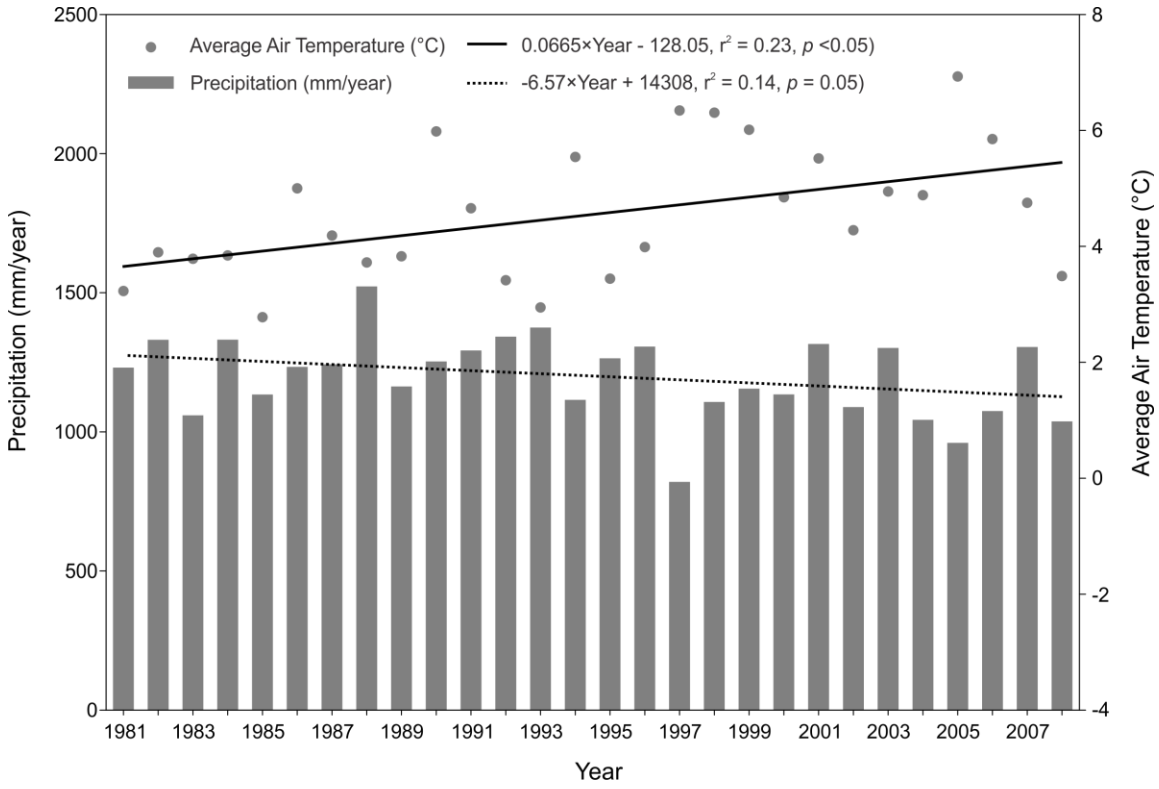


Figure 3.3: Annual hydroclimatic variation in the Turkey Lakes Watershed region.

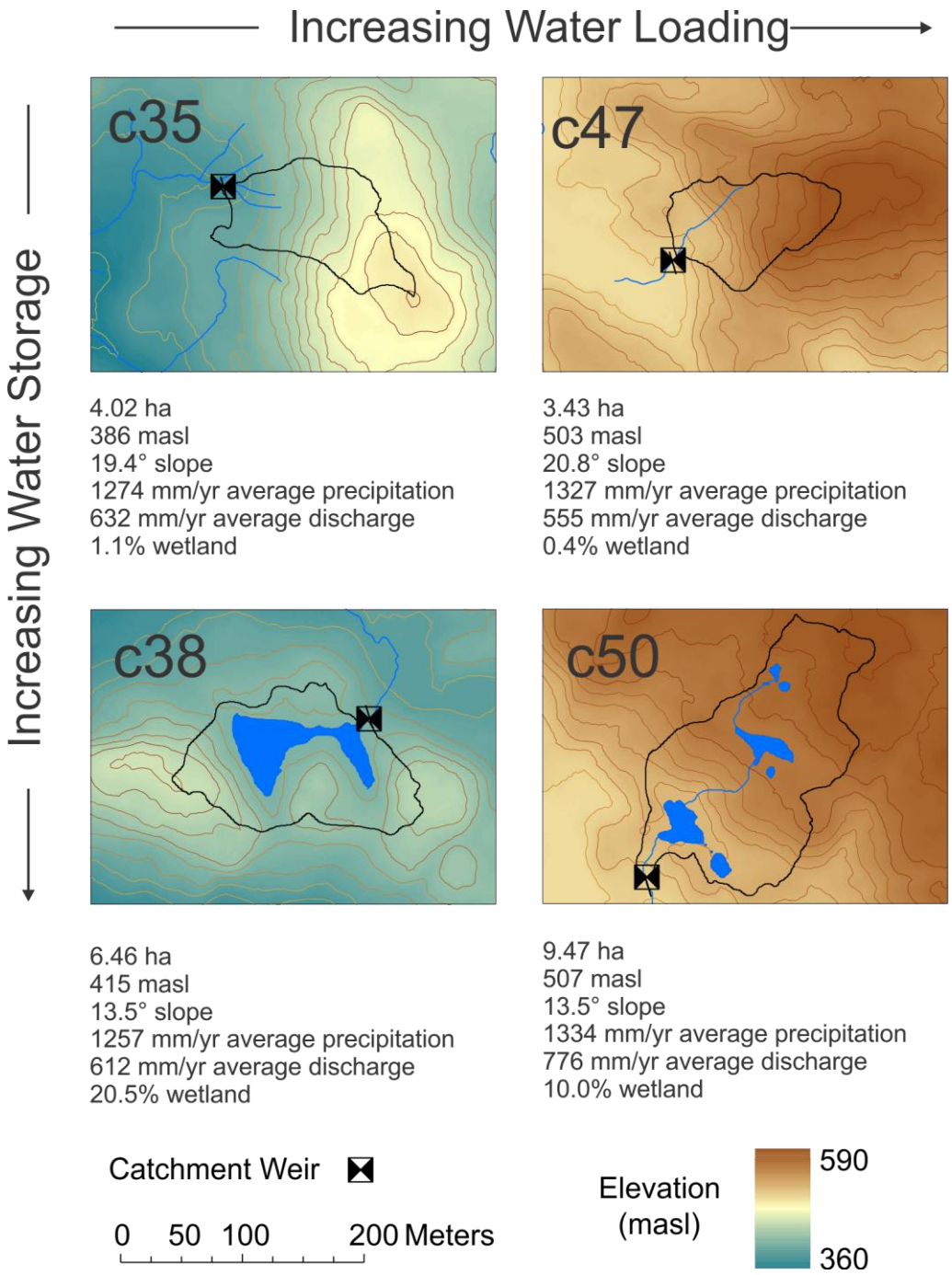


Figure 3.4: Topographic maps and descriptions of the four catchments selected from the Turkey Lakes Watershed for analysis. In c47, there is a buried side-channel, causing loss of groundwater (F. Beall, pers. comm). Catchment c49 is a high-elevation catchment that has similar average water loading (1327mm/yr) and a relatively small wetland (4%) with average discharge of 710 mm/yr, giving a closer approximation to the total discharge expected from c47.

Table 3.1: Characteristics of catchments in the Turkey Lakes Watershed.

Characteristics	**c35**	**c38**	**c47**	**c50**
Size (ha)	4.02	6.46	3.43	9.47
% Wetland	1.06	20.54	0.36	10.03
Elevation of weir (masl)	386	415	503	507
Slope (degrees)	19.36	13.51	20.84	13.45

representation of precipitation gauges, or to undetected water inputs from groundwater systems passing through fractured bedrock from outside of the catchment boundary.

To establish the magnitude in the gradient in water storage, we assumed the water storage capacity per unit area of the upland soils to be similar. The thin till that overlies the bedrock consists of two layer: an upper ablation till that is relatively permeable, and a lower basal till which is relatively impermeable. The ablation till that overlies the basal till has an average depth of 0.5 m (ranging from <0.2 to 1.0+ m) (Nicolson, 1988). However, some of the catchments contain wetlands that may modify water storage capacity. For example, catchments c35 and c47 have low water storage potential (1.1% and 0.4% wetland, respectively), whereas c38 and c50 contain high water storage potential (20.5% and 10.0%, respectively) (Creed *et al*., 2008). These wetlands likely vary in depth, but field measurements indicate that they can have depths up to about 10 m (Creed, Unpubl. Data). The modifying affect of these wetlands can either be to increase or decrease water export, depending on the antecedent water conditions within the wetlands (i.e., when wetlands are full of water, upland drainage waters bypass the storage by flowing over the surface of the wetland, and when wetlands are empty of water, upland drainage waters are trapped in the wetland as the water table within the wetland is below the weir.

3.3 Methods

3.3.1 Analytical Framework

The analytical framework for analysing non-stationary (linear trends) and stationary (non-linear oscillations) signals from the computed yearly water yield time series is presented in Figure 3.5.

3.3.2 Non-stationary linear trends

Annual data were used because daily, monthly and seasonal water yield data were too variable and linear trends were not statistically significant (data not shown). Daily water yield data from four catchments (c35, c38, c47 and c50) in the TLW were summed to derive a yearly time series of water yield running from 1981 to 2008 water years (June-

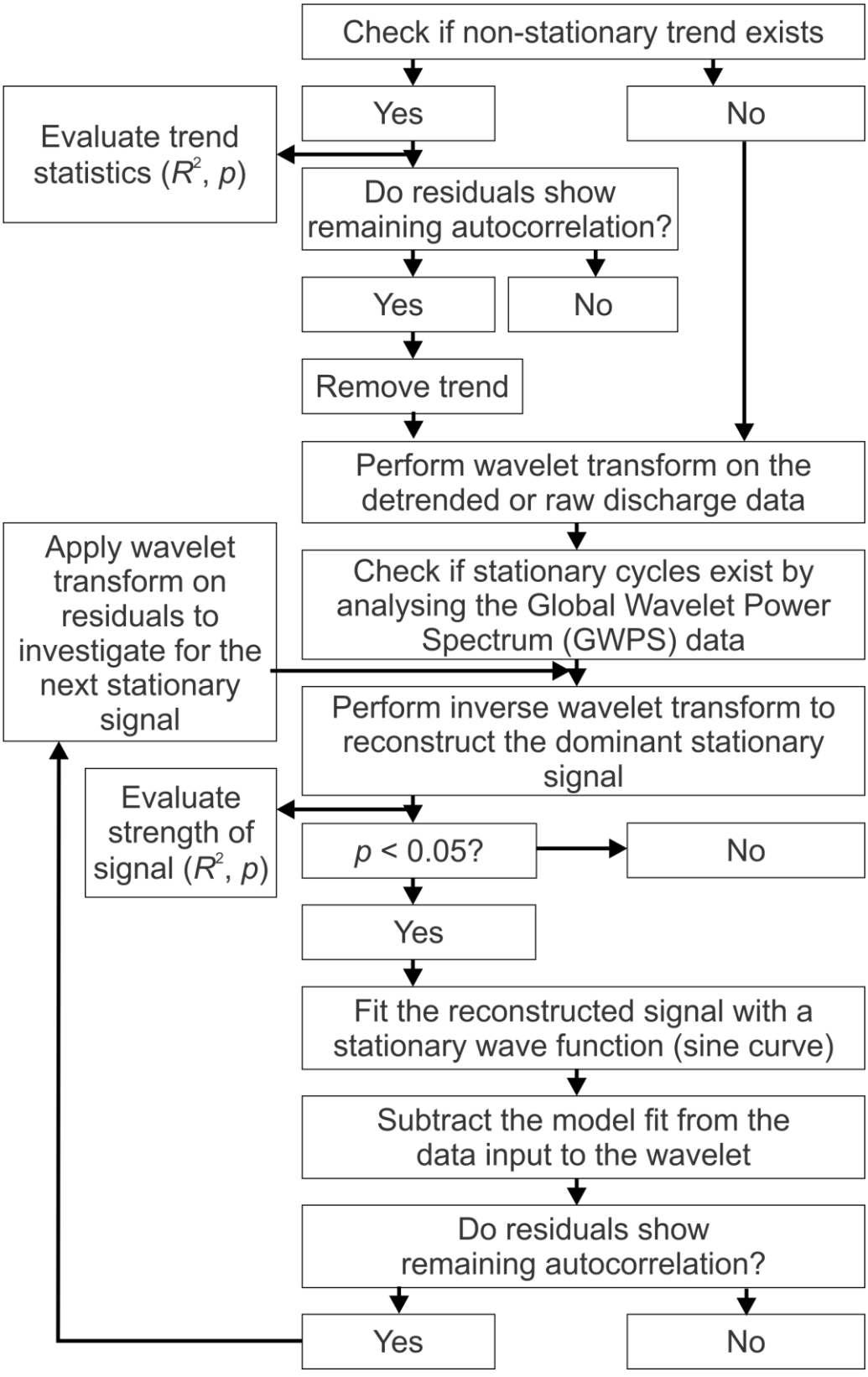


Figure 3.5: Flow chart summarizing the analytical steps.

May, with the water year indicated as the calendar year in which the water year began). The computed yearly time series of water yields were analysed for non-stationarity, which was then removed. The detrended portions were then further studied for the presence of multiple stationary signals using wavelet analysis.

3.3.3 Stationary non-linear oscillations

Following the method outlined in Torrence and Compo (1998), wavelet power spectra of the detrended portion of the yearly water yield data were derived for the catchments under investigation. The spectrums were computed by convoluting each time series with a scaled and translated version of a transforming wavelet function, usually known as the "mother wavelet." Assuming an equal time interval of Δt in a time series Xn ($n = 0, 1\ldots N-1$), the corresponding wavelet function, $\psi_o(\eta)$ (η is a non-dimensional time parameter on which the function depends), must have a zero mean and be localized in time and frequency space (Farge, 1992). A Morlet wavelet was chosen due to its extensive applications in similar studies involving hydroclimatic time series analysis. In addition to its ability to represent the shape of hydrological signals (Kang and Lin, 2007), Morlet wavelets provide adequate time and superior frequency resolution compared to other wavelet types (Labat, 2005; Soniat et al., 2006).

The Morlet wavelet is characterized by a Gaussian modulated plane wave:

$$\psi_o(\eta) = \pi^{-\frac{1}{4}} e^{i\omega_o \eta} e^{-\frac{\eta^2}{2}} \qquad (3.1)$$

Where i = an imaginary unit for complex valued Morlet function to overcome disadvantages of shift sensitivity, poor directionality and lack of phase information in using conventional real valued wavelets; ω_o is the non-dimensional angular frequency, which by default is taken to be 6 to satisfy the admissibility condition (Farge, 1992). The continuous wavelet transform of time series X_n, for each scale s at all n, with respect to the wavelet function $\psi_o(\eta)$ is mathematically represented as (3.2).

$$W_n(s) = \frac{1}{N} \sum_{n'=0}^{N-1} x_{n'} \psi^* \left[\frac{(\eta' - \eta)\Delta t}{s} \right] \qquad (3.2)$$

Where $W_n(s)$ stands for wavelet transform coefficients, ψ for the normalized wavelet, (*) for the complex conjugate, s for wavelet scale, n for localized time index, and n' for translated time index.

The transformed signal, $W_n(s)$, is a function of the wavelet scale and translation parameters found by conducting the convolution N (the number of data in the time series) times for each scale. Other than (3.2), a faster way of performing such a transform is to simultaneously calculate all the N convolutions in a Fourier space using discrete Fourier transform (DFT) of Xn (3.3).

$$\hat{x}_k = \frac{1}{N}\sum_{n=0}^{N-1} x_n e^{-2\pi i k n / N} \qquad (3.3)$$

Where $k = 0 \ldots N$ is the frequency index. In the Fourier space the wavelet transform equation (3.2) can be expressed as (3.4).

$$W_n(s) = \sum_{k=0}^{N-1} \hat{x}_k \hat{\psi}^*(s\omega_k) e^{i\omega_k n \Delta t} \qquad (3.4)$$

Where $\hat{\psi}(s\omega)$ is Fourier transform of a function $\psi(t/s)$ and ω_k is an angular frequency defined as (3.5):

$$\omega_k = \begin{cases} \dfrac{2\pi k}{N\Delta t} & if \quad k \le \dfrac{N}{2} \\ -\dfrac{2\pi k}{N\Delta t} & if \quad k > \dfrac{N}{2} \end{cases} \qquad (2.5)$$

The wavelet power spectrum was calculated as the square of the absolute value of the wavelet transform, $|W_n(s)|^2$.

The global wavelet power spectrum (GWPS) based analysis is considered a simple and robust technique for characterizing variability in time series (Santos and De Morais, 2008). Once the wavelet power spectra were calculated, the GWPS values were computed by time-averaging of wavelet spectrum values over all the local spectra. Generally, in wavelet based time series analysis, it is believed that the GWPS values provide useful information in terms of assessing the scale(s) (or period(s)) contributing most to the spectral energy of the time series under investigation. Scales with large GWPS values were considered to contribute more spectral energy, while the contribution of small GWPS scales were assumed to be little or insignificant. The GWPS values were,

therefore, used to identify scale(s) with high potential of periodic signals of stationary nature.

Inverse wavelet transfer of the forward wavelet transform (3.2) above was employed to reconstruct signals based on the coefficients of scales identified to have dominant GWPS. The inverse wavelet function is mathematically represented as (3.6).

$$x_n = \int_0^N \int_{s_1}^{s_k} W_n(s).\left[\frac{(\eta' - \eta)}{s}\right] \frac{dsdn}{s^2} \qquad (3.6)$$

Maintaining the coefficients of the chosen scale(s) while replacing all scale coefficients by zero and performing backwards (inverse) wavelet transform on the result generated the signals characterizing the identified scale. When choosing two or more consecutive scales, the inverse transform function builds the reconstructed signal as the sum of wavelets of different scales, *s*, at localized time, *n*.

Autocorrelation tests were used to examine if there was temporal autocorrelation between yearly time series of water yield. The autocorrelation was tested using Matlab's *autocorr* function and the confidence bounds were found using (3.7).

$$\frac{nSTDs}{\pm\ sqrt\ (N)} \qquad (3.7)$$

Where *nSTD*s is the number of standard deviations used in determining significance, and *N* is the number of independent sample data points. Two standard deviations were used to approximate 95% significance.

3.3.4 Searching for multiple stationary signals

Stationary signals were extracted from the water yield data time series using a step-wise methodology involving multiple cycles. The first step of the first cycle used the wavelet power spectrum of the detrended water yield time series to identify the dominant periodicity in the detrended time series, which was followed by inverse wavelet transform to extract the signal of dominant periodicity corresponding to scale(s) of peak GWPS values. The extracted signal was then fitted with a periodic function to model and statistically analyse the stationarity of the extracted signal. The same steps were followed in the second cycle using the residual of the detrended data (detrended water yield minus modeled stationary signal from cycle 1) as the input to the wavelet analysis. In the

following cycles, subsequent residuals (input data of the previous cycle minus modeled stationary signal in the same cycle) were similarily analysed.

For each cycle, the following "rules" were used to identify existing stationary signals: (1) A baseline of GWPS values was determined to select scales with the largest GWPS peaks above the set baseline; (2) Peak GWPS values were only considered for scales that were able to complete at least two full cycles in the available data (*i.e.*, cycles with periods less than 14 years); (3) Subsequent peak GWPS values were analysed until their inclusion in the model was not significant; and (4) The same scale could not appear twice among signals. After selecting the stationary signals for each catchment, each signal was added to the model using forward step-wise regression against the raw water yield data, first with the non-stationary signal.

After independent stationary signals were identified for each nutrient from each catchment, an overall stationary model was also developed for each nutrient from each catchment by modeling the sum of the independent stationary signals identified. The amplitude (difference between maximum and minimum) of the overall stationary signals was used to determine the range of change exhibited by stationarity over the study period.

3.3.5 Wavelet cross coherence analysis

Wavelet cross coherence analysis was used to understand the dominant oscillations that have detectable periodic patterns in the yearly time series of water yield within the chosen catchments. Wavelet coherence (Torrence and Webster, 1999; Grinsted *et al.*, 2004) of two time series X and Y, with wavelet transforms $W_n^X(s)$ and $W_n^Y(s)$, is defined as

$$R_n^2(s) = \frac{\left|S(s^{-1}W_n^{XY}(s))\right|^2}{S(s^{-1}\left|W_n^X(s)\right|^2) \times S(s^{-1}\left|W_n^Y(s)\right|^2)} \qquad (3.8)$$

Where S is a smoothing operator both in time and space that can be written as

$$S(W) = S_{\text{scale}}(S_{\text{time}}(W_n(s))) \qquad (3.9)$$

Where, S_{scale} denotes smoothing along the wavelet scale axis and S_{time} for the time axis.

Equation 3.8 closely resembles that of a traditional correlation coefficient. As a result, it is logical to consider wavelet coherence as a localized correlation coefficient in time frequency space (Grinsted *et al.*, 2004). The purpose of a smoothing operator is to

help locate local maxima or high regions in a plot, such as the cross coherence plot. The operation involves a smoothing or bin parameter, which determines the number of nearby frequencies, relative to one of interest, averaged (in a manner depending on the smoothing filter) to obtain the estimate of the cross coherence at the given frequency, producing an estimator that achieves small mean square error, which simultaneously keeps the variance and bias small.

We used wavelet cross coherence to correlate annual average indices for water years that were computed from monthly average indices of large scale climatic oscillations with the detrended water yield of the chosen catchments at each period using a Matlab package from Grinsted *et al*. (2002). The Multivariate El Niño Southern Oscillation (ENSO) Index (MEI), Atlantic Multidecadal Oscillation (AMO), Northern Atlantic Oscillation (NAO), Pacific Decadal Oscillation (PDO) indices were selected due to their global influence (Figure 3.6, Table 3.2). Wavelet transform plots map the correlations of wavelets of varying periods with the water yield time series, and wavelet cross coherence plots map the correlations of wavelets of varying periods with two different time series, the large scale climatic oscillations and the local water yield time series. In both cases, the cone of influence (COI) delimits regions of the plot that can be considered as part of the analysis. By analysing the plots, significant associations are indicated using warmer colours, and relationships with 95% confidence are circled. For wavelet cross coherence plots, arrows indicate the nature of the correlation: arrows to the left indicate negative correlations and arrows to the right indicate positive correlations (Grinsted *et al.*, 2004).

3.3.6 Climate drivers of yearly water yield time series

Correlation tests were performed among the global climate oscillations and between the global climate oscillations and local meteorological conditions. To examine correlations among the global climate oscillations, Pearson Product Moment correlation tests were performed between each of the four climate indices selected. Significant correlations were not expected if the global climate oscillations were significantly correlated for a short period (*i.e.*, if they were only strongly correlated for 5 years in a 28-year data

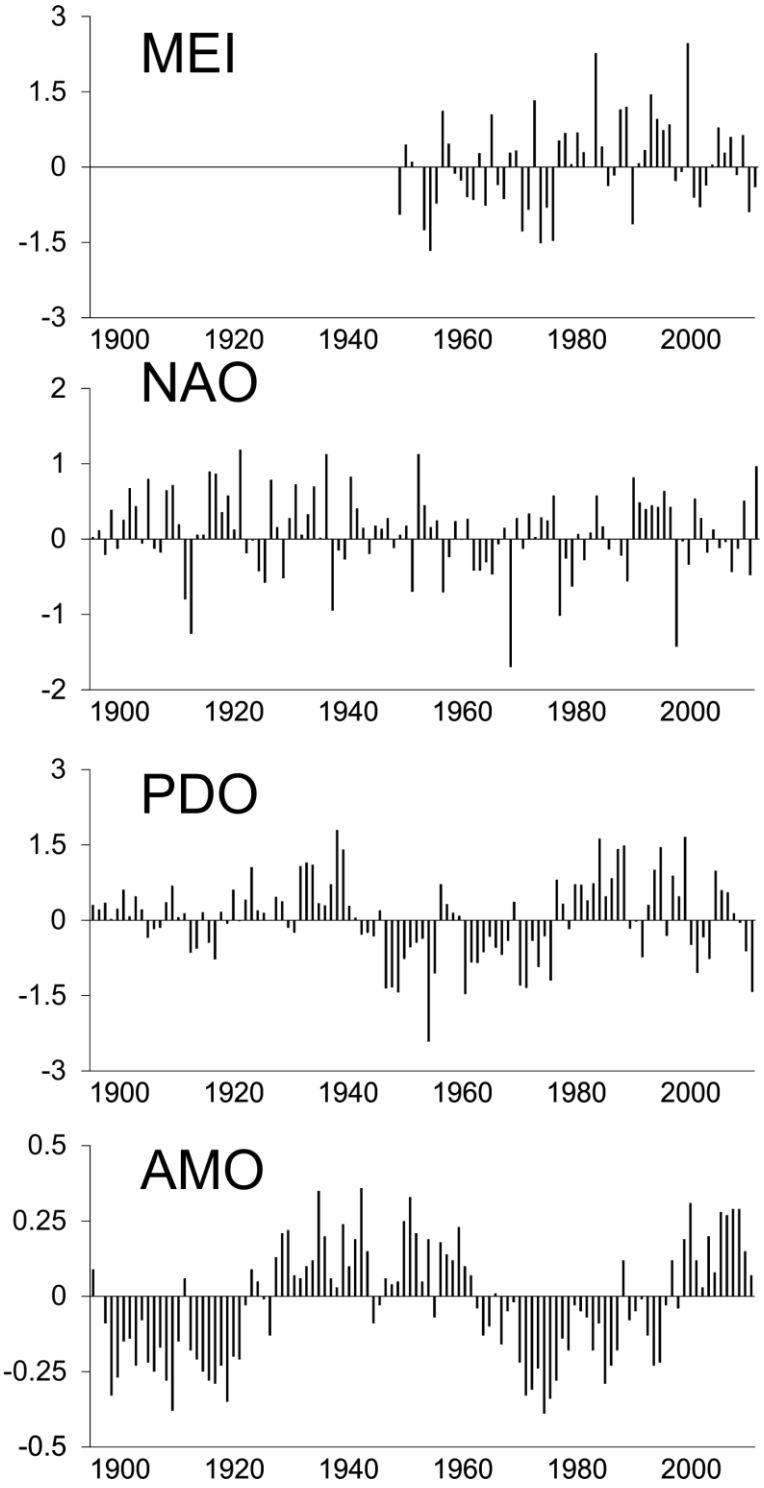


Figure 3.6: Time series of the Multivariate El Niño Southern Oscillation (ENSO) Index (MEI), Atlantic Multidecadal Oscillation (AMO), Northern Atlantic Oscillation (NAO), and Pacific Decadal Oscillation (PDO) indices.

Table 3.2: Large-scale climatic oscillations used for cross-coherence analysis.

Indices (Data Source)	**Periodicity**	**Climatic influence**
Multivariate El Nino Southern Oscillation (ENSO) Index (MEI) (NOAA – ESRL 2012a)	The periodicity of strong ENSO events is approximately 2 to 7 years (Huggett, 1997).	A positive MEI index (an ENSO episode), is associated with warmer than normal autumn to spring temperatures at the study site (Shabbar and Khandekar, 1996, Shabbar and Bonsal, 2004).
Northern Atlantic Oscillation (NAO) (NCAR 2012)	There is no statistically significant periodicity, although there is some evidence of a 7 to 9 year and approximately 20 years periodicities (Burroughs, 2005).	A positive NAO is associated with colder than normal winters at the study site (Bonsal *et al.*, 2001).
Pacific Decadal Oscillation (PDO) (JISAO 2012)	PDO tends to occur with a periodicity of around 20 to 30 years (Burn, 2008; Mantua and Hare, 2002; Minobe, 1997)	A positive PDO is associated with warmer and drier winters, while negative phases are associated with cooler and wetter winters at the study site (Burn, 2008).
Atlantic Multidecadal Oscillation (AMO) (NOAA – ESRL 2012b)	AMO is characterised by a 60- to 90-year oscillation (Knudsen *et al.*, 2011).	A positive AMO anomaly is associated with warmer winters and lower rainfall at the study site (Knight *et al.*, 2006).

series). Therefore significant correlations among the global climate oscillations occurred only if they existed for nearly the entire time series.

To examine correlations between the global climate oscillations and local climatic conditions, we sought the longest possible meteorlogical records located near the four catchments in the TLW: the National Climatic Data Center's Global Historical Climatology Network v2 (GHCN-Monthly) station at Sault Ste. Marie, Michigan (Station identifier 42572734000, with a record from 1889 to 2011) and Environment Canada's station at Sault Ste. Marie, Ontario (Station identifier 71260, with a record from 1962 to 2011). Furthermore, data from the Michigan station were split into two periods (1901-1963 and 1964-2010) to compare the relationship between AMO and temperature/precipitation during distinct cycles of the estimated 60- to 90-year AMO global climate oscillation.

3.4 Results

There were significant non-stationary signals in water yields. Catchments showed significant negative linear trends in the yearly water yield time series over the past 28 years (Figure 3.7). The rate of decline in water yield was highest (-14.6 mm/yr) in the catchment with lower water loading and lower water storage capacity (c35) ($r^2 = 0.52$, $p < 0.001$) and nearly as high (-13.0 mm/yr) in the catchment with similar water loading but higher water storage capacity (c38) ($r^2 = 0.44$, $p < 0.001$). In contrast, the rate of decline in water yields was lowest (no significant signal) in the catchment with higher water loading and lower water storage capacity (c47) ($r^2 = 0.04$, $p = 0.306$), and higher (-8.9 mm/yr) in the catchment with higher water loading and higher water storage capacity (c50,) ($r^2 = 0.18$, $p < 0.05$), but not as high as the lower water loading catchments. Non-stationary signals were influenced more by water loading than by water storage capacity.

There were also significant stationary signals in water yields. The sequence of steps for detecting significant stationary signals is illustrated for c35 in Figures 3.8, 3.9 and 3.10. After removing the linear trend in the water yield data of each catchment (Figures 3.8A-3.10A), wavelet transforms (Figures 3.8B-3.10B) and peak analysis (Figures 3.8C-3.10C) revealed periods that explained significant amounts of variance in the detrended water yield. Sine curves were modeled to the detrended water yield data

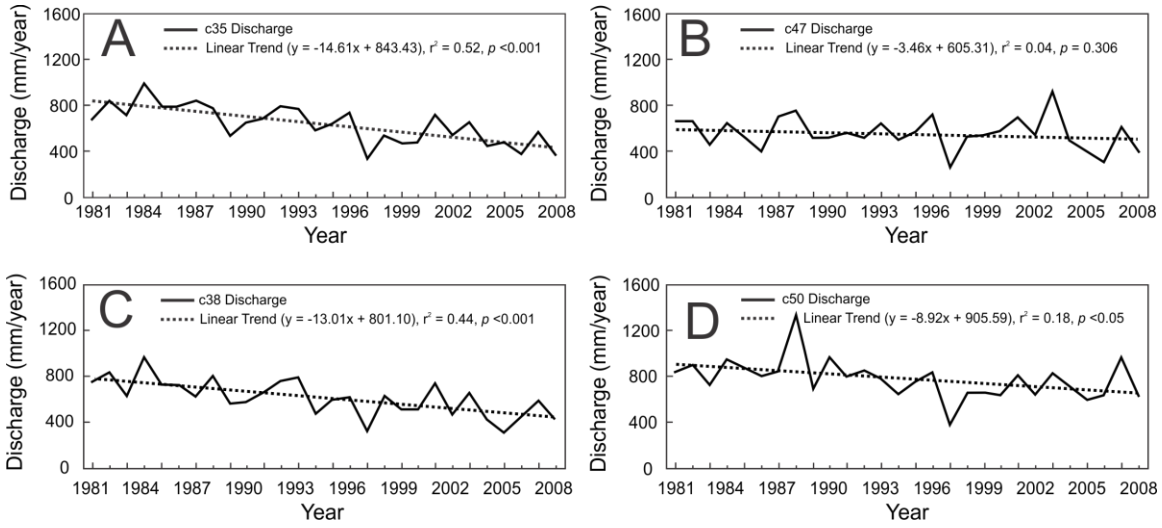


Figure 3.7: Non-stationary trends in water yield for (A) c35, (B) c47, (C) c38 and (D) c50.

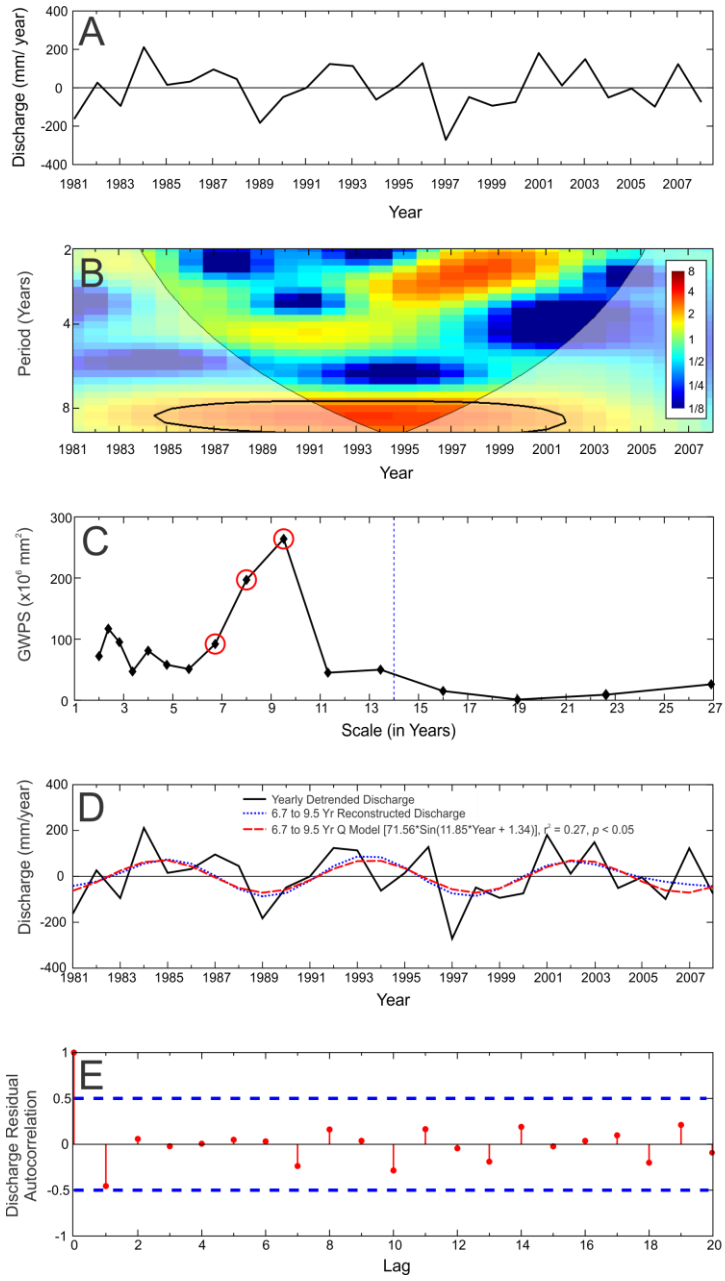


Figure 3.8: Stationary trend analysis for the first signal in c35: (A) c35 yearly detrended water yield data, (B) wavelet transform (from Equation 3.6) of c35 water yield data [strong and weak contributions to the power spectrum are indicated by warm (red) colours and cold (blue) colours, respectively, on a logarithmic scale; the thin solid line represents the cone of influence, the thick solid lines show the 95% significance level], (C) scale selection based on Global Wavelet Power Spectrum [the dotted line at 14 years indicates the cutoff for selecting periods of signals (half the 28-year time series)], (D) modeling the sine function to the detrended water yield data, and (E) Auto-correlation function analysis for the residuals between the observed and modeled water yield. Subsequent steps repeated the same process until fitting scales were no longer statistically significant.

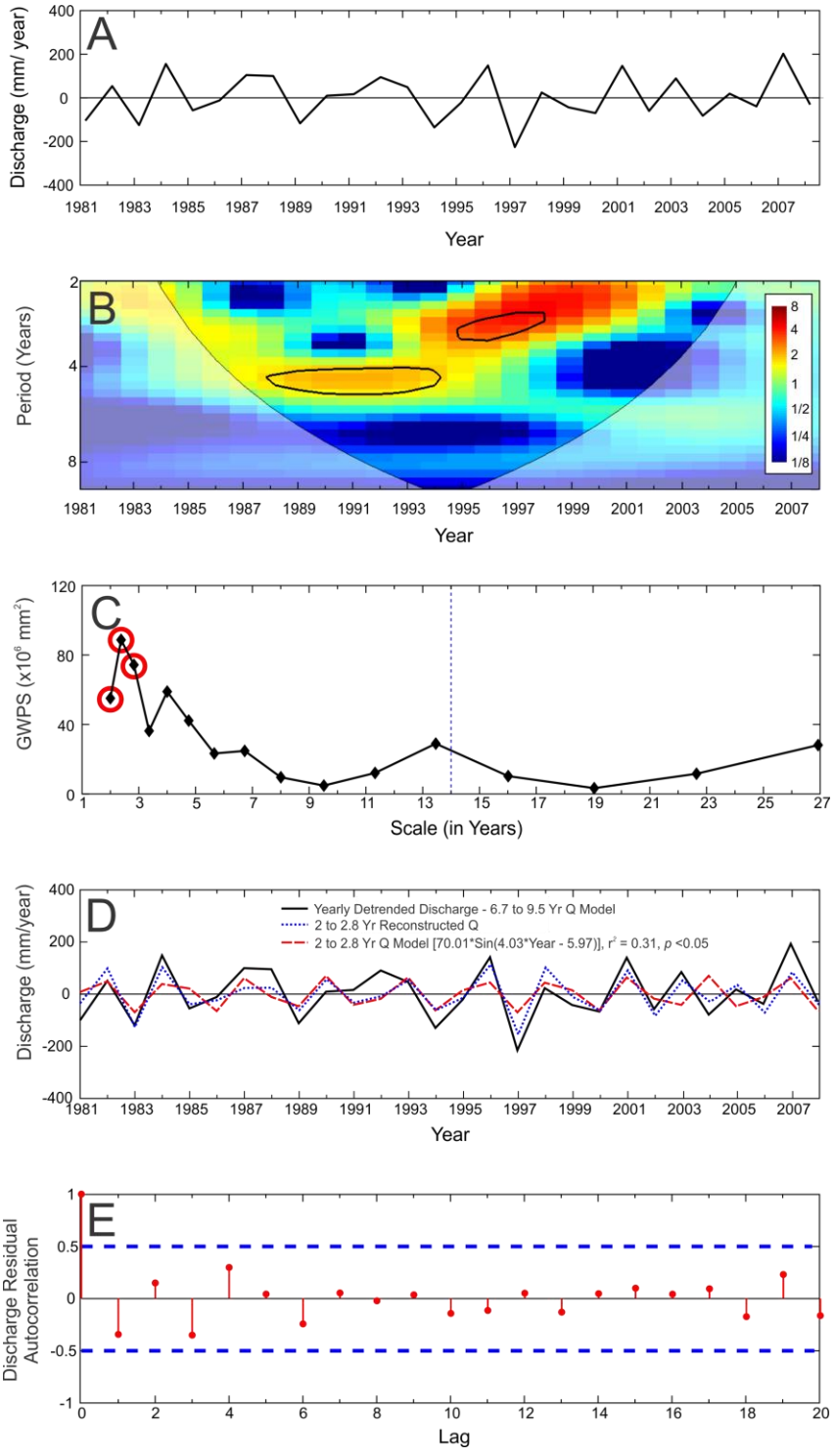


Figure 3.9: Stationary trend analysis for the second signal in c35: (A) c35 yearly detrended water yield data, (B) wavelet transform of c35 water yield data, (C) scale selection based on Global Wavelet Power Spectrum (D) modeling the sine function to the detrended water yield data, and (E) Auto-correlation function analysis for the residuals between the observed and modeled water yield.

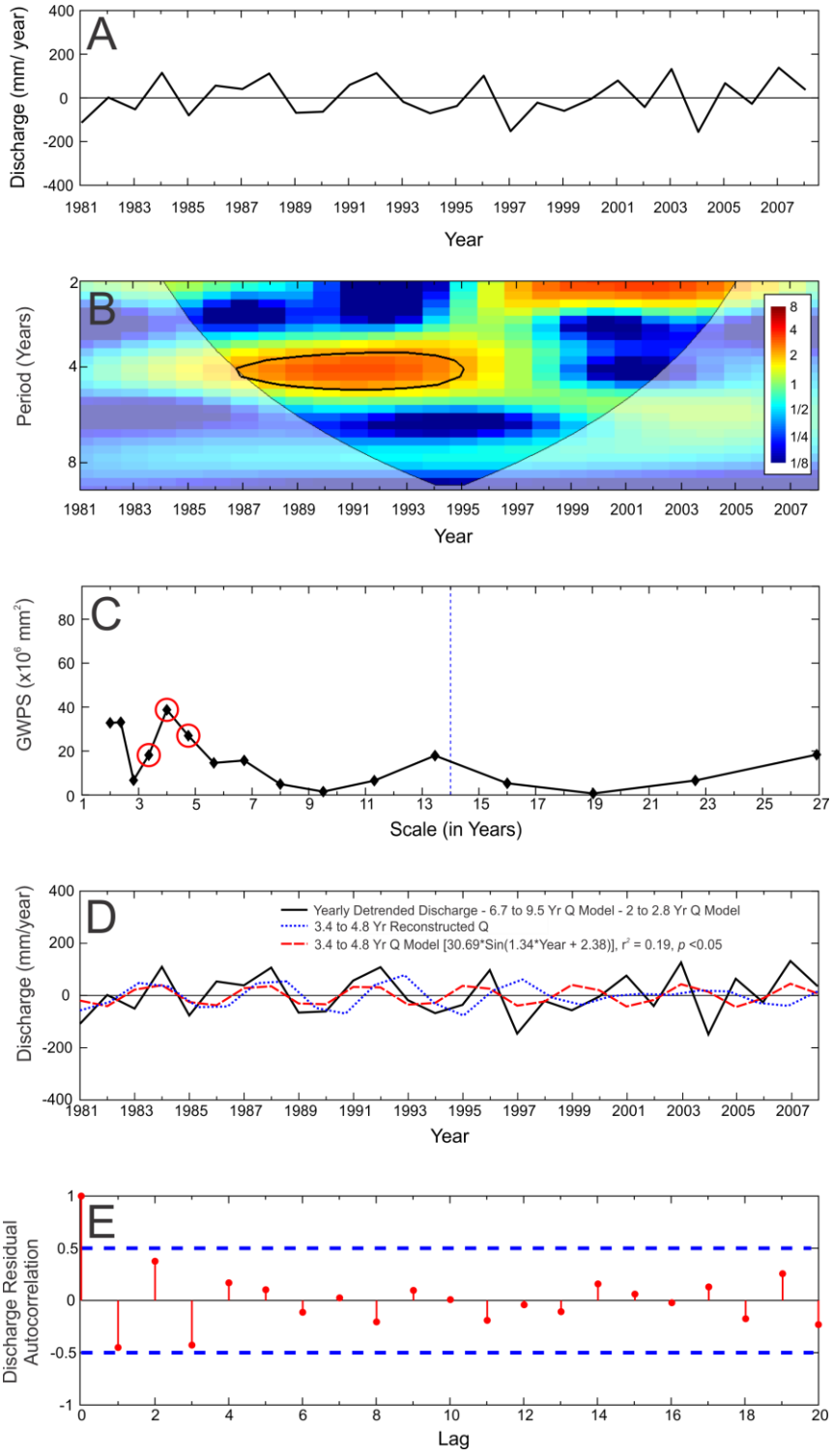


Figure 3.10: Stationary trend analysis for the third signal in c35: (A) yearly detrended water yield data, (B) wavelet transform of c35 water yield data, (C) scale selection based on Global Wavelet Power Spectrum (D) modeling the sine function to the detrended water yield data, and (E) Auto-correlation function analysis for the residuals between the observed and modeled water yield.

(Figures 3.8D-3.10D), and the autocorrelation function values from the residuals were all between 0.5 and -0.5 (Figures 3.8E-3.10E), indicating no significant autocorrelation with 95% confidence. However, the residuals suggested that periodic characteristics remained, so the framework was applied until fitted scales were no longer statistically significant.

Each of the four catchments showed three significant stationary signals with the same periods (*i.e.*, 2 to 2.83 years, 3.36 to 4.76, and 6.73 to 9.51 years), except for c50, which had a stationary signal of 5.66 to 8 years instead of 6.73 to 9.51 years (Tables 3.3 and 3.4). The relative dominance of these three periods varied among the catchments. The two catchments with lower water storage capacity (c35, c47) showed the same sequence of the 6.73 to 9.51 period detected first, followed by the 2 to 2.83 period, and then the 3.36 to 4.76 years period. In contrast, the two catchments with higher water storage capacity (c38, c50) showed a different sequence from both the lower water storage capacity catchments and each other.

The 2 to 2.83 year signal was detected first in both c38 and c50, but the sequence was 6.73 to 9.51 years, and then 3.36 to 4.76 years in c38 and the opposite in c50 (Table 3.3). Signals with shorter periods dominated the detrended water yield time series in catchments with high water storage capacity, whereas the signals with longer periods dominated the time series in the catchments with small wetlands.

The combination of non-stationary and stationary signals explained the majority of variation in water yields for each of the four catchments: 81% (c35), 76% (c38), 56% (c47), and 63% (c50) (Figure 3.11, Table 2.4). For catchments with lower water loading (c35, c38), the non-stationary signal was stronger than the combination of stationary signals. For c35 (low water storage capacity), the non-stationary signal explained 52% of the temporal variation in water yields, whereas the stationary signals together explained an additional 29%. For c38 (high water storage capacity), the relative importance of the two signals shifted slightly, with the non-stationary signal explaining 44% of the temporal variation in water yields, whereas the stationary signals together explained an additional 32%. In contrast, for catchments with higher water loading (c47, c50), the non-stationary signals were lower than the combination of stationary signals. For c47 (low water storage capacity), the non-stationary signal explained no variation in water yields, whereas the stationary signals explained 56% of the variation in water yields. Similarly,

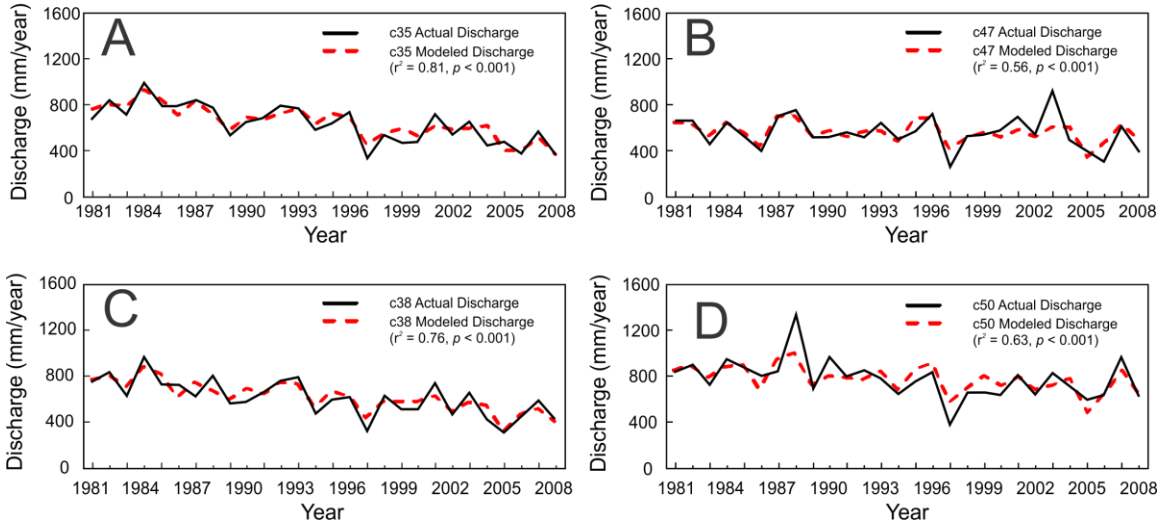


Figure 3.11: Time series for the observed and modelled yearly water yields over the study time period for the catchments (A) c35, (B) c47, (C) c38, and (D) c50.

Table 3.3: Global wavelet power spectrum (GWPS) values of water yield generated from Equation 3.6 in catchments c35 (A), c38 (B), c47 (C) and c50 (D). The detrended water yield was used to generate the first signal from the wavelet transform. Water yield used for subsequent signals is the difference between water yield from the previous step and modeled water yield at the step of investigation. The highlighted values indicate the p*eak GWPS values selected as the stationary signal* in each step. See Figures 3.5-3.7 for sample peak selection.

A – c35

Level	Period (Years)	Stationary Signal 1	Stationary Signal 2	Stationary Signal 3	Stationary Signal 4
1	2	72,742,838.99	52,559,388.15	32,799,491.02	27,446,013.24
2	2.38	117,046,896.11	86,142,685.27	33,099,842.66	27,794,912.71
3	2.83	95,367,771.17	71,792,782.62	6,696,663.58	4,232,105.67
4	3.36	47,741,733.74	33,848,471.69	18,165,496.28	2,583,822.86
5	4	81,074,024.78	56,401,908.76	38,739,832.75	10,806,888.73
6	4.76	58,234,715.87	39,741,839.00	26,980,918.02	17,925,972.20
7	5.66	51,335,670.69	20,873,913.33	14,592,670.07	10,317,740.44
8	6.73	92,205,150.66	22,340,644.25	15,694,400.58	11,632,192.79
9	8	197,102,724.56	7,197,672.74	4,958,396.31	3,739,473.63
10	9.51	264,112,013.58	2,417,747.20	1,526,098.69	1,211,442.02
11	11.31	45,201,766.78	9,685,764.83	6,538,213.21	5,017,783.08
12	13.45	50,842,798.77	26,525,867.07	17,936,846.25	13,754,007.79
13	16	15,053,551.08	7,880,583.29	5,330,643.82	4,090,358.01
14	19.03	1,053,004.09	969,869.79	691,324.14	586,426.30
15	22.63	9,521,102.60	9,229,953.56	6,601,178.77	5,632,752.84
16	26.91	26,474,669.50	25,665,094.95	18,355,442.43	15,662,607.47

B – c38

Level	Period (Years)	Stationary Signal 1	Stationary Signal 2	Stationary Signal 3	Stationary Signal 4
1	2	106,001,656.86	65,500,872.94	48,315,829.46	37,976,716.25
2	2.38	176,776,699.36	73,227,373.56	56,593,670.61	41,443,685.28
3	2.83	163,347,155.50	29,417,499.54	24,119,780.39	11,899,508.67
4	3.36	94,230,821.75	53,245,045.28	40,833,464.41	7,754,080.30
5	4	94,604,196.33	73,783,452.65	46,187,212.25	10,742,035.21
6	4.76	72,194,221.50	55,545,861.64	29,425,631.37	15,231,178.55
7	5.66	63,011,768.80	51,616,100.99	17,665,216.18	9,873,949.32
8	6.73	121,492,134.14	95,498,143.63	25,383,305.84	15,629,556.19
9	8	135,031,783.10	99,286,457.90	8,232,465.30	5,436,313.37
10	9.51	153,895,573.39	110,475,543.03	1,763,117.56	1,617,943.44
11	11.31	18,359,957.45	12,445,607.56	2,421,615.86	1,806,002.61
12	13.45	7,256,840.78	3,152,322.63	6,311,266.97	4,617,283.87
13	16	2,184,458.85	974,902.91	1,906,954.17	1,391,336.79
14	19.03	967,872.18	978,304.53	871,358.10	562,080.93
15	22.63	9,648,040.81	9,846,927.33	8,690,551.80	5,593,546.42
16	26.91	26,827,644.36	27,380,675.06	24,165,220.47	15,553,590.24

Table 3.3. (*Continued*)

C – c47

Level	Period (Years)	Stationary Signal 1	Stationary Signal 2	Stationary Signal 3	Stationary Signal 4
1	2	157,378,239.90	130,985,771.78	103,534,002.71	64,157,739.24
2	2.38	238,019,826.75	197,689,749.78	93,014,746.78	62,664,581.73
3	2.83	236,765,895.02	197,011,424.17	51,846,652.20	18,944,890.45
4	3.36	193,389,465.55	160,463,022.85	105,140,813.67	10,874,058.26
5	4	197,170,649.88	162,055,920.48	129,181,221.50	4,760,670.53
6	4.76	66,672,825.22	44,838,963.34	37,913,995.80	9,819,489.91
7	5.66	161,946,538.57	25,973,696.09	23,481,299.18	18,331,077.33
8	6.73	423,081,833.54	45,421,536.92	39,531,938.84	28,953,133.67
9	8	207,480,165.06	81,090,984.09	62,461,506.46	46,627,686.57
10	9.51	135,564,307.08	110,929,919.49	83,073,858.35	62,119,444.50
11	11.31	92,175,460.96	79,159,848.22	56,239,813.54	39,268,364.16
12	13.45	220,101,911.49	190,401,174.75	134,047,200.73	92,409,319.83
13	16	65,257,544.17	56,448,360.73	39,748,733.61	27,397,450.38
14	19.03	5,489,763.99	4,678,540.27	3,451,728.12	2,293,780.81
15	22.63	50,655,197.95	43,105,691.36	31,948,504.04	21,155,114.85
16	26.91	140,853,402.31	119,861,011.50	88,836,994.23	58,824,563.32

D – c50

Level	Period (Years)	Stationary Signal 1	Stationary Signal 2	Stationary Signal 3	Stationary Signal 4
1	2	347,530,485.98	237,768,185.59	179,026,156.86	153,497,536.92
2	2.38	392,660,317.07	129,919,942.14	91,315,689.24	78,293,766.94
3	2.83	437,477,169.71	60,073,959.61	21,922,598.28	18,783,311.38
4	3.36	300,915,850.89	178,837,671.90	16,154,965.00	13,633,355.93
5	4	323,010,771.88	248,900,020.12	11,055,093.84	7,544,101.66
6	4.76	110,746,232.35	78,420,959.73	18,871,232.68	7,017,206.14
7	5.66	100,538,905.89	81,222,487.51	50,338,414.75	2,258,900.74
8	6.73	176,988,435.47	165,444,943.04	113,468,010.56	623,426.91
9	8	67,184,433.77	65,711,576.85	43,635,232.31	2,342,173.59
10	9.51	53,122,685.79	46,737,650.63	30,147,648.03	14,541,131.78
11	11.31	309,051,767.56	215,367,355.62	153,370,958.01	122,549,864.32
12	13.45	853,003,199.84	591,660,421.54	422,246,007.10	340,091,344.81
13	16	253,770,934.12	176,267,394.30	125,815,125.46	101,392,846.08
14	19.03	38,213,673.55	31,454,954.80	22,839,047.47	19,529,737.85
15	22.63	368,033,540.57	305,451,014.96	221,951,169.09	190,267,619.61
16	26.91	1,023,365,499.83	849,346,601.61	617,164,331.78	529,064,070.81

Table 3.4: Amount of variation explained by and magnitude of change of non-stationary (linear trends) and stationary (oscillating cycles) signals in yearly water yield export data from catchments c35, c38, c47 and c50 in the Turkey Lakes Watershed. For variation, data reported are R^2 values (with $p < 0.05$; NS indicating not significant relationships). For magnitude, data reported are rate of change in export (mm/year) for non-stationary signals and amplitude (mm/year) for stationary cycles.

Water Export	**C35**	**C38**	**C47**	**C50**
Variation				
Non-stationary signal (%)	52	44	NS	18
Trend + Cycle 1 (%)	*65*	*59*	*19*	*39*
Trend + Cycle 1 + 2 (%)	*76*	*68*	*38*	*56*
Trend + Cycle 1 + 2 + 3 (%)	*81*	*76*	*56*	*63*
Stationary signal (%)*	29	32	56	45
Magnitude				
Trend (slope) (mm/yr)	-15	-13	NS	-9
Cycles (amplitude) (mm/yr)	±72	±83	±79	±100

for c50 (high water storage capacity), the non-stationary signal explained 18% of the variation in water yields, while the stationary signals explained an additional 45% of the variation in water yields (Table 3.4). The modeled water yields represented the observed water yields in each of the four catchments; however, the modeled water yield sometimes failed to capture peak water yield, particularly in the catchments with high water loading, c47 (e.g., 2003 peak) and c50 (e.g., 1997 peak) (Figure 3.10).

The wavelet cross coherence plots revealed complex interactions between water yield and global climate oscillations (Figures 3.12-3.15). For each of the four catchments, there were significant correlations between each of global climate oscillations and water yields: (a) MEI was highly correlated to water yields at periods of 2 to 3.5 years, particularly in the 1990s (coincident with PDO), with greater MEI resulting in lower water yields (Figure 3.12A-3.15A); (b) AMO was correlated to water yields at periods of 3 to 5 years, although the correlations were stronger at the beginning of the time series compared to the end of the time series, with higher AMO resulting in lower water yields (Figure 3.12B-3.15B); (c) NAO was correlated to water yields at periods of 3 to 4.5 years, particularly in the first half of the time series; however, the nature of the correlation was unclear (arrows in different directions) (Figures 3.12C-3.15C); and (d) PDO was highly correlated to periods of 2 to 3.5 years, particularly during the five year window from 1998 to 2003, with higher PDO resulting in lower water yields (Figures 3.12D-3.15D).

There were significant relationships among major climatic oscillation indices (i.e., MEI, AMO, NAO, and PDO) (Table 3.5). The Pearson product moment correlation between the annual average values of the climate oscillations revealed significant correlations between the MEI and PDO ($p<0.001$) and the NAO and PDO ($p<0.05$). Of the 12 stationary signals observed in water yield data, six were significantly correlated with a climatic index (Table 3.6). MEI was the index most often strongly correlated with water yield (seven times total with four correlations being significant).

Comparing meteorological records at nearby stations with the major climatic oscillation indices, only the AMO index was significantly linked to annual temperature and precipitation at the TLW meteorological station. Temperature and the AMO index were positively linked from 1981 to 2008 ($r^2 = 0.46$, $p < 0.001$). This positive relationship

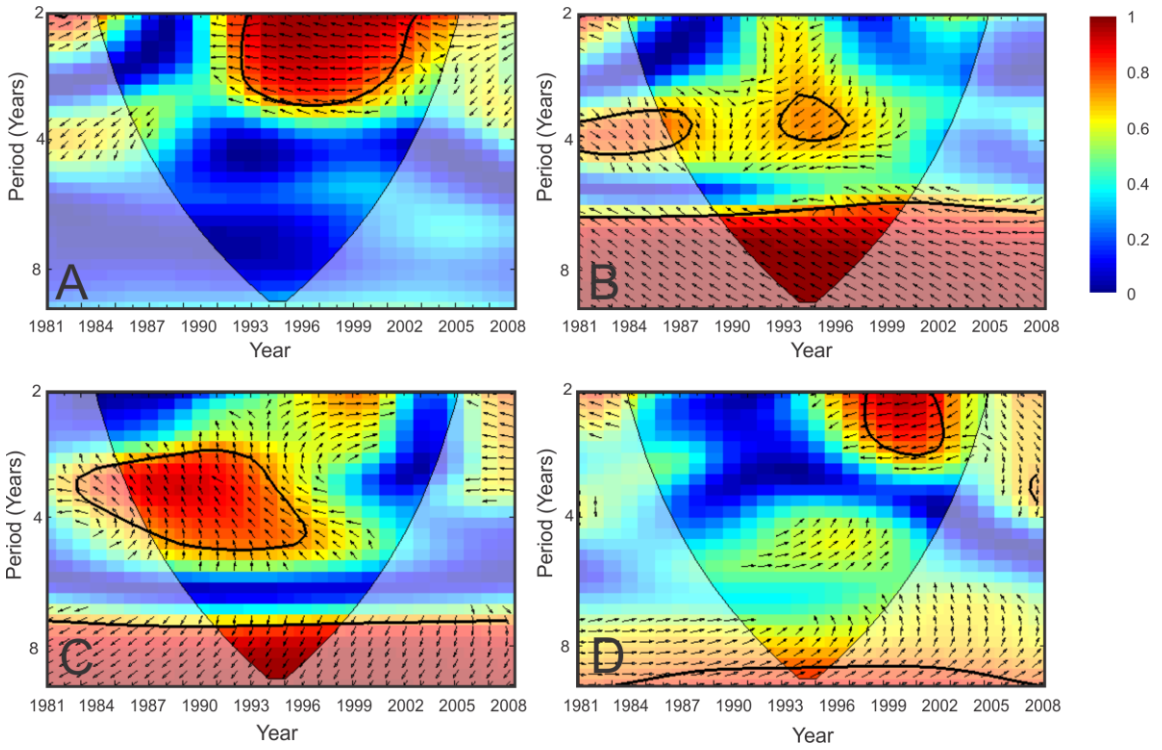


Figure 3.12: Cross coherence plots using Morlet mother wavelets to generate wavelet power spectra (from Equation 11) show correlations at each period between yearly water yield of c35 and (A) MEI, (B) AMO, (C) NAO, and (D) PDO. The thin solid line represents the cone of influence, the thick contours indicate the 95% significance level, arrows show the relative phase relationship (left arrows for negative correlations and right arrows for positive correlations). Warm colours indicate strong correlations and cool colours indicate weak relationships along a linear scale.

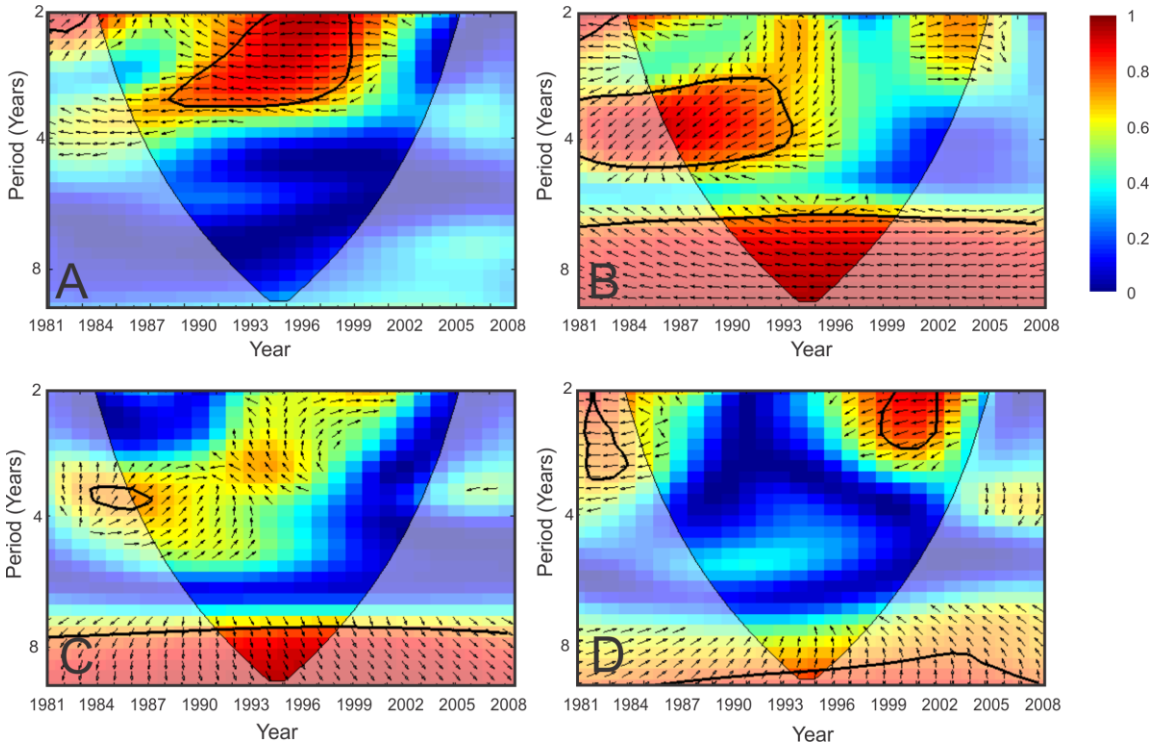


Figure 3.13: Cross coherence plots using Morlet mother wavelets to generate wavelet power spectra (from Equation 11) show correlations at each period between yearly water yield of c38 and (A) MEI, (B) AMO, (C) NAO, and (D) PDO. The thin solid line represents the cone of influence, the thick contours indicate the 95% significance level, arrows show the relative phase relationship (left arrows for negative correlations and right arrows for positive correlations). Warm colours indicate strong correlations and cool colours indicate weak relationships along a linear scale.

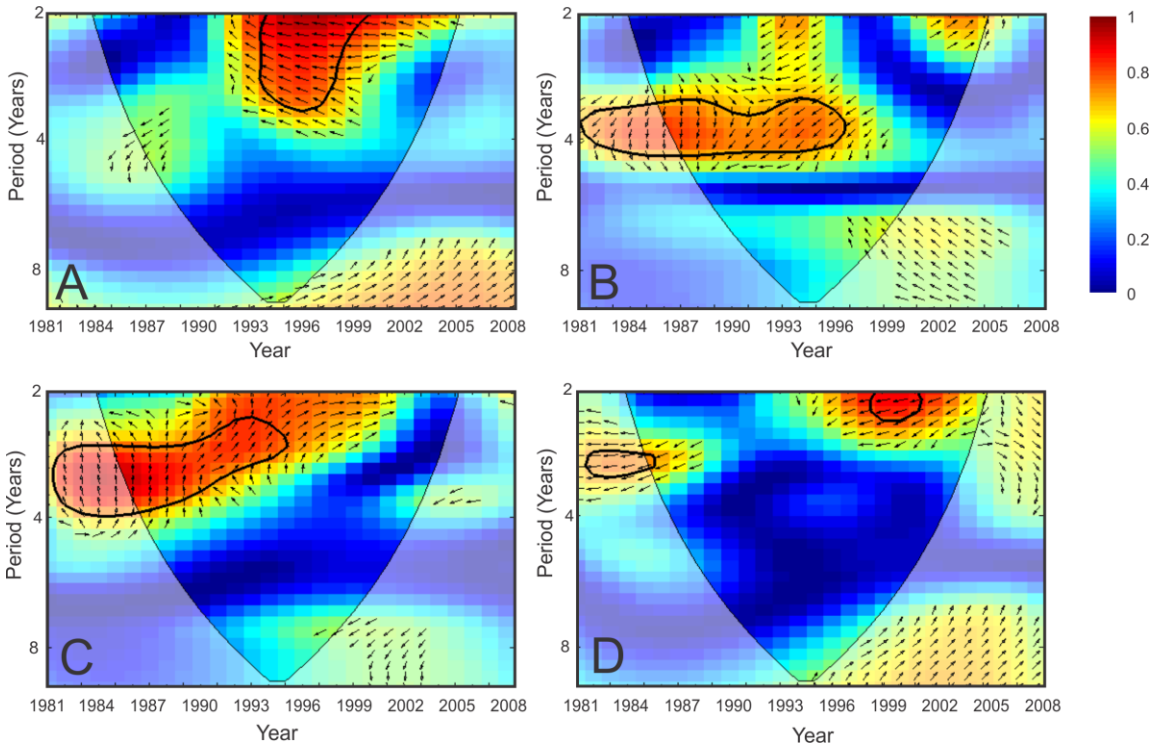


Figure 3.14: Cross coherence plots using Morlet mother wavelets to generate wavelet power spectra (from Equation 11) show correlations at each period between yearly water yield of c47 and (A) MEI, (B) AMO, (C) NAO, and (D) PDO. The thin solid line represents the cone of influence, the thick contours indicate the 95% significance level, arrows show the relative phase relationship (left arrows for negative correlations and right arrows for positive correlations). Warm colours indicate strong correlations and cool colours indicate weak relationships along a linear scale.

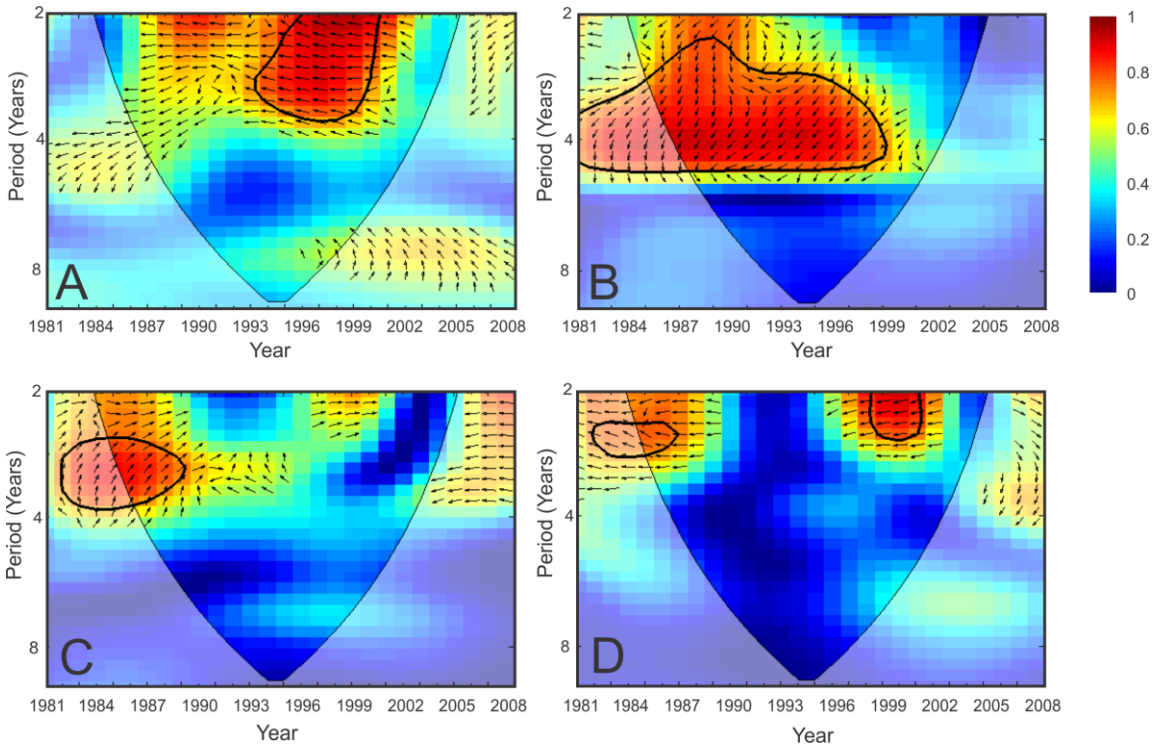


Figure 3.15: Cross coherence plots using Morlet mother wavelets to generate wavelet power spectra (from Equation 11) show correlations at each period between yearly water yield of c50 and (A) MEI, (B) AMO, (C) NAO, and (D) PDO. The thin solid line represents the cone of influence, the thick contours indicate the 95% significance level, arrows show the relative phase relationship (left arrows for negative correlations and right arrows for positive correlations). Warm colours indicate strong correlations and cool colours indicate weak relationships along a linear scale.

Table 3.5: Pearson Product Moment Correlations between the annual average values of Multivariant El Niño Southern Oscillation (ENSO) Index (MEI), Atlantic Multidecadal Oscillation (AMO), Northern Atlantic Oscillation (NAO), and Pacific Decadal Oscillation (PDO) (* indicates $p<0.05$; *** indicates $p<0.001$).

	MEI	AMO	NAO	PDO
MEI	-	-0.152	0.011	0.600***
AMO	-	-	-0.387	-0.314
NAO	-	-	-	-0.387*
PDO	-	-	-	-

Table 3.6: Correlations between climatic indices and the identified stationary signals for four catchments in the Turkey Lakes Watershed demonstrating the indices that are the most strongly correlated.

Catchment	Stationary Signal	Periods (years)	Strongest Correlated Index	r^2 (Direction of Correlation)	*p*
c35	1	6.73 to 9.51	PDO	0.220 (+)	**0.013**
	2	2 to 2.83	MEI	0.026 (-)	0.414
	3	3.36 to 4.76	MEI	0.150 (-)	**0.039**
c38	1	2 to 2.83	NAO	0.010 (-)	0.619
	2	6.73 to 9.51	AMO	0.250 (-)	**0.007**
	3	3.36 to 4.76	MEI	0.240 (-)	**0.009**
c47	1	6.73 to 9.51	NAO	0.009 (-)	0.636
	2	2 to 2.83	MEI	0.014 (-)	0.552
	3	3.36 to 4.76	MEI	0.210 (-)	**0.015**
c50	1	2 to 2.83	MEI	0.012 (-)	0.575
	2	3.36 to 4.76	MEI	0.210 (-)	**0.014**
	3	5.66 to 8	PDO	0.054 (-)	0.232

was confirmed using the longer records of the Sault Ste. Marie, Michigan station (1889-2010, $r^2 = 0.19$, $p < 0.001$) and the Sault Ste. Marie, Ontario station (1962-2010; $r^2 = 0.35$, $p < 0.001$). Precipitation and the AMO index were negatively linked at the TLW station ($r^2 = 0.34$, $p < 0.001$), though no significant relationships were observed with data from the Michigan or Ontario stations.

Splitting the Michigan meteorological data according to distinct AMO cycles (1901-1963 and 1964-2010) revealed a change in the relationships. Split temperature records confirmed consistent positive relationships between the AMO index and temperature (Figure 3.16A), but split precipitation records indicated that from 1901 to 1963, AMO was significantly positively correlated to precipitation ($r^2 = 0.16$, $p < 0.05$), but AMO was negatively correlated with precipitation during 1964 to 2010 ($r^2 = 0.08$, $p < 0.05$) (Figure 3.16B).

Looking at the complete AMO cycle from 1901 to 1963 versus temperature (Figure 3.16A), the minimum AMO value of -0.39 corresponds to an interpolated temperature value of 3.81°C and the maximum AMO value of 0.36 corresponds to a temperature value of 4.96°C. The difference of 1.15°C over 31 years (half the AMO period) indicates that 0.037°C per year in climate warming can be explained by a shift from a low point in the AMO cycle to a high point, about 55% of the observed 0.067 °C per year rate observed in the TLW (Figure 3.3).

3.5 Discussion

This paper examined the effects of changing climatic conditions on water yields from headwater catchments in a natural (generally undisturbed) northern forested landscape. Northern latitudes are expected to see substantial environmental changes based on projected climate change scenarios (Carey *et al.*, 2010). We were interested to see if and how these effects are already being manifested. By focusing on headwater catchments on natural landscapes, we examined the hydrological systems that are most sensitive and that have the potential to serve as early warning sentinels of climate change effects to more regional catchments, including those that provide water supplies to downstream communities.

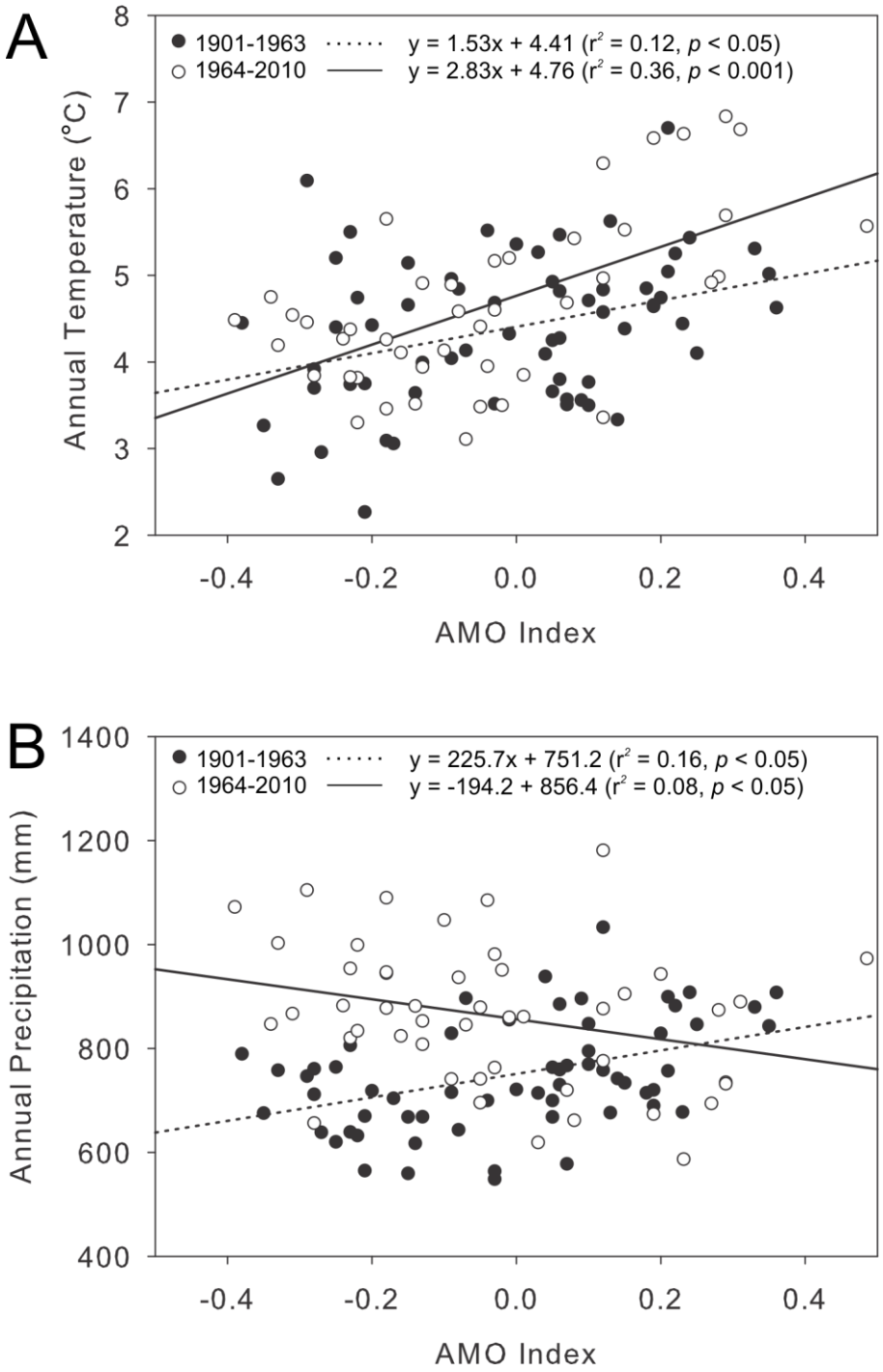


Figure 3.16: Regressions between the AMO Index and the mean annual precipitation (A) and temperature values (B) from the Sault Ste. Marie, Michigan weather station during two distinct AMO cycles (1901-1964 and 1964-2010).

3.5.1 Climate change has effects on water yields

The analytical framework outlined in this paper (Figure 3.5) enabled the detection of climate signals in the water yields of four catchments in the Turkey Lakes Watershed (TLW). The framework detected non-stationary linear trends, then after removing these trends, detected stationary non-linear cycles caused by climate oscillations. Without applying this framework, the non-stationary climate signals would not have been identified, discriminated, nor quantified from the original time series of water yields.

Climate had a substantial non-stationary effect on water yields. A shift to warmer and drier conditions resulted in a linear decline in water yields that ranged from 0% (c47) to 52% (c35). This decline of yearly water yield may be related to a unidirectional change towards warmer and drier conditions over the past 28 years. However, climate also had a substantial stationary effect on water yields. Multiple scales of nested periodic cycles were detected in the water yield data, explaining variation in addition to the non-stationary trends that ranged from c35 (29%) to c47 (56%). The three periodic cycles, which occurred from 2 to 2.83 years, 3.36 to 4.76 years, and 6.73 to 9.51 years, were found in all catchments, except for c50, where the longest periodic trend was 5.66 to 8.00 years rather than 6.73 to 9.51 years. A comparison of the periods from the wavelet analysis (Figures 3.8-3.10, Table 3.3) and the wavelet cross coherence analysis (Figures 3.12-3.15) suggests that the 2 to 2.83 year signal was influenced by the MEI and PDO; the 3.36 to 4.76 year signal was influenced by the AMO; and the 6.73 to 9.51 year signal was influenced partially by the NAO, though it was only strongly correlated to water yields for the higher water loading catchments, c35 and c38. A 28-year dataset is particularly short for wavelet analysis. It is likely that signals with longer periods are also present, but they could not be detected with the data available.

3.5.2 Climate change results in differential responses among catchments

There were substantial differences in the non-stationary rate of decline and a marginal difference in stationary oscillations in water yield signals among the catchments, despite their close proximity (Figure 3.7, Table 3.4). Catchments with lower water loading were more sensitive to the non-stationary climate signals (Table 3.4), showing declines in water yields of -14.6 mm/year (c35) and -13.0 mm/year (c38). Our findings suggest that

there is a higher rate of change in net water loading (precipitation *minus* evapotranspiration and sublimation) on sites that experience less overall water loading, leading to a higher rate of change in catchment water yields at low water loading sites compared to higher water loading sites.

Catchments with wetlands formed by topographic depressions and/or flats store water (Lindsay *et al.*, 2004; Creed *et al.*, 2003; 2008). Catchments with higher water storage capacity buffered the effects of climate warming. The declines in water yield in catchments with lower water loading (c35 and c38) were of a greater magnitude than in those with higher water loading (c47 and c50). For the catchments with lower water loading (c35, c38), a lower water storage capacity increased the amount of variation explained in water yields attributed to non-stationary signals (52% for c35 *versus* 44% for c38), but increased the amount of model variation attributed to stationary signals (an additional 29% for c35 *versus* 32% for c38). For the catchments with higher water loading (c47, c50), a lower water storage decreased the amount of variation explained in water yields attributed to non-stationary signals (0% for c47 *versus* 18% for c50), and increased the amount of model variation attributed to stationary signals (an additional 56% for c47 and 45% for c50). Higher water storage capacity appeared to reduce the effects of shorter periods on discharge, perhaps reflecting the buffering capacity of storage capacity on water discharge fluctuations associated with shorter-term periods, but not longer term periods.

Our study indicates that drier (lower water loading) catchments with minimal water storage capacity may be more responsive to climate change in humid regions. The catchment with the lower water loading and lower water storage capacity (c35) was the most sensitive to the non-stationary signal (decline in water yield of -14.6 mm/year) and was the catchment for which we were able to explain the most variation (81%) in water yields through a combination of the non-stationary and stationary signals. In contrast, the catchment with higher water loading and lower water storage capacity (c47), was the least sensitive to the non-stationary signal (no significant decline in water yields) and only 56% of the variation in water yields could be explained through a combination of non-stationary and stationary signals. It is difficult to compare our findings with similar studies in the region or elsewhere because there are few studies that investigate the effect

of catchment water loading on water yield responses to climate change. Nonetheless, our study clearly shows that the climatic characteristics of a region within which a catchment is located must be considered prior to selecting the best sentinel for climate change.

Potential water storage impacted the amplitude of stationary signals, as detailed in the conceptual framework in Figure 3.17. In the low water storage catchments (c35 and c47), there is minimal storage, so the amplitude of the stationary signals should not fluctuate greatly. In the high water storage catchments, low water loading (e.g., c38) should result in less discharge because water is stored (bucket empty), while high water loading (e.g., c50) should result in more discharge because the wetland is filled (bucket full). Accordingly, the amplitude of the stationary signals in high water storage catchments is larger, showing a greater response to stationary signals, which could not be detected when comparing average water yields (e.g., c35 and c38 in Figure 3.4).

3.5.3 Global drivers of local responses in water yields

In the last few decades, scientists have recognized the effects of global climate oscillations on regional climate, particularly on the interannual variability of temperature and precipitation in regions thousands of kilometres away from the sites of the initial fluctuations (Ropelewski and Halpert, 1996; Shabbar *et al.*, 1997; Ionita *et al.*, 2012; Zhou *et al.*, 2012). Furthermore, the effects of global climate oscillations on hydrology and associated hydroecological processes of water bodies are well documented (Foley *et al.*, 2002; Kawahata *et al.*, 2003; Kondrashov *et al.*, 2005; Labat, 2008; Keener *et al.*, 2010). We contributed to this body of knowledge by exploring the effects of global climate oscillations on headwater catchment water yields.

The non-stationary trend was linked to climate warming. One of the original assumptions of this research is that at least part of the observed increase in temperature in the TLW (0.067 °C per year, Figure 3.3) is being caused by anthropogenic climate warming. We were able to show that the AMO index and temperature are significantly correlated both using the TLW data and the longer-term data from the Sault Ste. Marie, Michigan weather station over two distinct AMO cycles (1901 to 1963 and 1963 to 2010). By using the longer-term data, we were able to show that temperature at the minimum AMO values increases by approximately 0.037°C per year until the maximum AMO

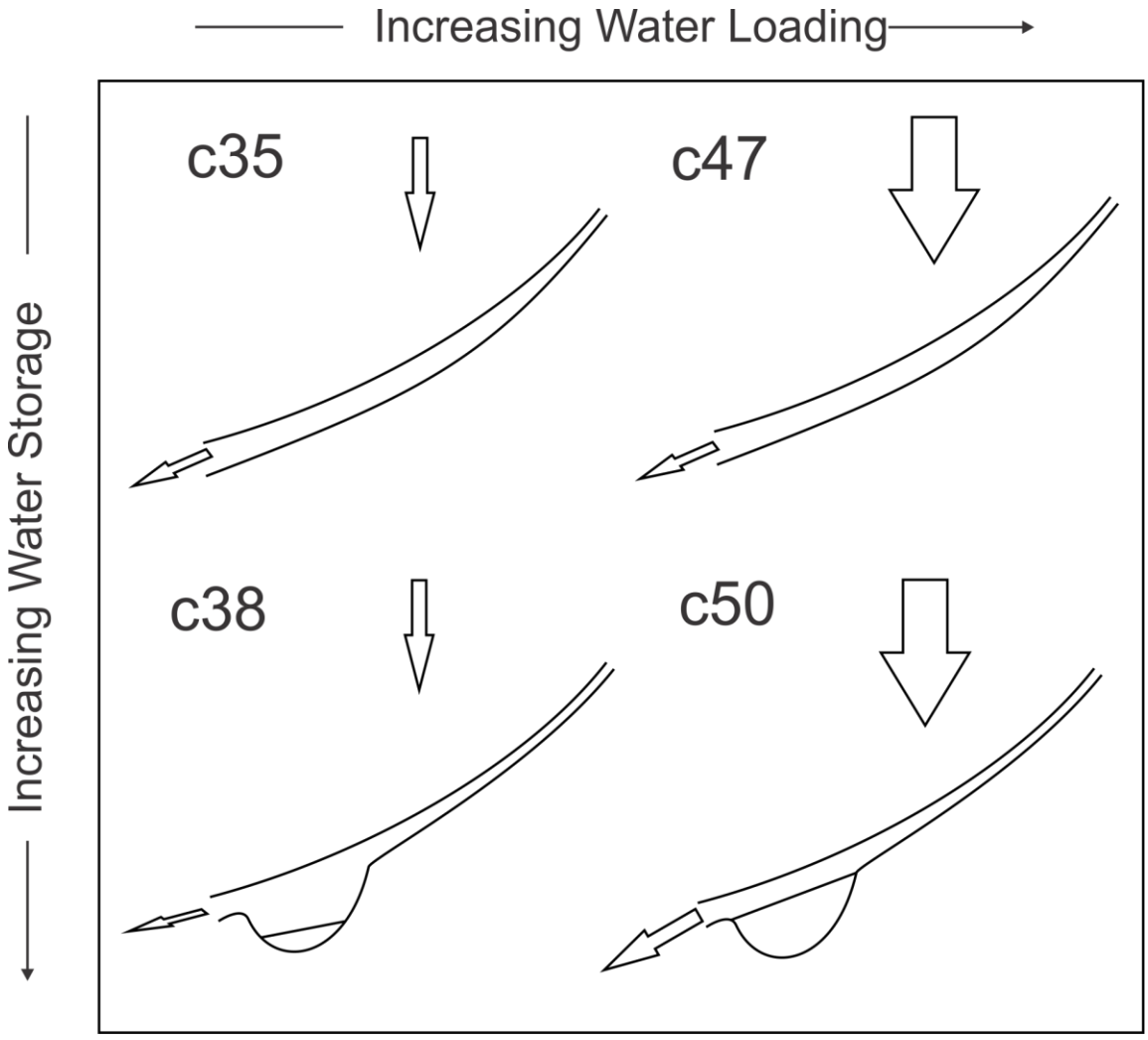


Figure 3.17: Conceptual model of role of potential water storage on amplitude of stationary signals water yield time series.

values (approximately 30 years). Coincidentally, the TLW data record (1981 to 2008) corresponded with an AMO minimum to maximum half cycle (Figure 3.6), meaning that the TLW was being affected both by strong non-stationary and stationary signals. We estimate that of the 0.067 °C per year increase in temperature observed from 1981 to 2008, 0.037°C per year can be explained by the AMO index (from interpolated temperatures of 3.81°C at the minimum AMO value and 4.96°C at the maximum value over a 31-year half-cycle, Figure 3.16A), leaving 0.030°C for other causes, including anthropogenic climate change. It is possible that some of the increase in temperature ascribed to AMO is also, at least in part, caused by anthropogenic climate change. For example, Guan and Nigam (2009) state that non-stationary trends, such as anthropogenic climate warming, can affect Atlantic Sub-surface Temperature, potentially aliasing effects of global warming into natural climate oscillations.

The stationary trend was linked to global climate oscillations, with the highest frequency (2 to 3.6 years) associated with MEI and PDO, a moderate frequency (3.5 to 6 years) associated with AMO, and the lowest frequency (6.73 to 9.51) associated with NAO. Each of these global climate oscillation indices was correlated to local water yields, but the timing, persistence, and direction of correlations varied and only MEI was consistent across basins. From the complex patterns in the wavelet cross coherence plots (Figures 3.9-3.12), the following generalizations were made: (a) The period of high, negative correlations between MEI or PDO and water yields was longer in duration in the lower water loading catchments (c35, c38) compared to higher water loading catchments (c47, c50) – as the MEI or PDO increase, climate is warmer, drier and water yields decrease; (b) The period of high, generally negative correlations between the AMO and water yields was shorter in duration in the lower water loading catchments (c35, c38) compared to higher water loading catchments (c47, c50) – as the AMO increases, the climate gets warmer with less rain and water yields decrease; and (c) The period of high, generally positive correlations between the NAO and water yields was longer in duration in the lower water storage capacity catchments (c35, c47) compared to higher water storage capacity catchments (c38, c50) – as the NAO increases, climate is cooler, wetter and water yields increase. Global climate oscillations have prolonged effects on water

yields from catchments with lower water loading (c35, c38) and lower water storage capacity (c35, c47).

Some of the global climate oscillation indices had interactive effects. The positive correlation between the MEI and PDO indicates that as the MEI increases (reflecting warmer, drier conditions) or decreases (reflecting cooler, wetter conditions), the effects on climatic conditions may be amplified by the PDO. The negative correlation between the NAO and PDO indicates that as the NAO index increases (reflecting cooler, wetter conditions) or decreases (reflecting warmer, drier conditions), the effects on climatic conditions may be amplified or dampened by the PDO (Table 3.5).

3.5.4 Future consideration of finer time series of water yield data

This study used yearly time series of water yields rather than finer time scales. In our data analysis, the residuals (observed data minus trend) are consistent with white noise, but there may be additional features that this type of data cannot detect, for example persistent wetness levels over a period of a few months. Future work using finer time scales may reveal if there is a stochastic persistence such as autoregressive time series dependence in the noise, or if there is coherence with respect to other climate oscillation indices such as NOA or PDO on this finer scale. The cross coherence analysis shows there is some correlation or dependence between the catchment data and the global climate oscillation indices. In future studies that focus on intra-annual data, we will explore if there is lag dependence between the catchment data and previous values of these indices. We have not checked the cross coherence of the indices with the residuals due to the length of the time series and the fact that the residuals are consistent with white noise. This additional step would be interesting to see if the regression**s** mean estimates account for the influence of the climate oscillation indices, or if there is further dependence.

A limitation of the presented analyses (and similar analyses in other studies) is the short length of the available data time series. The TLW has one of the longest monitoring records in Canada (Creed *et al.*, 2011); even so, it does not allow for full consideration of some of the multi-decadal global climate oscillations. For example, the MEI has a 2- to 7-year cycle (Huggett, 1997); NAO has no statistically significant periodicity, although

there is some evidence of a 7- to 9-year and approximately a 20-year cycle (Burroughs, 2005); PDO has a 20- to 30-year cycle (Burn, 2008); and AMO has a 60- to 90-year cycle (Knudsen *et al*. 2011). Complete cycles for MEI and NAO only would be captured in the 28-year record for the TLW. A potential danger of this short time series is that the apparent non-stationary signal may exaggerate the stated influence of climate warming. Even still, with an observation window that included only half of the AMO cycle, we were able to observe significant correlations between climate and the AMO index and to ascribe more than half the non-stationary temperature increase in the TLW to this relationship. Continued support and investment in long-term catchment studies, and analysis of social factors that influence water supply and demand, will help civic institutions adapt to future scenarios of climate and land-use change (Creed *et al.*, 2011; Jones *et al.*, 2012).

3.6 Conclusions

Climatic change has complex influences on headwater catchment water yields. To determine effects of climate change, we must be able to discriminate between anthropogenic climate warming (non-stationary trends) and natural climate oscillation (stationary cycles) signals on catchment water yields from catchments. Using our analytical framework, we were able to show that (A) headwater catchments showed a general non-stationary decline in water yields, which may have been caused by the 1 degree Celsius per decade climate warming that has occurred within the region; however, individual catchments varied in their responsiveness to climate change, with catchments that have lower water loading and lower water storage capacity being the most sensitive; (B) headwater catchments showed stationary cycles in water yields caused by specific climate oscillations or possibly the interactive impacts of multiple global climate oscillations, which are sometimes significantly correlated with each other; and (C) by combining the models of stationary and non-stationary signals identified, it was possible to explain the majority of the variance in water yields within each catchment. AMO was identified as the index most closely associated with climate in the Turkey Lakes Watershed, and it explained approximately 0.037°C of the observed 0.067 °C per year increase in temperature from 1981 to 2008. The methodology developed in this study can

be used not only to understand hydrologic responses to climate change, but also associated biogeochemical responses, including carbon, nitrogen, phosphorus export. Future work will extend the analytical framework to include seasonal, monthly and daily data as well as predicting both water and solute yields from headwater catchments within the TLW and will apply this methodology to other catchments from long-term monitoring stations with the longest available records in forested landscapes across northern latitudes in North America.

3.7 References

Arnell N. 2004. Climate change and global water resources: SRES emissions and socio-economic scenarios. *Global Environmental Change-Human and Policy Dimensions* 14: 31-52. DOI: 10.1016/j.goenvcha.2003.10.006.

Bishop K, Buffam I, Erlandsson M, Folster J, Laudon H, Seibert J, Temnerud J. 2008. Aqua Incognita: the unknown headwaters. *Hydrological Processes* **22**: 1239-1242. DOI: 10.1002/hyp.7049

Burn DH. 2008. Climatic influences on streamflow timing in the headwaters of the Mackenzie River Basin. *Journal of Hydrology* **352**: 225-238. DOI: 10.1016/j.jhydrol.2008.01.019.

Burroughs WJ. 2005. Cycles and periodicities. In Encyclopedia of World Climatology, Oliver JE (ed). Springer-Dordrecht: The Netherlands; 173-177.

Canada Soil Survey Committee. 1978. Canadian system of soil classification, Publ. 1646, 164 pp., Dep. of Agri., Ottawa.

Carey SK, Tetzlaff D, Seibert J, Soulsby C, Buttle J, Laudon H, McDonnell J, McGuire K, Caissie D, Shanley J, Kennedy M, Devito K, Pomeroy JW. 2010. Inter-comparison of hydro-climatic regimes across northern catchments: synchronicity, resistance and resilience. *Hydrological Processes* **24**: 3591-3602. DOI: 10.1002/hyp.7880.

Chen Y, Takeuchi K, Xu C, Chen Y, Xu Z. 2006. Regional climate change and its effects on river runoff in the Tarim Basin, China. *Hydrological Processes* **20**: 2207-2216. DOI: 10.1002/hyp.6200.

Christensen NS, Wood AW, Voisin N, Lettenmaier DP, Palmer RN. 2004. The effects of climate change on the hydrology and water resources of the Colorado River basin. *Climatic Change* **62**: 337-363. DOI: 10.1023/B:CLIM.0000013684.13621.1f.

Clarke A, Mac Nally R, Bond N, Lake PS. 2008. Macroinvertebrate diversity in headwater streams: a review. *Freshwater Biology* **53**: 1707-1721. DOI: 10.1111/j.1365-2427.2008.02041.x.

Cowell DW, Wickware GM. 1983. Preliminary analyses of soil chemical and physical properties, Turkey Lakes Watershed, Algoma, Ontario, Rep. 83-08, Turkey Lakes Watershed, Algoma, Ontario, Canada.

Creed IF, Sanford SE, Beall FD, Molot LA, Dillon PJ. 2003. Cryptic wetlands: integrating hidden wetlands in regression models of the export of dissolved organic carbon from forested landscapes. *Hydrological Processes* **17**: 3629-3648. DOI: 10.1002/hyp.1357.

Creed IF, Beall FD, Clair TA, Dillon PJ, Hesslein RH. 2008. Predicting export of dissolved organic carbon from forested catchments in glaciated landscapes with shallow soils. *Global Biogeochemical Cycles* **22**: GB4024. DOI: 10.1029/2008GB003294.

Creed IF, Sass GZ, Beall FD, Buttle JM, Moore RD, Donnelly M. 2011. Scientific theory, data and techniques for conservation of water resources within a changing forested landscape. A State of Knowledge report. *Sustainable Forest Management Network, Edmonton*, Alberta, 136.

Eimers M, Dillon P, Watmough S. 2004. Long-term (18-year) changes in sulphate concentrations in two Ontario headwater lakes and their inflows in response to decreasing deposition and climate variations. *Hydrological Processes* **18**: 2617-2630. DOI: 10.1002/hyp.5570.

Elliot H. 1985. Geophysical survey to determine overburden thickness in selected areas within the Turkey Lakes Watershed basin, Algoma District, Ontario, Rep. 85-09, Turkey Lakes Watershed, Algoma, Ontario, Canada.

Farge M. 1992. Wavelet transforms and their applications to turbulence. *Annual Review of Fluid Mechanics* **24**: 395-457. DOI: 10.1146/annurev.fluid.24.1.395.

Feminella J. 1996. Comparison of benthic macroinvertebrate assemblages in small streams along a gradient of flow permanence. *Journal of the North American Benthological Society* **15**: 651-669. DOI: 10.2307/1467814.

Foley J, Botta A, Coe M, Costa M. 2002. El Nino-Southern Oscillation and the climate, ecosystems and rivers of Amazonia RID A-5695-2009. *Global Biogeochemical Cycles* **16**: 1132. DOI: 10.1029/2002GB001872.

Giblin PE, Leahy EJ. 1977. Geological compilation of the Batchawana sheet, Districts of Algoma and Sudbury, Ontario, Preliminary Map 302, Geol. Surv. Can., Ontario.

Gomi T, Sidle R, Richardson J. 2002. Understanding processes and downstream linkages of headwater systems. *Bioscience* **52**: 905-916. DOI: 10.1641/0006-3568(2002)052[0905:UPADLO]2.0.CO;2.

Grinsted A, Moore J, Jevrejeva S. 2002. Cross wavelet and wavelet coherence Matlab Package. Downloaded from http://www.pol.ac.uk/home/research/waveletcoherence/ on October 15, 2011.

Grinsted A, Moore J, Jevrejeva S. 2004. Application of the cross wavelet transform and wavelet coherence to geophysical time series. *Nonlinear Processes in Geophysics* **11**: 561-566.

Guan B, Nigam S. 2009. Analysis of Atlantic SST variability factoring interbasin links and the secular trend: Clarified structure of the Atlantic Multidecadal Oscillation. *Journal of Climate* **22**: 4228-4240. DOI:10.1175/2009JCLI2921.1.

Haycock NE, Pinay G, Walker C. 1993. Nitrogen-retention in river corridors - european perspective. *Ambio* **22**: 340-346.

Huggett RJ. 1997. Environmental change. The evolving ecosphere. Routledge: London; 119.

Ionita M, Lohmann G, Rimbu N, Chelcea S, Dima M. 2012. Interannual to decadal summer drought variability over Europe and its relationship to global sea surface temperature. *Climate Dynamics* **38**: 363-77. DOI: 10.1007/s00382-011-1028-y.

Jeffries D, Kelso J, Morrison I. 1988. Physical, Chemical, and Biological Characteristics of the Turkey Lakes Watershed, Central Ontario, Canada. *Canadian Journal of Fisheries and Aquatic Sciences* **45**: 3-13.

Jeffries DS, Semkin RS. 1982. Basin description and information pertinent to mass balance studies of the Turkey Lakes Watershed. Rep. 82-01, Turkey Lakes Watershed, Algoma, Ontario, Canada.

Joint Institute for the Study of the Atmosphere and Ocean (JISAO). 2012. Pacific Decadal Oscillation (PDO) data. Accessed from http://jisao.washington.edu/pdo/PDO.latest on April 10, 2012

Jones JA, Creed IF, Hatcher KL, Warren RJ, Adams MB, Benson MH, Boose E. Brown WA, Campbell JL, Covich A, Clow DW, Clifford CN, Elder K, Ford CR, Grimm NB, Henshaw DL, Larson KL, Miles ES, Miles KM, Sebestyen S, Spargo AT, Stone AT, Vose JM, Williams MW. 2012. Ecosystem processes and human influences regulate streamflow response to climate change at Long-Term Ecological Research Sites. *BioScience* **62**: 390-404.

Kang S, Lin H. 2007. Wavelet analysis of hydrological and water quality signals in an agricultural watershed. *Journal of Hydrology* **338**: 1-14. DOI: 10.1016/j.jhydrol.2007.01.047.

Kawahata H, Gupta L. 2003. El Nino Southern Oscillation (ENSO) related variations in particulate export fluxes in the western and central equatorial Pacific. Journal of *Oceanography* **59:** 663-670. DOI: 10.1023/B:JOCE.0000009595.79408.13.

Keener VW, Feyereisen GW, Lall U, Jones JW, Bosch DD, Lowrance R. 2010. El-Nino/Southern Oscillation (ENSO) influences on monthly NO(3) load and concentration, stream flow and precipitation in the Little River Watershed, Tifton, Georgia (GA). *Journal of Hydrology* **381:** 352-363. DOI: 10.1016/j.jhydrol.2009.12.008.

Kirkby MJ (ed). 1978. Hillslope hydrology. John Wiley and Sons: Chichester, United Kingdom.

Knight JR, Folland CK, Scaife AA. 2006. Climate impacts of the Atlantic Multidecadal Oscillation. *Geophysical Research Letters* **33**: L17706. DOI: 10.1029/2006GL026242.

Knudsen MF, Seidenkrantz M, Jacobsen BH, Kuijpers A. 2011. Tracking the Atlantic Multidecadal Oscillation through the last 8,000 years RID A-3451-2012 RID A-4854-2012. *Nature Communications* **2**: 178. DOI: 10.1038/ncomms1186.

Kondrashov D, Feliks Y, Ghil M. 2005. Oscillatory modes of extended Nile River records (AD 622-1922). *Geophysical Research Letters* **32**: L10702. DOI: 10.1029/2004GL022156.

Labat D. 2005. Recent advances in wavelet analyses: Part I. A review of concepts. *Journal of Hydrology* **314**: 275-288. DOI: 10.1016/j.jhydrol.2005.04.003.

Labat D. 2008. Wavelet analysis of the annual water yield records of the world's largest rivers. *Advances in Water Resources* **31**: 109-117. DOI: 10.1016/j.advwatres.2007.67.004.

Lindsay JB, Creed IF, Beall FD. 2004. Drainage basin morphometrics for depressional landscapes. *Water Resources Research* **40**: W09307. DOI: 10.1029/2004WR003322

Mantua N, Hare S. 2002. The Pacific decadal oscillation. *Journal of Oceanography* **58**: 35-44. DOI: 10.1023/A:1015820616384.

Meyer JL, Wallace JB. 2001. Lost linkages and lotic ecology: Rediscovering small streams. In Ecology: Achievement and Challenge, Huntly NJ, Levin S (eds). Blackwell Publishing: Oxford; 295-317.

Minobe S. 1997. A 50-70 year climatic oscillation over the North Pacific and North America. *Geophysical Research Letters* **24**: 683-6. DOI: 10.1029/97GL00504.

National Center for Atmospheric Research (NCAR). 2012. Northern Atlantic Oscillation (NAO) data. Accessed from https://climatedataguide.ucar.edu/sites/default/files/cas_data_files/asphilli/nao_station_monthly_0.txt on April 10, 2012.

National Oceanic and Atmospheric Administration – Earth System Research Laboratory (NOAA – ESRL). 2012a. Multivariate El Niño Southern Oscillation (ENSO) Index (MEI) data. Accessed from http://www.esrl.noaa.gov/psd/enso/mei/table.html on April **10**, 2012.

National Oceanic and Atmospheric Administration – Earth System Research Laboratory (NOAA – ESRL). 2012b. Atlantic Multidecadal Oscillation (AMO) data. Accessed from http://www.esrl.noaa.gov/psd/data/correlation/amon.us.long.data on April 10, 2012.

Nicolson JA. 1988. Water and chemical budgets for terrestrial basins at the Turkey Lakes Watershed. *Canadian Journal of Fisheries and Aquatic Sciences* **45**: 88-95.

Pike RG, Spittlehouse DL, Bennett KE, Egginton VN, Tschaplinski PJ, Murdock TQ, Werner AT. 2008. Climate Change and Watershed Hydrology: Part I - Recent and Projected Changes in British Columbia. *Streamline Watershed Management Bulletin* **11**: 1-7.

Price DT, McKenney DW, Joyce LA, Siltanen RM, Papadopol P, Lawrence K. 2011. High-resolution interpolation of climate scenarios for Canada derived from General Circulation Model Simulations. *Natural Resources Canada Information Report* NOR-X-421.

Rabeni C, Wallace G. 1998. The influence of flow variation on the ability to evaluate the biological health of headwater streams. *Hydrology, Water Resources and Ecology in Headwaters*: 411-417.

Ropelewski C, Halpert M. 1996. Quantifying Southern Oscillation - Precipitation relationships. *Journal of Climate* **9**: 1043-1059. DOI: 10.1175/1520-0442(1996)009<1043:QSOPR>2.0.CO;2.

Santos CAG, De Morais BS. 2008. Hydrological zones of San Francisco river basin by wavelet transform. In Proceedings of HydroPredict 2008, Bruthans, Kovar, Hrkal (eds). Prague, Czech Republic; 1-8.

Shabbar A, Bonsal B, Khandekar M. 1997. Canadian precipitation patterns associated with the southern oscillation. *Journal of Climate* **10**: 3016-3027. DOI: 10.1175/1520-0442(1997)010<3016:CPPAWT>2.0.CO;2.

Shabbar A, Bonsal B. 2004. Associations between low frequency variability modes and winter temperature extremes in Canada. *Atmosphere-Ocean* **42**: 127-140. DOI: 10.3137/ao.420204.

Shabbar A, Khandekar M. 1996. The impact of El Nino-Southern Oscillation on the temperature field over Canada. *Atmosphere-Ocean* **34**: 401-416.

Sidle R, Tsuboyama Y, Noguchi S, Hosoda I, Fujieda M, Shimizu T. 2000. Stormflow generation in steep forested headwaters: a linked hydrogeomorphic paradigm. *Hydrological Processes* **14**: 369-385. DOI: 10.1002/(SICI)1099-1085(20000228)14:3<369::AID-HYP943>3.0.CO;2-P.

Soniat TM, Klinck JM, Powell EN, Hofmann EE. 2006. Understanding the success and failure of oyster populations: Climatic cycles and Perkinsus marinus. *Journal of Shellfish Research* **25**: 83-93. DOI: 10.2983/0730-8000(2006)25[83:UTSAFO]2.0.CO;2.

Strand LT, Haaland S, Kaste O, Stuanes AO. 2008. Natural variability in soil and runoff from small headwater catchments at Storgama, Norway. *Ambio* **37**: 18-28. DOI: 10.1579/0044-7447(2008)37[18:NVISAR]2.0.CO;2.

Torrence C, Compo G. 1998. A practical guide to wavelet analysis. *Bulletin of the American Meteorological Society* **79**: 61-78. DOI: 10.1175/1520-0477(1998)079<0061:APGTWA>2.0.CO;2.

Torrence C, Webster P. 1999. Interdecadal changes in the ENSO-monsoon system. *Journal of Climate* **12**: 2679-2690. DOI: 10.1175/1520-0442(1999)012<2679:ICITEM>2.0.CO;2.

Wickware GM, Cowell DW. 1985. Forest Ecosystem Classification of the Turkey Lake Watershed, Ecol. Classif. Ser. 18, Lands Dir., Environ, Ottawa, Canada.

Winter TC. 2000. The vulnerability of wetlands to climate change: A hydrologic landscape perspective. *Journal of the American Water Resources Association* **36**: 305-11. DOI: 10.1111/j.1752-1688.2000.tb04269.x.

Wipfli M, Gregovich D. 2002. Export of invertebrates and detritus from fishless headwater streams in southeastern Alaska: implications for downstream salmonid production. *Freshwater Biology* **47**: 957-69. DOI: 10.1046/j.1365-2427.2002.00826.x.

Zhou T, Zhang L, Li H. 2008. Changes in global land monsoon area and total rainfall accumulation over the last half century. *Geophysical Research Letters* **35**: L16707. DOI: 10.1029/2008GL034881

Zhou W, Chen W, Wang DX. 2012. The implications of El Niño-Southern Oscillation signal for South China monsoon climate. *Aquatic Ecosystem Health & Management* **15**:14-19.

Zwiers FW, Schnorbus MA, Maruszeczka GD. 2011. Hydrologic impacts of climate change on BC water resources. Summary report for Campbell, Columbia and Peace River watersheds. Pacific Climate Impacts Consortium: University of Victoria, Victoria, BC.

Chapter 4: Nutrient export from catchments on forested landscapes reveal complex non-stationary and stationary climate signals

Preface

The previous chapter focused on the role of topography in influencing temporal variation in annual water yield, whereas this chapter focuses on the role of topography in influencing temporal variation in annual nutrient export. This chapter tests the hypotheses that that (1) annual time series of nutrient export contain both non-stationary and stationary signals; (2) non-stationary signals are the major signal in terms of contributing to high rates of nutrient export over time and may obscure the contributions of stationary signals on nutrient export; (3) non-stationary signals of metabolically more active nutrients (e.g., nitrogen and phosphorus containing nutrients) show higher rates of change than metabolically less active nutrients (e.g., carbon containing nutrients); and (4) catchments with topographic characteristics that lead to lower hydrologic storage potential and lower hydrologic loading potential show the greater rates of changes in the trends in nutrient export because the hydrological condition that influence biogeochemical processes and nutrient transport are at risk of fundamental changes from climate change in these systems. The analytical framework presented in the previous chapter is applied to detect trends and cycles in the annual time series of nutrient export of carbon (DOC), nitrogen (DON, NO_3^--N), and phosphorus (TDP) in the same catchments. The significance of this chapter is that it uses the analytical framework for deconstructing export signals to reveal changes in trends and cycles in nutrient export signals that will affect the absolute and relative magnitude of nutrient export, which in turn will influence downstream aquatic productivity and biodiversity.

4.1 Introduction

Scientific evidence for climate change is supported by an increasing body of research (IPCC, 2007, Hansen *et al.*, 2012). Climate directly affects water export from catchments by controlling the water export (Mengistu *et al*., 2012), and by extension may also affect the export of nutrients dissolved in this water. However, much less is known about this

relationship, especially in surface waters (Whitehead *et al.*, 2009). Changes in nutrient flow may impact water quality, affecting aquatic productivity and biodiversity, and potentially leading to algal blooms that can severely hamper human drinking water and recreational activities (e.g., Paerl and Paul, 2012). An understanding of the complex links between climate and water resources is needed for planning mitigation and adaptation procedures to ensure the sustainability of water resources.

Climate is inherently dynamic and contains an often complex mixture of non-stationary and stationary signals. Non-stationary climate signals have statistical mean and standard deviation values that change over time, (e.g., directional climatic warming driven by anthropogenic climate change). In contrast, stationary climate signals have statistical means and standard deviations that do not change over time (e.g., global climate oscillations that are naturally occurring at scales ranging from several years to several decades). Discriminating non-stationary signals from the stationary signals that characterize natural climatic variability will contribute to a predictive understanding of changes in both the quantity and quality of surface waters (Adrian *et al.*, 2009*).*

Lakes are a good place to detect changes in climatic conditions because they integrate changes that occur within their catchments (Williamson *et al.*, 2008); however, headwater catchments may be the best places to detect climate signals for the following reasons: (1) they constitute a large spatial extent and contribute a large proportion of water to downstream systems (Bishop *et al.*, 2008); (2) they are located at relatively high topographic positions, they collect precipitation over a relatively small area, and have thin soils for water storage, making their hydrologic regime more sensitive to climate related changes in environmental conditions (Strand *et al.*, 2008); (3) their geomorphic and geologic complexity influences hydrological flow partitioning (surface/subsurface) and pathways tapping into biogeochemical source areas (Creed *et al.*, 1996; Creed and Band, 1998); (4) they are found in areas that are usually relatively undisturbed by human activities (Blenckner et al., 2007); and (5) there are existing long term monitoring networks of headwater catchments particularly in the northern hemisphere (e.g., Creed *et al*., 2011; Jones *et al.*, 2012). For these reasons, greater focus should be placed on headwater systems and their potential to serve as early warning systems for effects of climate change on surface water quantity and quality.

In a recent study, we examined catchment water yield responses to climate signals in a temperate forest region of eastern North America (Mengistu *et al.*, 2012). We developed an approach to remove non-stationary trends and then detect the most prominent nested oscillations within the dataset. We found that catchments showed a general non-stationary decline in water yields, which may have been caused by the 1ºC per decade climate warming that has occurred within the region over the past three decades; however, individual catchments varied in their responsiveness to changing climatic conditions. Catchments with lower water loading and minimal water storage capacity were more sensitive to non-stationary and stationary signals both in terms of magnitude of change in water yield and proportion of the total variation in year-to-year water yield (Mengistu *et al.*, 2012).

In this study, we extend the analysis presented in Mengistu et al. (2012) to identify climate signals within nutrient export records from the same catchments. Climate trends and oscillations will affect nutrient export indirectly through alteration of water flow partitioning and pathways as well as directly through changes in biogeochemistry. This study tested the following hypotheses: (1) yearly nutrient export time series for dissolved organic carbon (DOC), dissolved organic nitrogen (DON), nitrate-nitrogen (NO_3^--N) and total dissolved phosphorus (TDP) from TLW headwater catchments has significant non-stationary and stationary climatic signals; (2) unidirectional non-stationary trends are the major signal as a result of their greater rate of contribution to nutrient export over time and may obscure the contributions of stationary signals on nutrient export; (3) sensitivity to non-stationary signals is greater for nutrients that are more metabolically active (e.g., DON, NO_3^--N and TDP) than less metabolically active (e.g., DOC) nutrients; and (4) sensitivity to these signals is greatest in catchments with relatively low water loading and low water storage capacity, where the hydrological system and its hydrological connections that influence biogeochemical processes are at risk of fundamental changes from climate change. By examining catchment nutrient export responses to changing climatic conditions, it may be possible to infer what types of catchments are the most sensitive sentinels of climate change and to evaluate the potential magnitude of continued climate warming impacts on dissolved nutrient export

to surface waters on forested landscapes. This information could be used to support policies of reduced nutrient loads into surface waters.

4.2 Study Area

The Turkey Lakes Watershed (TLW) is an experimental forest (47°80'30''N, 84°82'50''W) located on the Algoma Highlands on the northern edge of the Great Lakes–St. Lawrence Forest region (Figure 4.1) and established in 1980 by the Canadian federal government (Jeffries *et al.*, 1988). The TLW rests on Precambrian silicate greenstone formed from metamorphosed basalt, with small outcrops of felsic igneous rock near Batchawana Lake and Little Turkey Lake (Giblin and Leahy, 1977). The overall relief ranges from 644 m above sea level at the summit of Batchawana Mountain to 244 m above sea level at the outlet to the Batchawana River. A thin and discontinuous till overlies the bedrock and ranges in depth from <1 m at higher elevations (with infrequent surface exposure of bedrock) to 1–2 m at lower elevations, with till deposits up to 65 m occasionally in bedrock depressions. The podzolic soils in the tills are thin and undifferentiated near the ridge, gradually thickening, differentiating, and increasing in organic content on topographic benches and toward the stream, with highly humified organic deposits wetlands (Canada Soil Survey Committee, 1978; Creed *et al.*, 2002).

The watershed is covered by a northern tolerant hardwood forest dominated by sugar maple (*Acer saccharum* Marsh.) (*Wickware and Cowell*, 1985) with no disturbances since the 1950s. Average stand density (904 stems ha^{-1}), dominant height (20.5 m), diameter at breast height (15.3 cm) and basal area (25.1 m^2 ha^{-1}) are relatively uniform across the uplands, with stand density increasing and dominant height decreasing in the wetlands. The uplands overstory includes sugar maple associates, white pine (*Pinus strobes* L.), white spruce (*Picea glauca* Moench Voss.), ironwood (*Ostrya virginiana* (Mill.) K. Koch), and yellow birch (*Betula alleghaniensis* Britton), which comprise less than 10% of basal area in the uplands, and the sparse understory is dominated by saplings and seedlings of sugar maple and a variety of herbs and ferns. In the wetlands, the overstory is a mixture of black ash (*Fraxinus nigra* Marsh.), eastern white cedar (*Thuja occidentalis* L.), red maple (*Acer rubrum* L.), balsam fir (*Abies balsamea* (L.) Mill.), yellow birch, and tamarack (*Larix laricina* (DuRoi) K. Koch.), and the understory is

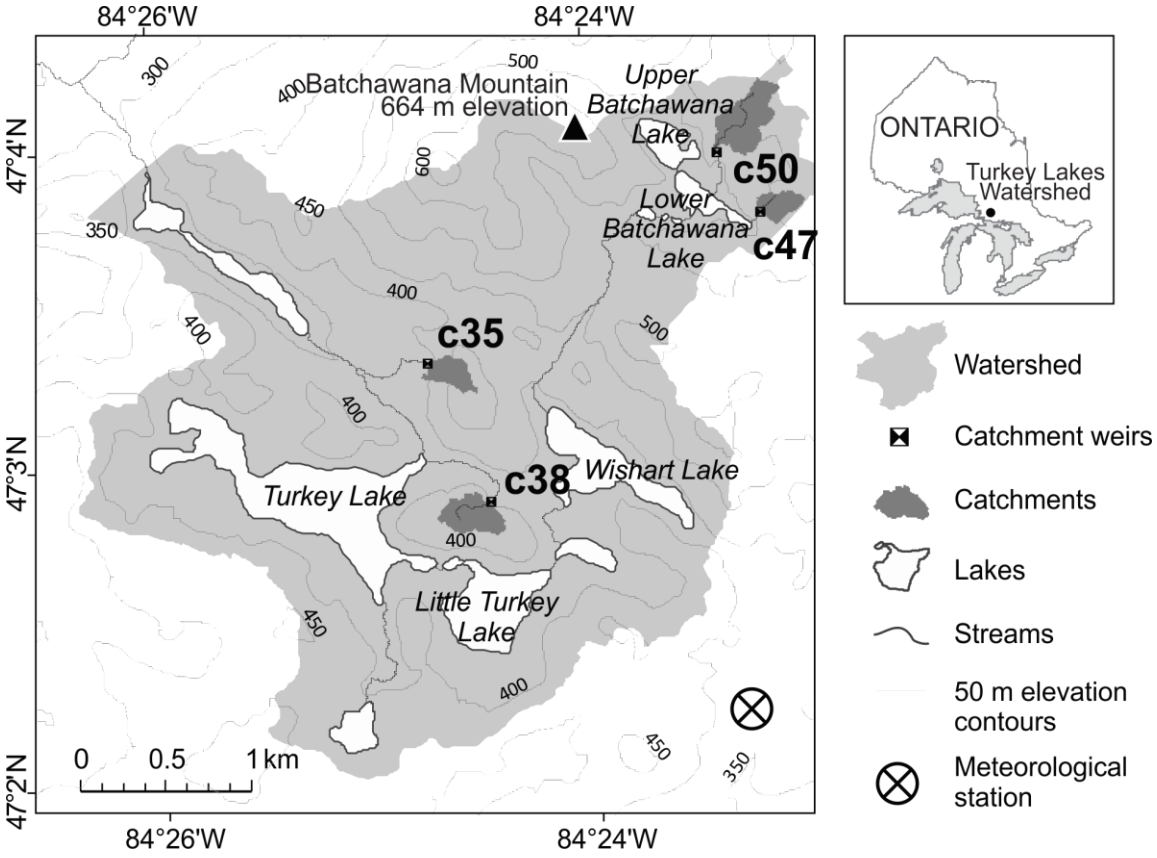


Figure 4.1: The Turkey Lakes Watershed.

composed of the seedlings and saplings of overstory trees and various herbs and ferns (Webster *et al.*, 2008).

The watershed is influenced by a continental climate. The average annual precipitation is 1200 mm and the average annual temperature is 5.0 ºC [based on a 28-year meteorological record (1981-2008) from the Canadian Air and Precipitation Monitoring Network (CAPMoN) station located just outside the TLW boundary (see Figure 4.1)]. Meteorological conditions within the TLW reflect significant influences from Lake Superior in the west and orographic effects created by Batchawana Mountain. Snowpack persists from late November, early December through to late March, early April, with peaks in stream discharge during snowmelt and again in September to November during autumn storms. The average annual atmospheric deposition of sulphur and nitrogen [based on a 28-year atmospheric acidic deposition record from the same CAPMoN station) show that sulphur deposition has been declining at a rate of almost 1 kg/ha/yr, but nitrogen deposition has been comparatively stable (Figure 4.2) (M. Shaw, Unpublished Data).

For this study, we examine four catchments, c35, c38, c47 and c50, which exhibit a water loading gradient in the form of rain and snow and a water storage gradient in wetlands (Figure 4.3). See the conceptual model from Chapter 3 for details on how the magnitudes of the gradients in water loading and water storage were determined. In summary, for water loading, average precipitation for the four catchmets was interpolated from local weather stations in the TLW using Anusplin 4.37. For water storage, we compared the wetland size by area of the four catchments and assumed that the water storage capacity per unit area of upland soils was similar.

4.3 Methods

4.3.1 Analytical framework

We applied an analytical framework to identify non-stationary and stationary signals in yearly time series of nutrient export from catchments c35, c38, c47 and c50 in the TLW (Figure 4.4). Daily, monthly and seasonal nutrient export data were too variable and linear trends were not statistically significant (data not shown) so annual data was used

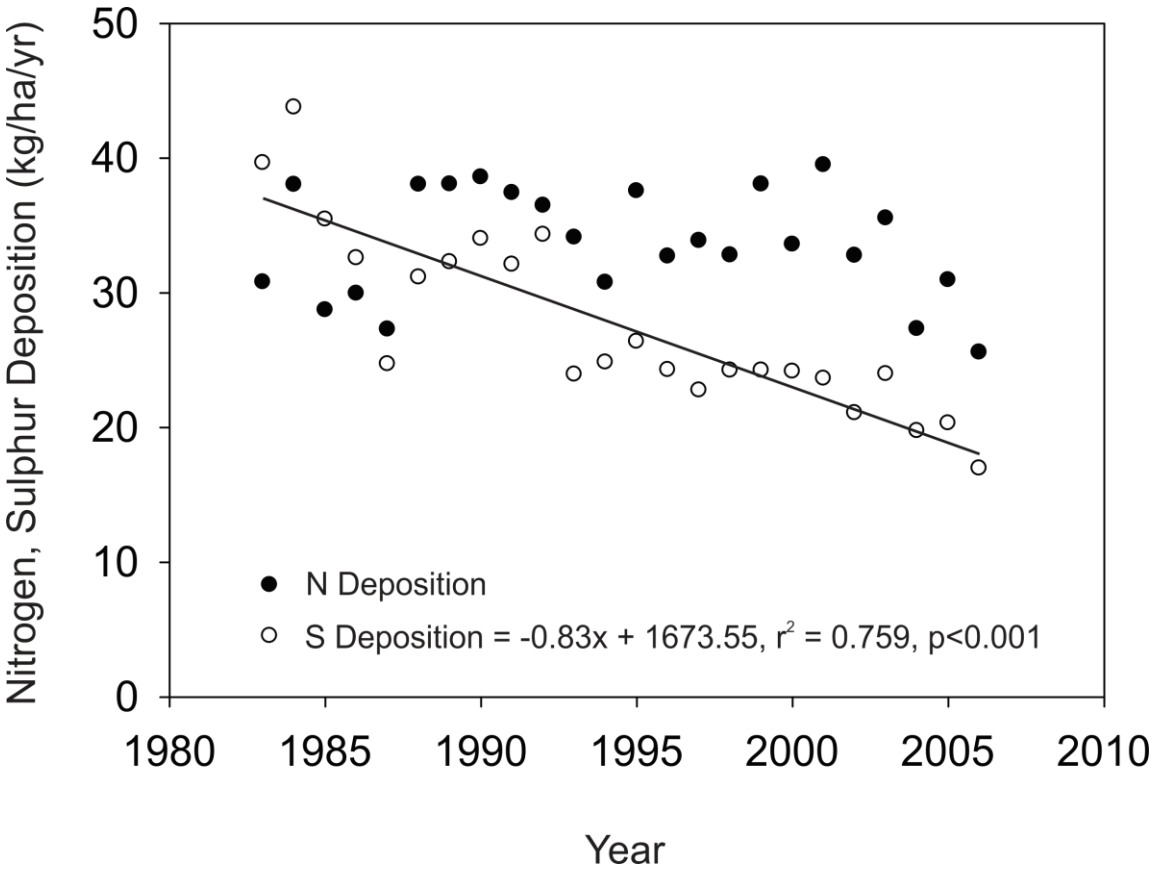


Figure 4.2: Nitrogen and sulphur deposition data from 1983 to 2006 (Unpublished data, M. Shaw, Environment Canada).

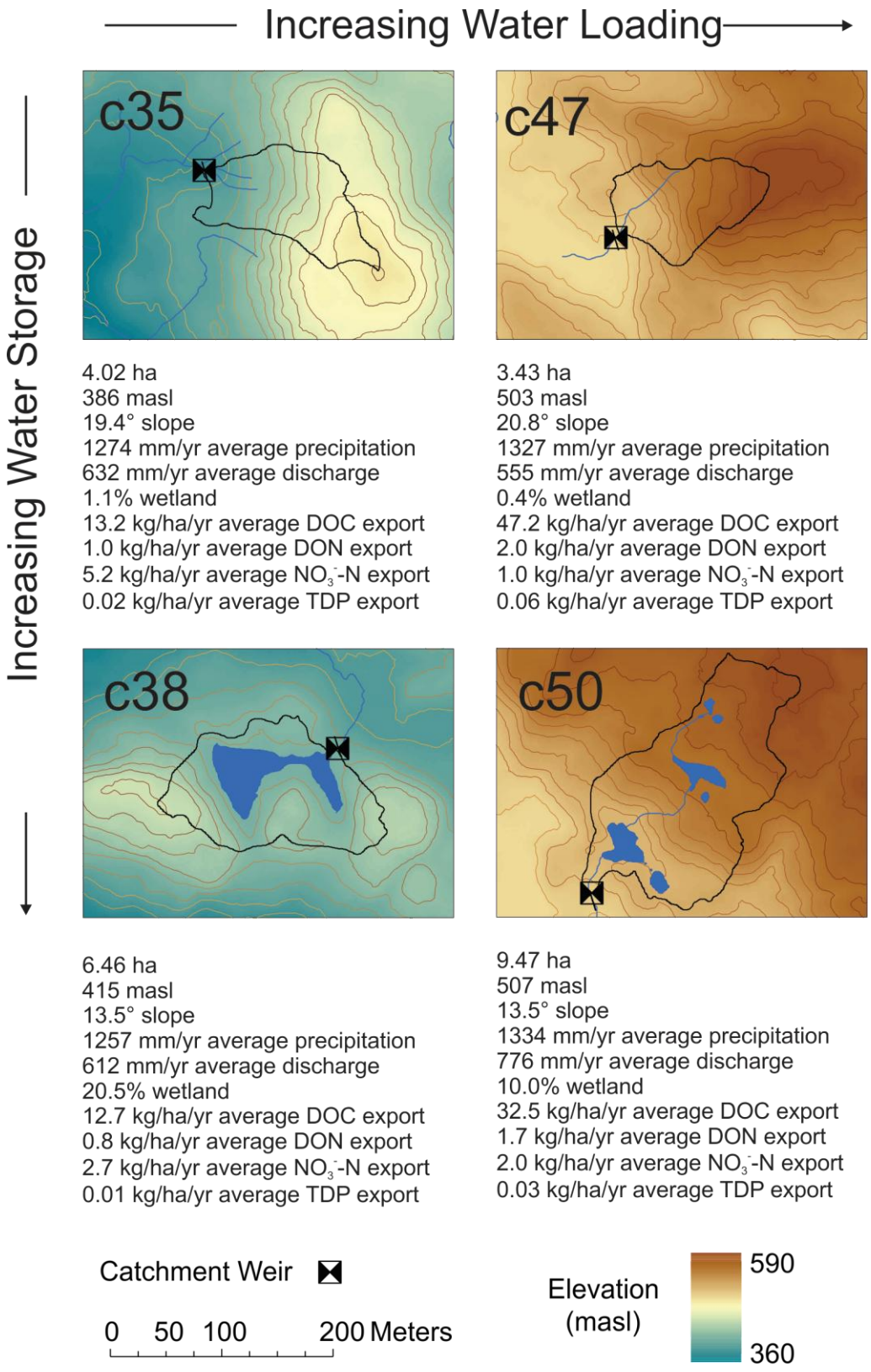


Figure 4.3: Topographic maps and descriptions of the four catchments selected from the Turkey Lakes Watershed for analysis.

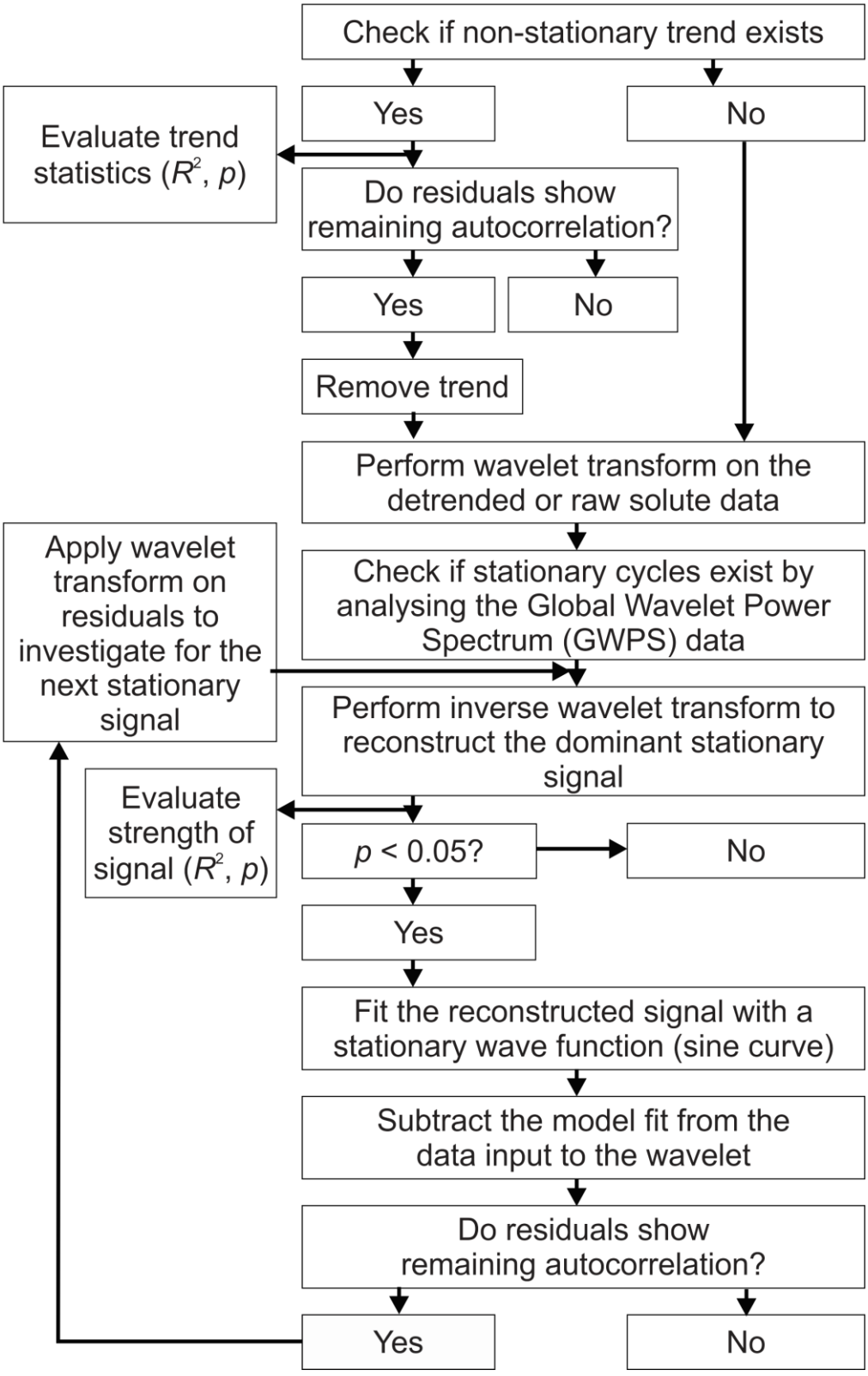


Figure 4.4: Diagram detailing the analytical framework of detecting non-stationary and stationary trends in nutrient data.

instead. We describe the analytical framework briefly here, but for further details refer to Mengistu *et al.* (2012).

4.3.2 Yearly nutrient export

Daily discharge and discharge chemistry data were provided by F. Beall at the Canadian Forest Service in Sault Ste. Marie, Ontario. Daily discharges were derived from continuously measured stream stage at V-notch weirs on each catchment. The concentrations of DOC, NH_4^+-N, NO_3^--N, and TDP in discharge were derived from samples collected every two weeks during the winter, daily during spring snowmelt, and weekly or every two weeks during the summer and autumn. Stream water samples were filtered through Fisher Q8 (coarse, fast flow) paper filters; extensive testing found no significant difference for samples filtered with fine vs. coarse filters.

NH_4^+-N, NO_3^--N, and total dissolved nitrogen (TDN) were analysed using sodium nitroprusside, cadmium reduction and cadmium reduction after autoclave digestion methods, respectively, on Technicon Autoanalysers. DON was calculated from TDN minus dissolved inorganic nitrogen (DIN = NH_4^+-N + NO_3^--N). DOC was determined by removing dissolved inorganic carbon (DIC) by purging with N_2 after acidification, converting DOC to DIC by persulfate oxidation catalyzed by UV, then converting the resulting DIC to CO_2 by acidification, which was measured by colorimetry. TDP was analysed on a Technicon Autoanalyser IIC after autoclave digestion using the molybdophosphoric acid colour reaction.

Daily nutrient concentrations were either measured or estimated by interpolation of the two measured values located directly before and directly after the unknown value. Daily nutrient exports were then calculated as the product of the total daily discharge and the interpolated daily concentrations in the discharge. Yearly nutrient exports were calculated as the yearly sum of the daily nutrient exports based on the water year (June 1 to May 31), before being normalized by catchment area.

4.3.3 Non-stationary linear trends

The computed yearly time series of nutrient exports were analysed for non-stationarity by linear regression. Significant stationary signals were subtracted from the observed data,

and the residuals (i.e., detrended data) were then examined for the presence of stationary signals using wavelet analysis. If there was no significance, then no stationary signals were removed.

4.3.4 Stationary non-linear oscillations

Wavelet transforms display the most prominent frequencies within a yearly nutrient export data in a wavelet power spectrum (WPS). WPSs of the detrended portion of the yearly nutrient export data were derived using the method outlined in Torrence and Compo (1998). A Morlet wavelet was chosen due to its extensive application to similar studies involving hydroclimatic time series analysis (Kang and Lin, 2007).

The WPSs were computed by convoluting each time series with a scaled and translated version of a transforming wavelet function. Assuming an equal time interval of Δt in a time series X_n ($n = 0, 1, \ldots, N-1$), the corresponding wavelet function, $\psi_o(\eta)$ (where η is a non-dimensional time parameter on which the function depends), must have a zero mean and be localized in time and frequency space. The wavelet was characterized by a Gaussian modulated plane wave:

$$\psi_o(\eta) = \pi^{-\frac{1}{4}} e^{i\omega_o \eta} e^{-\frac{\eta^2}{2}} \qquad (4.1)$$

Where i = an imaginary unit for complex valued Morlet function to overcome disadvantages of shift sensitivity, poor directionality and lack of phase information in using conventional real valued wavelets; ω_o is the non-dimensional angular frequency, which by default is taken to be 6 to satisfy the admissibility condition (Farge, 1992).

The continuous wavelet transform of time series X_n, for each scale s at all n, with respect to the wavelet function $\psi_o(\eta)$ is mathematically represented as 4.2:

$$W_n(s) = \frac{1}{N} \sum_{n'=0}^{N-1} x_n \psi^* \left[\frac{(\eta' - \eta)\Delta t}{s} \right] \qquad (4.2)$$

Where $W_n(s)$ stands for wavelet transform coefficients, ψ for the normalized wavelet, (*) for the complex conjugate, s for wavelet scale, n for localized time index, and η' for translated time index.

The transformed signal, $W_n(s)$, is a function of the wavelet scale, and translation parameters are found by conducting the convolution N (the number of data in the time

series) times for each scale. A faster way of performing such a transform is to simultaneously calculate all the N convolutions in a Fourier space using discrete Fourier transform of X_n (4.3):

$$\widehat{x}_k = \frac{1}{N}\sum_{n=0}^{N-1} x_n e^{-2\pi i k n / N} \qquad (4.3)$$

Where $k = 0 \ldots N$ is the frequency index.

In the Fourier space the wavelet transform equation (4.2) can be expressed as (4.4):

$$W_n(s) = \sum_{k=0}^{N-1} \widehat{x}_k \widehat{\psi}^*(s\omega_k) e^{i\omega_k n \Delta t} \qquad (4.4)$$

Where $\psi(s\omega)$ is Fourier transform of a function $\psi(t/s)$ and ω_k is an angular frequency defined as (3.5):

$$\omega_k = \begin{cases} \dfrac{2\pi k}{N\Delta t} & if \quad k \le \dfrac{N}{2} \\ -\dfrac{2\pi k}{N\Delta t} & if \quad k > \dfrac{N}{2} \end{cases} \qquad (4.5)$$

The WPSs were calculated as the square of the absolute value of the wavelet transform, $|W_n(s)|^2$.

Once the WPSs were calculated, the global wavelet power spectrum (GWPS) values were computed by time-averaging wavelet spectrum values over all the local spectra. GWPS values can be used to assess the scales (or periods) contributing most to the spectral energy of the time series under investigation. Scales with large GWPS values were considered to contribute more spectral energy, while the contribution of small GWPS scales were assumed to be little or insignificant. GWPS values were, therefore, used to identify the periods of strongest stationary periodic signals.

Inverse wavelet transformation of the forward wavelet transform (4.2) was employed to reconstruct signals based on the coefficients of scales identified to have dominant GWPS. The inverse wavelet function is mathematically represented as (4.6).

$$x_n = \int_0^N \int_{s_1}^{s_k} W_n(s) . \left\lfloor \frac{(\eta' - \eta)}{s} \right\rfloor \frac{dsdn}{s^2} \qquad (4.6)$$

Maintaining the coefficients of the chosen scales while replacing all scale coefficients with zero and performing backwards (inverse) wavelet transform on the result generated the signals characterizing the identified scale. For choices of two or more consecutive scales, the inverse transform function builds up the reconstructed signal as the sum of wavelets of different scales, *s*, at localized time, *n*.

Autocorrelation was used to detect temporal autocorrelation within yearly nutrient export data using the *autocorr* function in Matlab. The confidence bounds were found using 4.7:

$$\frac{nSTDs}{\pm\ sqrt\ (N)} \qquad (4.7)$$

Where *nSTD*s is the number of standard deviations used in determining significance, and *N* is the number of independent sample data points. Two standard deviations were used to approximate 95% significance.

4.3.5 Detecting stationary signals

Stationary signals were detected in the yearly nutrient export data using a step-wise methodology. A wavelet power spectrum of the detrended nutrient export data was used to identify the dominant periodicity in the detrended time series, which was followed by an inverse wavelet transform to extract the signal of dominant periodicity corresponding to scales of peak GWPS values. The dominant peak was selected for further analysis only if it had not been selected previously, as spectral leaking from one cycle to the next could occur. The extracted signal was then fitted with a periodic function to model and statistically analyse the stationarity of the extracted signal. The same steps were followed in the second cycle using the residuals of the detrended nutrient export data minus modeled stationary signal from the first cycle as the input to the wavelet analysis. In each of the subsequent cycles, residuals (i.e., input data of the previous cycle minus modeled stationary signal in the same cycle) were similarily analysed.

Subsequent peak GWPS values were considered as long as they made a significant contribution to the regression models. After selecting the stationary signals for each catchment, each signal was added to the respective nutrient export model using forward step-wise regression, starting with the non-stationary signal. After modeling the

stationary structures at each step for each nutrient, the model at each step was added to the overall nutrient model using forward step-wise regression against the raw nutrient export data, beginning with the non-stationary component of the nutrient export time series.

An overall stationary model was also developed for each nutrient from each catchment by modeling the sum of the stationary structures identified at each step for each nutrient. The amplitude (difference between maximum and minimum divided by two) of the overall stationary model was used to determine the range of change exhibited by stationarity over the study period.

4.3.6 Wavelet cross coherence analysis

Wavelet cross coherence analysis was used to determine if there was an association between yearly indices of global climate oscillations and the detrended yearly nutrient export data from the catchments using a Matlab package based on one from Grinsted *et al.* (2002). Wavelet coherence of two time series X and Y, with wavelet transforms $W_n^X(s)$ and $W_n^Y(s)$, was defined as 4.8:

$$R_n^2(S) = \frac{\left|S(s^{-1}W_n^{XY}(s))\right|^2}{S(s^{-1}\left|W_n^X(s)\right|^2) \times S(s^{-1}\left|W_n^Y(s)\right|^2)} \qquad (4.8)$$

Where S is a smoothing operator to help locate local maxima both in time. In the plot this can be written as 4.9:

$$S(W) = S_{\text{scale}}(S_{\text{time}}(W_n(s))) \qquad (4.9)$$

Where, S_{scale} denotes smoothing along the wavelet scale axis and S_{time} smoothing along the time axis.

The Multivariate El Niño Southern Oscillation (ENSO) Index (MEI), Atlantic Multidecadal Oscillation (AMO), Northern Atlantic Oscillation (NAO), Pacific Decadal Oscillation (PDO) indices were selected due to their global influence. MEI (annualized from monthly data based on water year) was used instead of alternative indices [e.g., the Southern Oscillation index (Sea Level Pressure differences) and ENSO 3.4 (SST)] because it includes six variables: sea level pressure, surface zonal wind, meridional wind, cloudiness, sea surface temperature, and surface air temperature (Wolter and Timlin,

1998), which makes MEI effective at discriminating ENSO impacts on hydrology, including rainfall and runoff variability (Kiem and Franks, 2001).

The annual average oscillation indices were calculated from monthly index values. Wavelet transform plots mapped the correlations between wavelets of varying periods with the yearly nutrient flux time series to readily visualize the dominant frequencies, while wavelet cross coherence plots mapped the correlations of two wavelet transformed time series (in this case time series of yearly water yield and average annual oscillation indices) at local times and scales. The cone of influence delimits regions not influenced by edge effect as a result of using time series of finite length, warmer colours represent good matching between correlating time series and the thick black solid lines encircles regions of the 95% confidence level in relatioship. For wavelet cross coherence plots, arrows indicate the nature of the correlation: arrows to the left indicated the two signals are in anti-phase, while arrows to the right indicate the two signals are in-phase (Grinsted *et al.*, 2004). Angled arrows give an indication of potential lags within the data. Arrows pointed downward indicate that X is leading Y by 90°, while upward pointing arrows indicate Y leading X by 90° (where 90° represents a time equivalent to one fourth of the periodicity represented by the scale of interest). Finally, Pearson Product Moment correlation tests were performed between each of the four climate indices studied and each of the stationary signal models isolated from within the time series of each nutrient. All statistical analyses were completed using Sigmaplot 12.0 (Systat Software, 2012), and MatLab version 2010b (Mathworks, 2010).

4.4 Results

4.4.1 Non-stationary and stationary signals

Significant negative linear trends were detected in DON, NO_3^--N, and TDP export flux data, but not DOC export data (Figures 4.5-4.8). These trends were often strongest in c35, the catchment with low water loading and low water storage, with rates of -48 g DON/ha/yr, -81 g NO_3^--N/ha/yr, and -0.8 g TDP/ha/yr. In contrast, these trends were lowest in c47, the catchment with high water loading and low water storage, with rates of -22 g DON/ha/yr and no significant trend in NO_3^--N or TDP. However, the weir in c47 was not ideally placed, and there was a bypass channel that circumvented the weir. The

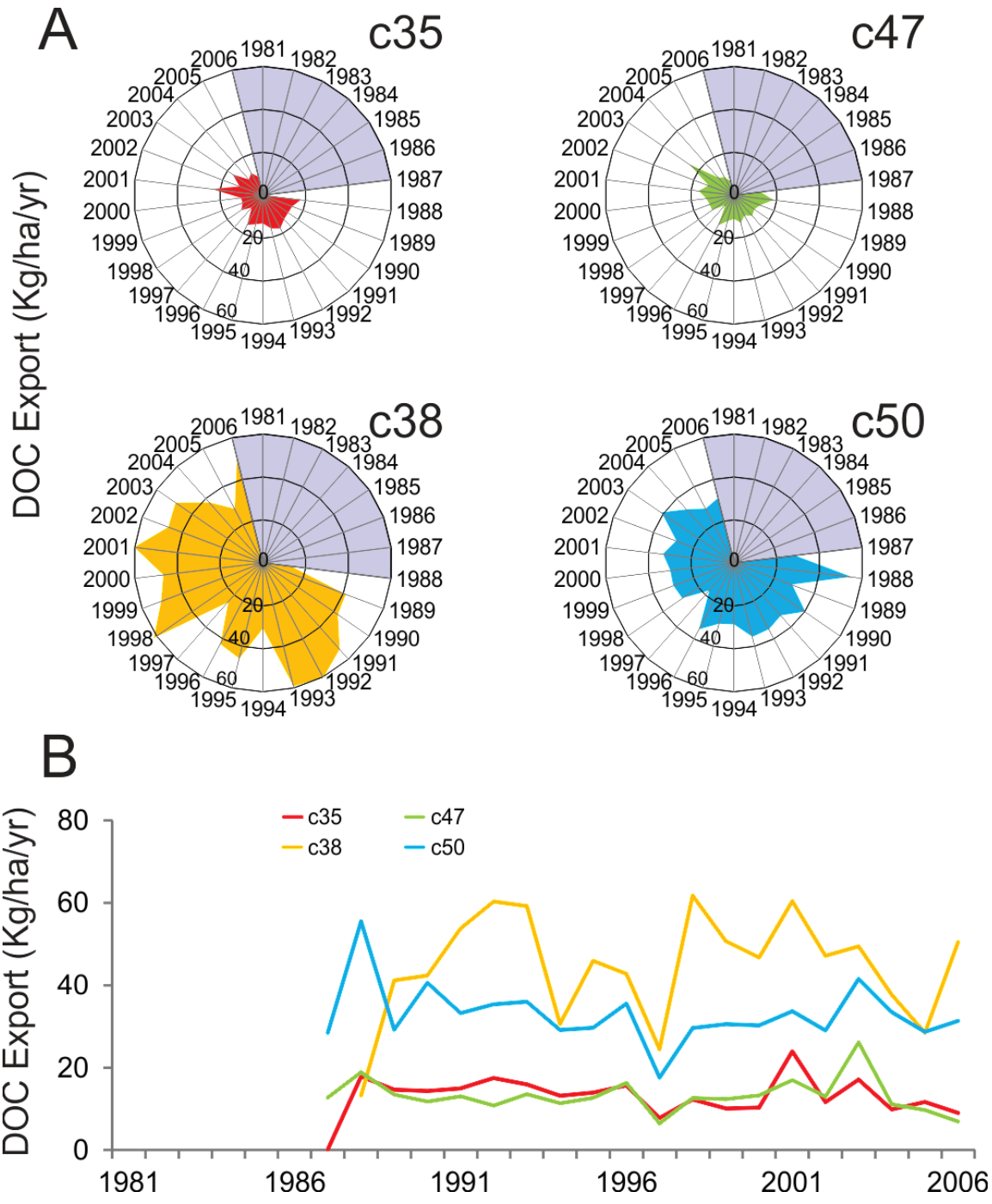


Figure 4.5: Spider plots (A) and line plots (B) showing time series of dissolved organic carbon (DOC) export in four catchments in the Turkey Lakes Watershed.

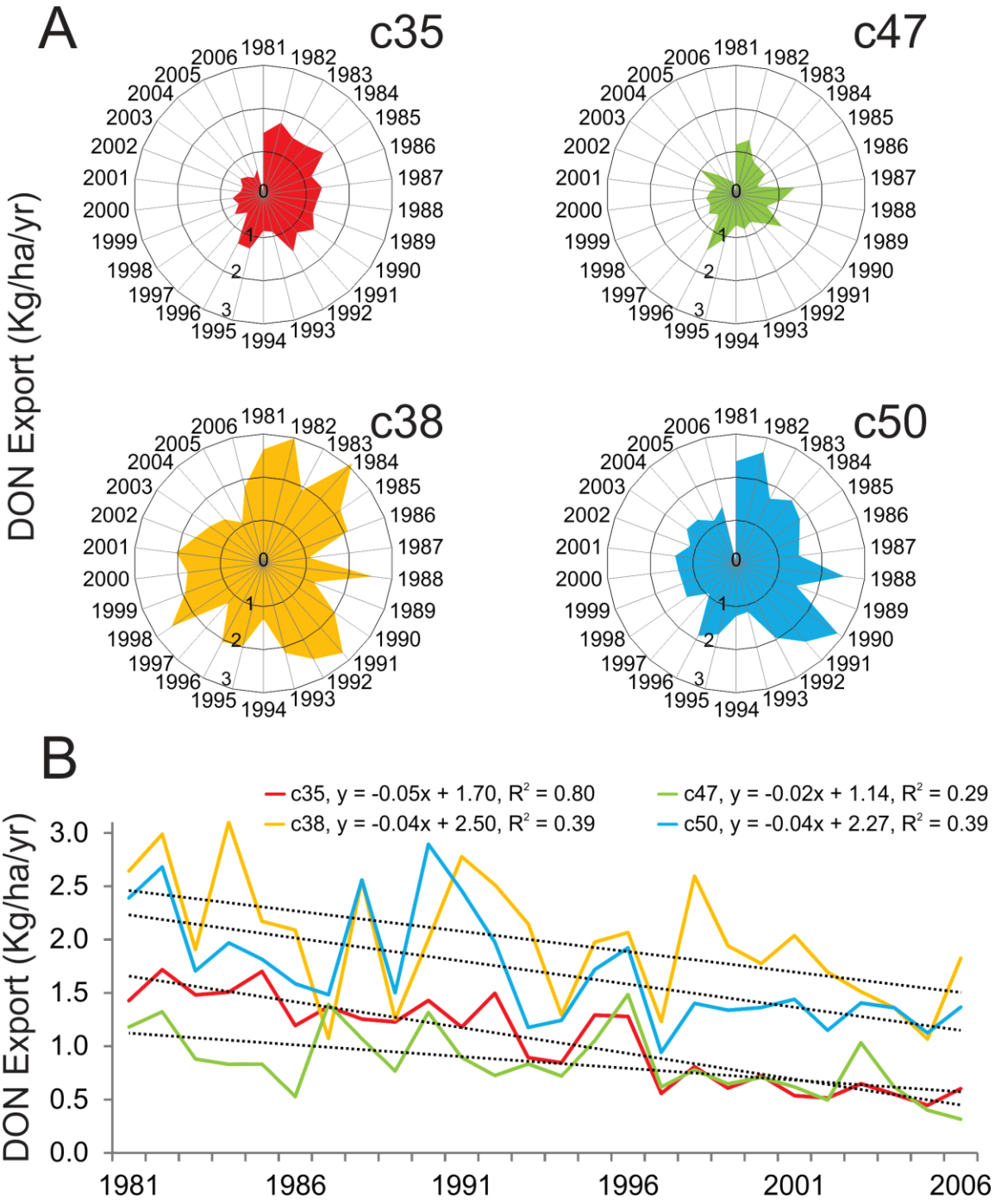


Figure 4.6: Spider plots (A) and line plots (B) showing time series of dissolved organic nitrogen (DON) export in four catchments in the Turkey Lakes Watershed.

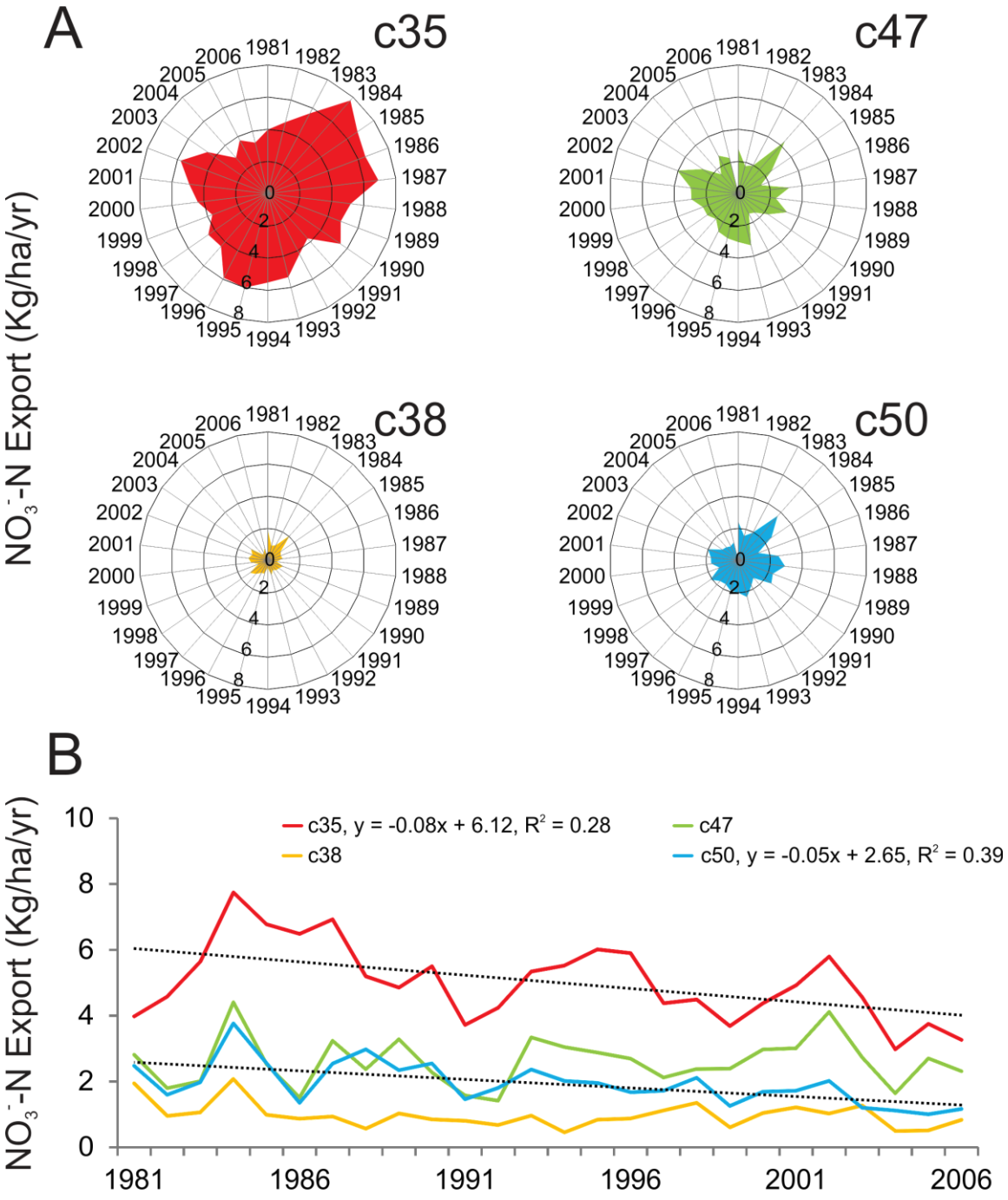


Figure 4.7: Spider plots (A) and line plots (B) showing time series of nitrate (NO_3^--N) export in four catchments in the Turkey Lakes Watershed.

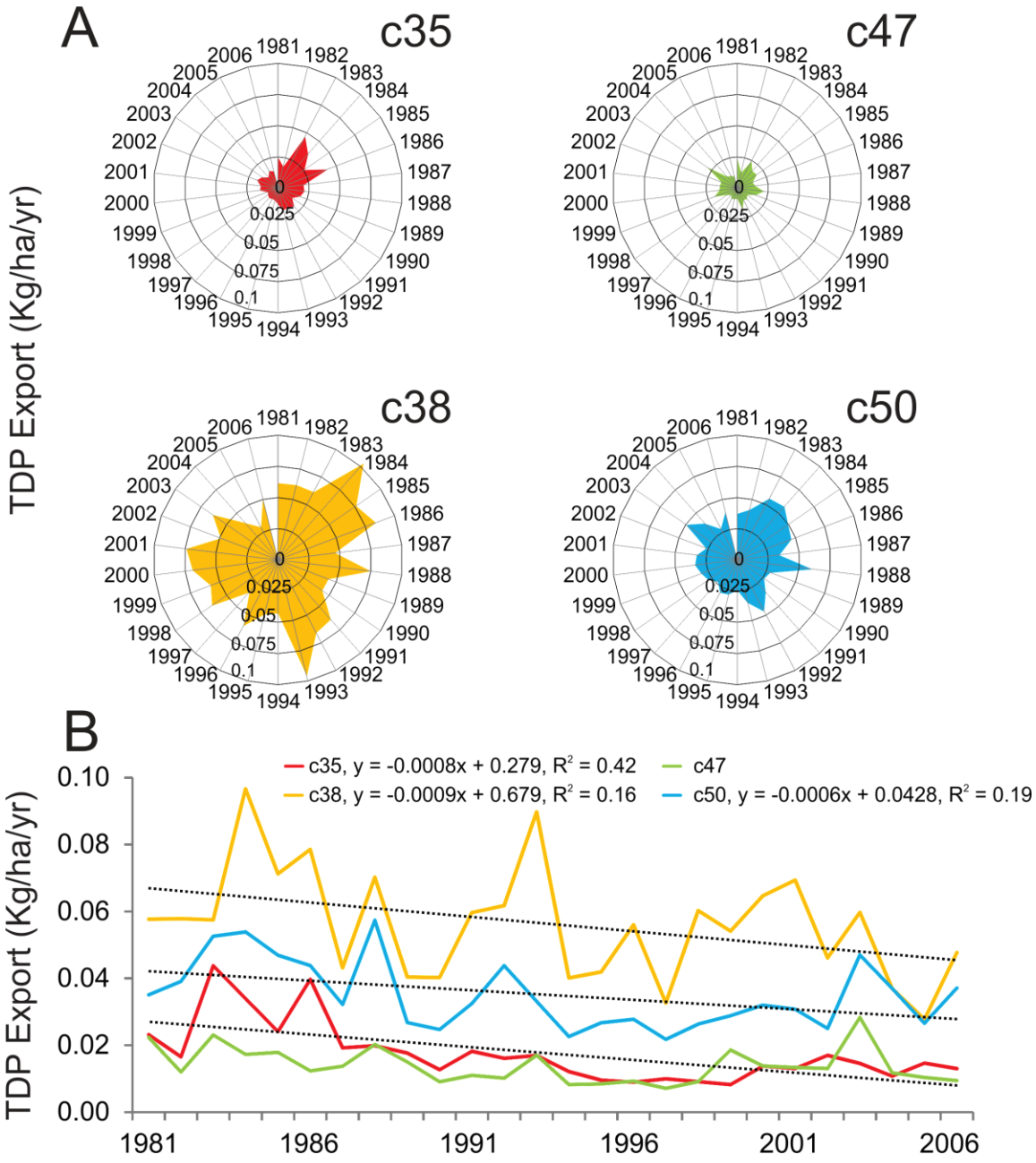


Figure 4.8: Spider plots (A) and line plots (B) showing time series of total dissolved phosphorus (TDP) export in four catchments in the Turkey Lakes Watershed.

closest comparable catchment is c49, which had significant declines in DON and NO_3^--N (R^2 = 0.165 and 0.199, respectively) of -21 g DON/ha/yr and -52 g NO_3^--N/ha/yr, respectively. Where nitrogen declines were detected, rates were higher in NO_3^--N than in DON. Where DON and TDP declines were detected, rates were higher in DON than TDP by almost two orders of magnitude (Tables 4.1-4.4).

Significant nested stationary cycles were detected in all nutrient export data and in all catchments (Figures 4.9-4.12, Tables 4.1-4.4). Stationary signals were identified at very short (2 to 3 year), short (3 to 5 year), medium (5 to 9 year) and long (9 to 13 year) scales (Table 4.5). The very short (very high frequency) 2.0 to 2.8 year signal was observed for all nutrients in all catchments. The short (high frequency) 3.4 to 4.8 year signal was observed within the DON, NO_3^--N and TDP export time series in all catchments (except c35 for TDP). The short DOC signal was observed only in c38, the low water loading and high water storage catchment. A medium (moderate frequency) signal was identified in many catchments, at either 5.7 to 8.0 years or the overlapping period of 6.7 to 9.5 years. There was a long signal in all catchments for DOC, and a long signal for DON was observed in all catchments except c35. A medium signal was observed in only the low water storage catchments (c35, c47) for NO_3^--N. There was a medium stationary signal for TDP in the low water loading catchments (c35, c38). Generally, the earlier cycle (5.7 to 8.0 years) was identified in the nitrogen bearing nutrients (i.e., DON, NO_3^--N)), while the later cycle (6.7 to 9.5 years) was identified in the carbon and phosphorus bearing nutrients. The longest cycle identified across the sites was 9.5 to 13.5 years and was detected in DON (c50) and in NO_3^--N (c35 and c38).

For each catchment, the overll nutrient export stationary signals revealed temporally varying phase relationships (Figures 4.13 and 4.14), at times coupled and at time uncoupled, leading to temporal changes in the stoichiometry of nutrient export [i.e., temporally varying DOC: nitrogen export ratio and TDP and nitrogen export ratio].

4.4.2 Non-stationary vs. stationary signals

The relative strengths of the non-stationary and stationary signals were evaluated first by assessing the magnitude of export attributed to the signal. To assess whether non-stationary or stationary patterns contributed more to variability in nutrient export, the

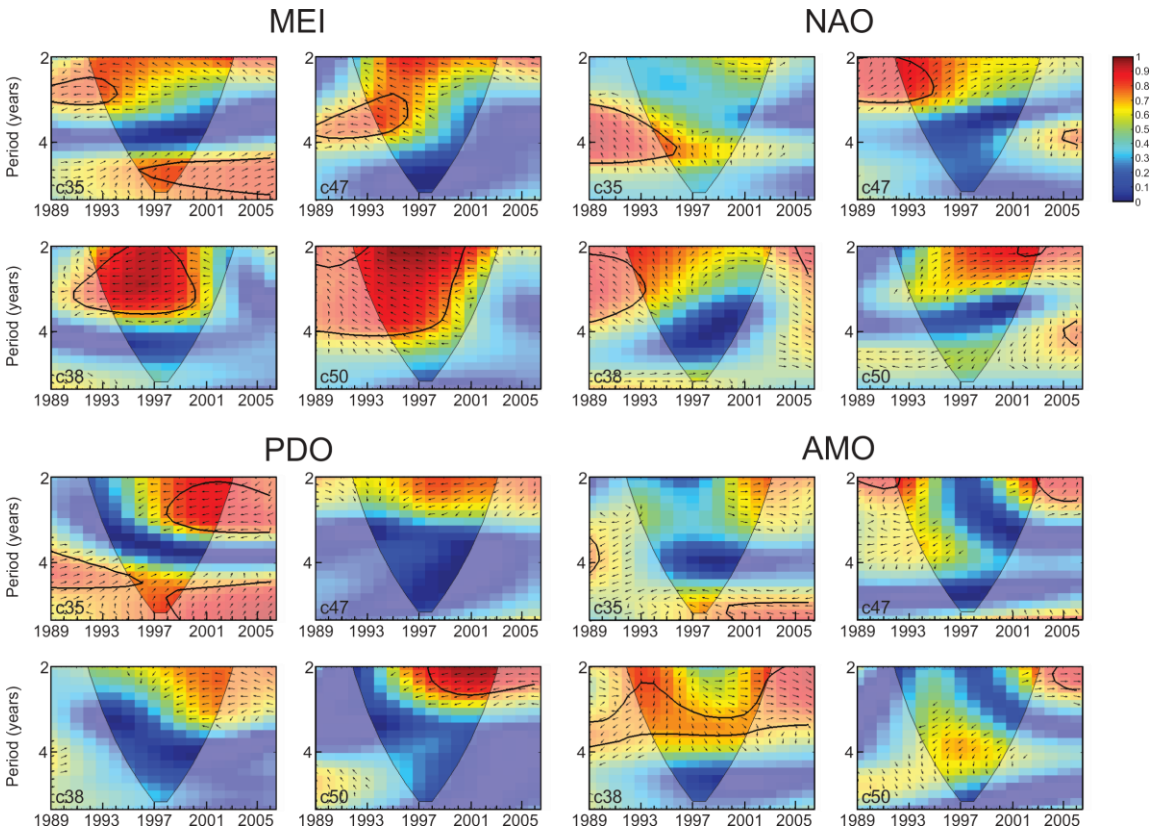


Figure 4.9: Wavelet cross coherence plots using Morlet wavelets showing correlations at each period between yearly DOC yield and MEI, NAO, PDO, and AMO at four catchments in the Turkey Lakes Watershed. The thin solid line represents the cone of influence, the thick contours indicate the 95% significance level, arrows show the relative phase relationship (left arrows for negative correlations and right arrows for positive correlations). Warm colours indicate strong correlations and cool colours indicate weak relationships along a linear scale.

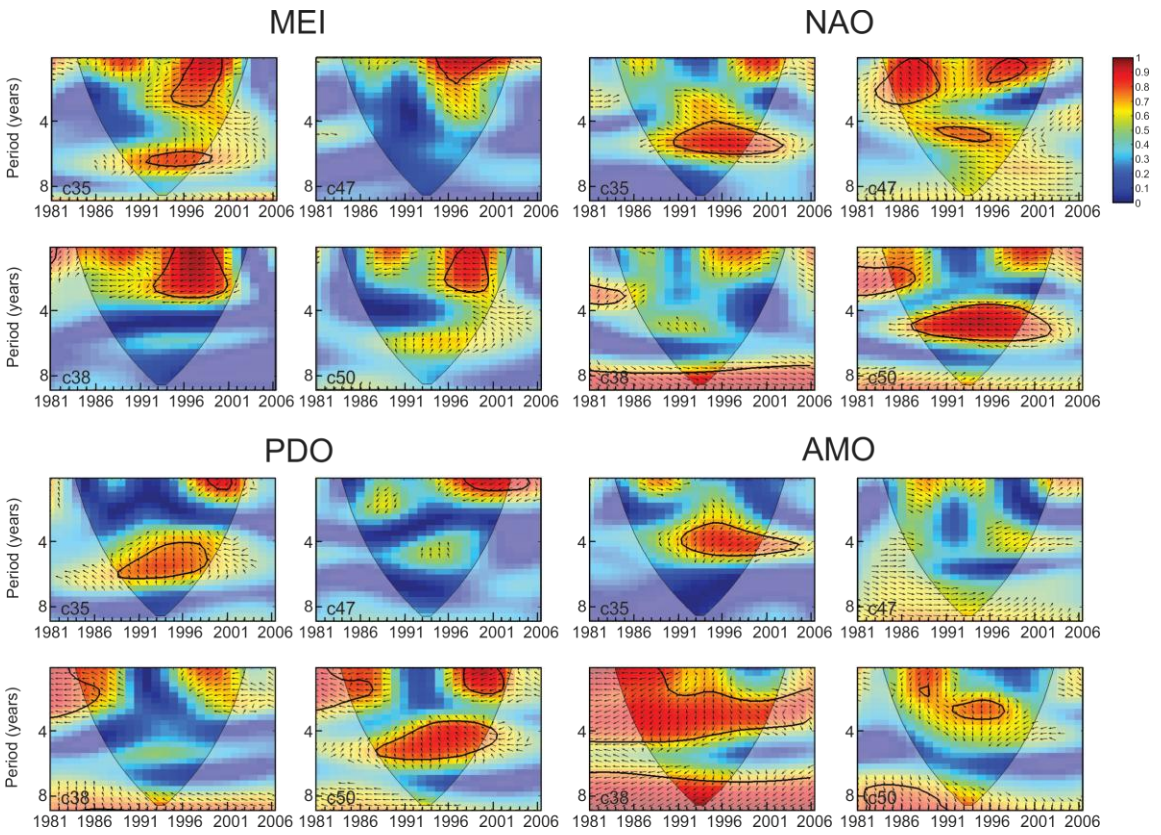


Figure 4.10: Wavelet cross coherence plots using Morlet wavelets showing correlations at each period between yearly DON yield and MEI, NAO, PDO, and AMO at four catchments in the Turkey Lakes Watershed.

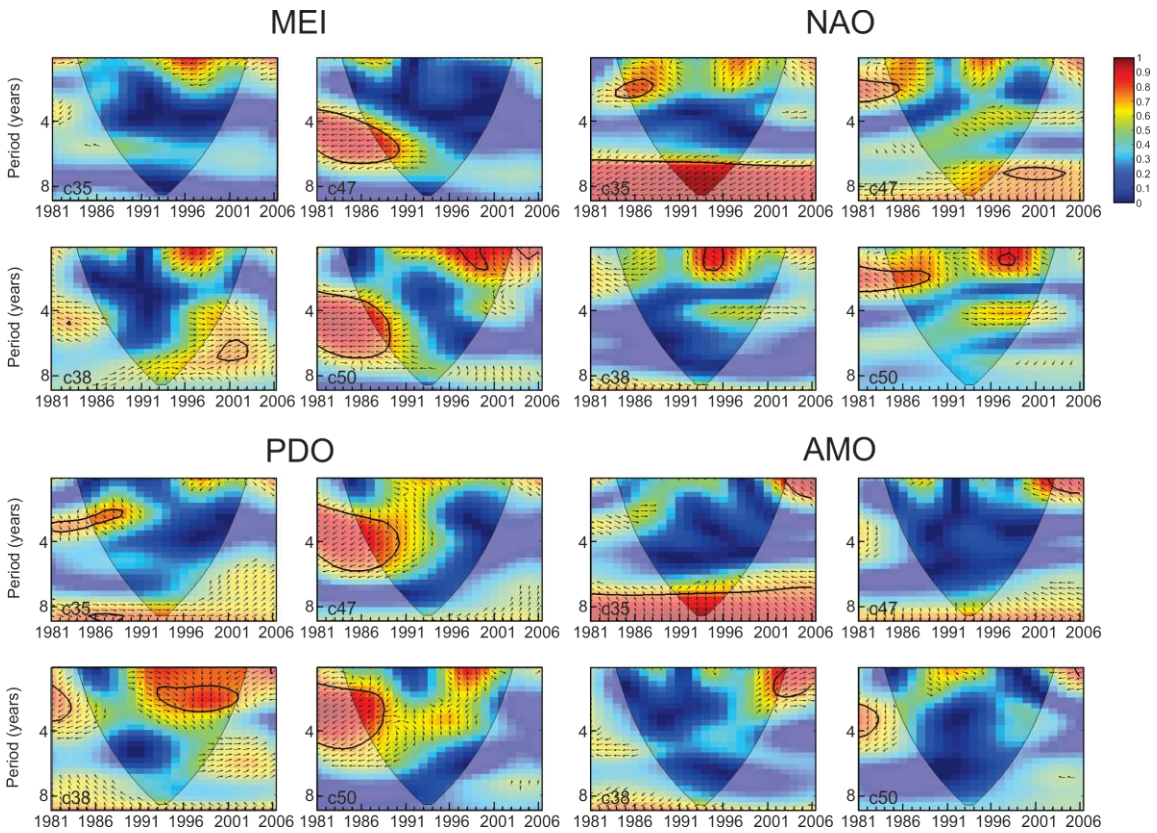


Figure 4.11: Wavelet cross coherence plots using Morlet wavelets showing correlations at each period between yearly NO_3^--N yield and MEI, NAO, PDO, and AMO at four catchments in the Turkey Lakes Watershed.

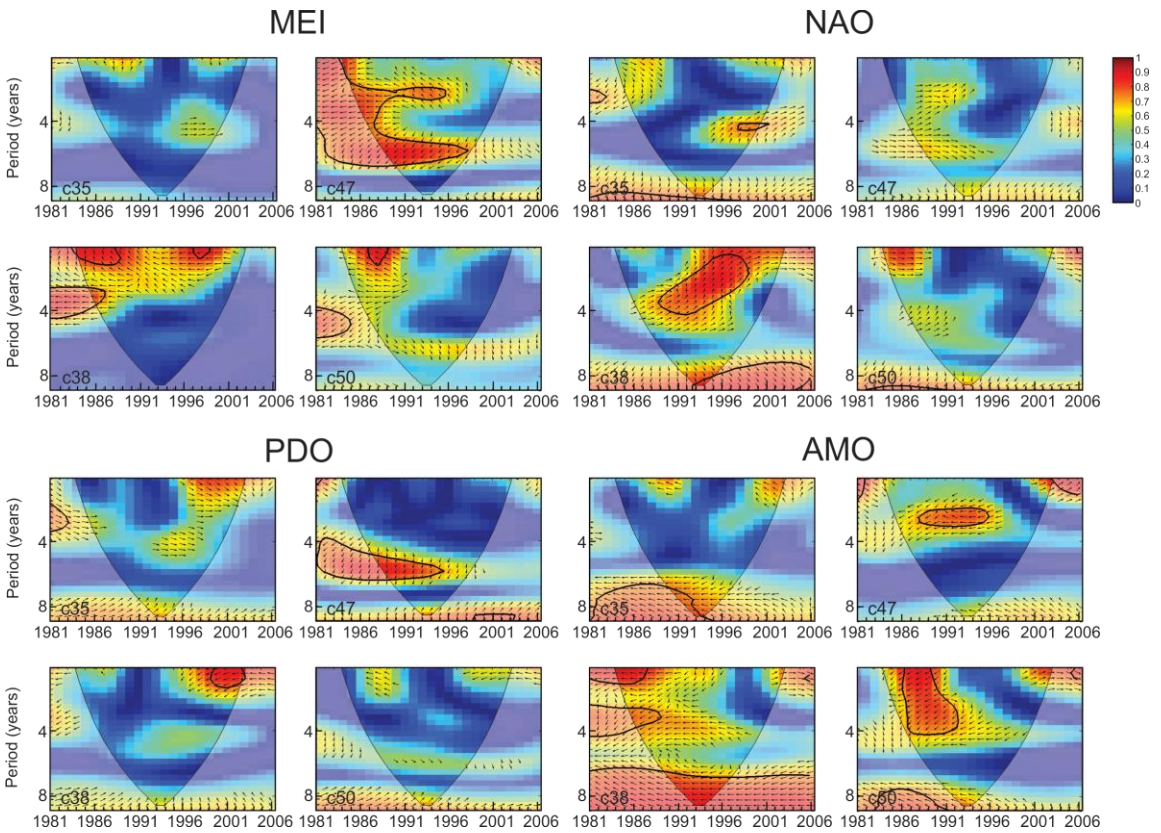


Figure 4.12: Wavelet cross coherence plots using Morlet wavelets showing correlations at each period between yearly TDP yield and MEI, NAO, PDO, and AMO at four catchments in the Turkey Lakes Watershed.

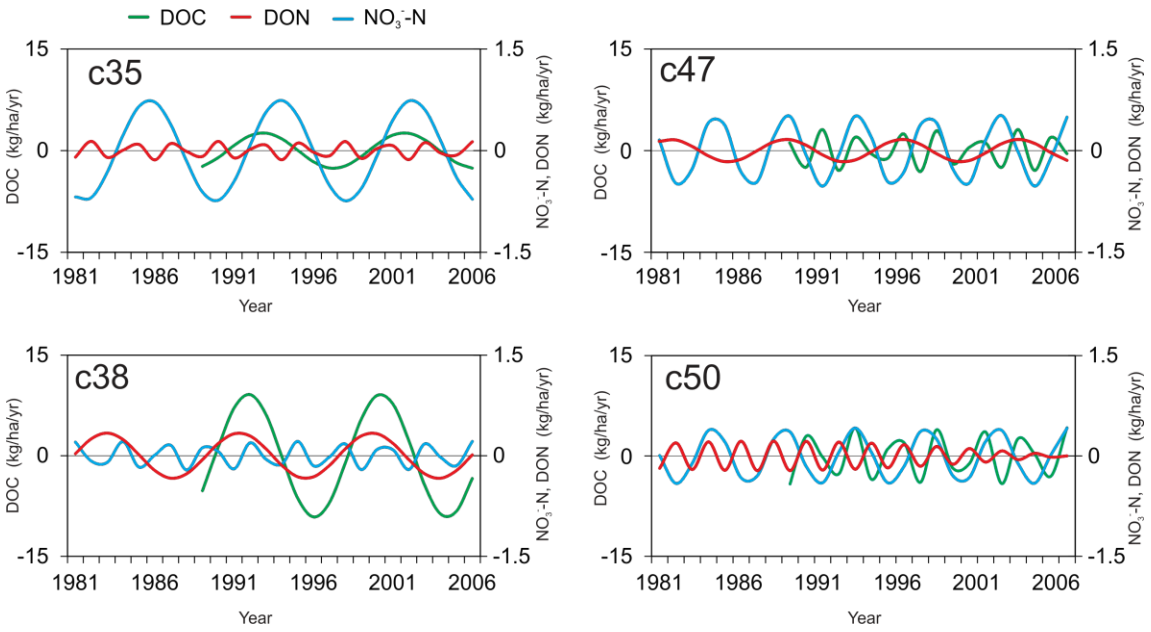


Figure 4.13: Final stationary signal models for DOC, NO_3^--N and DON export.

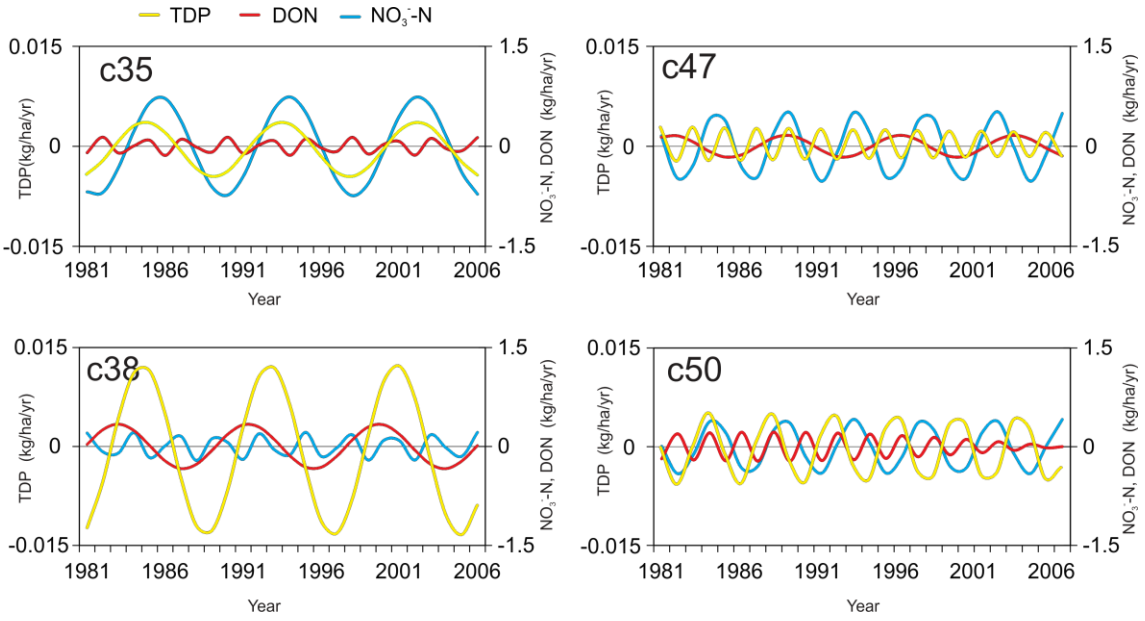


Figure 4.14: Final stationary signal models for TDP, NO_3^--N and DON export.

Table 4.1: Amount of variation and magnitude of change explained by non-stationary (linear) and stationary (periodic) trends in yearly DOC export data from catchments c35, c38, c47 and c50 in the Turkey Lakes Watershed. Data reported are R^2 values ($p < 0.05$; NS indicating not significant relationships), rate of change in export (mm/year) for non-stationary trends and amplitude for stationary cycles.

DOC Export	**C35**	**C38**	**C47**	**C50**
Variation				
Non-stationary signal (%)	NS	NS	NS	NS
Trend + Cycle 1 (%)	*29*	*34*	*20*	*18*
Trend + Cycle 1 + 2 (%)	*53*	*67*	*50*	*53*
Trend + Cycle 1 + 2 + 3 (%)	-[b]	*88*	*69*	-[b]
Stationary Signal (%)[a]	53	88	69	53
Magnitude				
Trend (slope) (g/ha/yr)	NS	NS	NS	NS
Trend related overall change (g/ha) [c]	-[e]	-[e]	-[e]	-[e]
Cycles (amplitude) (g/ha/yr)	±2,587	±9,121	±3,104	±4,217
Cycle related overall change (g/ha) [d]	5,174	18,242	6,208	8,434

[a] Amount of variation explained by the final model minus amount of variation explained by non-stationary trend.

[b] The last stationary signals identified in c35 and c50 DOC export data were not significant.

[c] Calculated as a product of magnitude of rate of decline (slope) and the number of study years.

[d] Calculated by multiplying sample amplitude by 2.

[e] Trend related overall decline was not calculated as the non-stationary signal identified in c38 and c47 NO_3^--N export data were not significant.

Table 4.2: Amount of variation and magnitude of change explained by non-stationary (linear) and stationary (periodic) trends in yearly DON export data from catchments c35, c38, c47 and c50 in the Turkey Lakes Watershed. Data reported are R^2 values ($p < 0.05$; NS indicating not significant relationships), rate of change in export (mm/year) for non-stationary trends and amplitude for stationary cycles.

DON Export	**C35**	**C38**	**C47**	**C50**
Variation				
Non-stationary signal (%)	80	26	29	39
Trend + Cycle 1 (%)	*86*	*43*	*50*	*51*
Trend + Cycle 1 + 2 (%)	*89*	*55*	*67*	*59*
Trend + Cycle 1 + 2 + 3 (%)	-[b]	*69*	*76*	*68*
Trend + Cycle 1 + 2 + 3 + 4 (%)	-[b]	-[b]	-[b]	*73*
Stationary Signal (%)[a]	9	43	47	34
Magnitude				
Trend (slope) (g/ha/yr)	-48	-38	-22	-43
Trend related overall change (g/ha) [c]	1,248	988	572	1,118
Cycles (amplitude) (g/ha/yr)	±137	±336	±163	±221
Cycle related overall change (g/ha) [d]	274	672	326	442

[a] Amount of variation explained by the final model minus amount of variation explained by non-stationary trend.

[b] The last stationary signals identified in c35, c38 and c47 DON export data were not significant.

[c] Calculated as a product of magnitude of rate of decline (slope) and the number of study years.

[d] Calculated by multiplying sample amplitude by 2.

[e] Trend related overall decline was not calculated as the non-stationary signal identified in c38 and c47 NO_3^--N export data were not significant.

Table 4.3: Amount of variation and magnitude of change explained by non-stationary (linear) and stationary (periodic) trends in yearly NO_3^--N export data from catchments c35, c38, c47 and c50 in the Turkey Lakes Watershed. Data reported are R^2 values ($p < 0.05$; NS indicating not significant relationships), rate of change in export (mm/year) for non-stationary trends and amplitude for stationary cycles.

NO_3^--N Export	**C35**	**C38**	**C47**	**C50**
Variation				
Non-stationary signal (%)	28	NS	NS	39
Trend + Cycle 1 (%)	*61*	*31*	*24*	*55*
Trend + Cycle 1 + 2 (%)	*73*	*42*	*39*	*65*
Trend + Cycle 1 + 2 + 3 (%)	*82*	*52*	*60*	-[b]
Trend + Cycle 1 + 2 + 3 + 4 (%)	*85*	-[b]	-[b]	-[b]
Stationary Signal (%)[a]	57	52	60	26
Magnitude				
Trend (slope) (g/ha/yr)	-81	NS	NS	-52
Trend related overall change (g/ha) [c]	2,106	-[e]	-[e]	1,352
Cycles (amplitude) (g/ha/yr)	±740	±213	±521	±413
Cycle related overall change (g/ha) [d]	1,480	426	1,042	826

[a] Amount of variation explained by the final model minus amount of variation explained by non-stationary trend.
[b] The last stationary signals identified in c38, c47 and c50 NO_3^--N export data were not significant.
[c] Calculated as a product of magnitude of rate of decline (slope) and the number of study years.
[d] Calculated by multiplying sample amplitude by 2.
[e] Trend related overall decline was not calculated as the non-stationary signal identified in c38 and c47 NO_3^--N export data were not significant.

Table 4.4: Amount of variation and magnitude of change explained by non-stationary (linear) and stationary (periodic) trends in yearly TDP export data from catchments c35, c38, c47 and c50 in the Turkey Lakes Watershed. Data reported are R^2 values ($p < 0.05$; NS indicating not significant relationships), rate of change in export (mm/year) for non-stationary trends and amplitude for stationary cycles.

TDP Export	**C35**	**C38**	**C47**	**C50**
Variation				
Non-stationary signal (%)	42	16	NS	19
Trend + Cycle 1 (%)	*51*	*49*	*14*	*38*
Trend + Cycle 1 + 2 (%)	*62*	*71*	*32*	*49*
Trend + Cycle 1 + 2 + 3 (%)	-[b]	*77*	-[b]	-[b]
Stationary Signal (%)[a]	20	61	32	30
Magnitude				
Trend (slope) (g/ha/yr)	-0.8	-0.9	NS	-0.6
Trend related overall change (g/ha) [c]	20.8	23.4	-[e]	15.6
Cycles (amplitude) (g/ha/yr)	±4	±12	±3	±5
Cycle related overall change (g/ha) [d]	8	24	6	10

[a] Amount of variation explained by the final model minus amount of variation explained by non-stationary trend.
[b] The last stationary signals identified in c35, c47 and c50 TDP export data were not significant.
[c] Calculated as a product of the magnitude of rate of decline (slope) and the number of study years.
[d] Calculated by multiplying sample amplitude by 2.
[e] Trend related overall decline was not calculated as the non-stationary signal identified in c38 and c47 NO_3^--N export data were not significant.

Table 4.5: Observed stationary signals for DOC, DON, NO_3^--N, and TDP in four catchments in the Turkey Lakes Watershed.

Nutrient	**Signal**	**Periods for observed stationary signals in each catchment (years)**			
		c35	**c38**	**c47**	**c50**
DOC	1	6.7 – 9.5	6.7 – 9.5	6.7 – 9.5	6.7 – 9.5
	2	2.0 – 2.8	2.0 – 2.8	2.0 – 2.8	2.0 – 2.8
	3		3.4 – 4.8	4.0 – 5.7	
DON	1	2.0 – 2.8	5.7 – 8.0	6.7 – 9.5	9.5 – 13.5
	2	3.4 – 4.8	2.0 – 2.8	2.0 – 2.8	5.7 – 8.0
	3		3.4 – 4.8	3.4 – 4.8	2.0 – 2.8
	4				3.4 – 4.8
NO_3^--N	1	5.7 – 8.0	2.0 – 2.8	3.4 – 4.8	3.4 – 4.8
	2	9.5 – 13.5	3.4 – 4.8	5.7 – 8.0	2.0 – 2.8
	3	3.4 – 4.8	9.5 – 13.5	2.0 – 2.8	
	4	2.0 – 2.8			
TDP	1	6.7 – 9.5	6.7 – 9.5	2.0 – 2.8	3.4 – 4.8
	2	2.0 – 2.8	2.0 – 2.8	3.4 – 4.8	2.0 – 2.8
	3		3.4 – 4.8		

magnitude of declines (maximum minus minimum) in nutrient export associated with the linear trend was compared with the range between amplitudes of the nutrient export associated with the overll stationary signal models (Tables 4.1-4.4). For DOC, no significant trends were identified at any catchments and therefore the non-stationary signal was less strong than the stationary signals and dominated variability within the DOC export time series. For DON, NO_3^--N, and TDP, the magnitude of the overall change in the non-stationary signal was larger than the range of variation between the amplitudes of the overall stationary signal (Tables 4.2-4.4). For DON, all catchments had non-stationary signals that accounted for more of the range in the observed export fluxes than any of the identified stationary frequencies. Stationary cycles resulted in greater export of DON from the catchments with high water storage capacity (c38, c50) than those with low water storage (c35, 47). For NO_3^--N, where trends existed, the magnitude of change in nutrient export explained by non-stationary signals was higher than that explained by overall stationary signals. For TDP, signals were more complex. The magnitude of change explained by c38 non-stationary and overall stationary models was almost the same, and there was no significant non-stationary signal for c47, while the magnitude of the non-stationary signal change in c35 and c50 was larger than the overll stationary signal models.

The strength of the non-stationary and stationary signals was also assessed by examining the magnitude of variation in export attributed to each signal (Tables 4.1-4.4). In most catchments, stationary signals explained more variation in nutrient export than non-stationary signals. The exceptions were c35 (low water loading, low water storage), where 0.80 of the total 0.89 variation in DON (i.e., 90%) and 0.42 of the total 0.62 variance in TDP (68%) and c50 (high water loading, high water storage), where 0.39 of the total 0.73 variation in DON (53%) and 0.39 of the total 0.65 variation (60%) in NO_3^--N, were due to the non-stationary signal. For all other catchments and nutrients, the non-stationary signals explained less of the total explained variation in nutrient export (Table 4.1-4.4). Looking at the nutrients, 53% to 0.88% of the variation in DOC concentrations was explained by stationary signals and no significant non-stationary signal was identified in any of the catchments. The other nutrients behaved more similarly to each

other. For DON, 0.09 to 0.47 of the variation was explained by stationary signals; for NO_3^--N, 0.20 to 0.61 of the variation was explained by stationary signals; and for TDP, 0.26 to 0.60 of the variation was explained by stationary signals. Therefore, other nutrients had weaker, but still important stationary signals.

4.4.3 Combined signal strength

Coefficient of determination values were derived by correlating the linear trend model added to the sine wave oscillatory models with the raw data. The combined non-stationary and stationary models were able to explain 66% of variation within DOC, 77% for DON, 66% for NO_3^--N, and 55% for TDP (Tables 4.1-4.4) when averaged across the four catchments. In general, the combined stationary and non-stationary signals were able to explain the most variation in nutrient export in catchments with low water loading (0.72 for both c35 and c38).

4.4.4 Linking climate and nutrient signals

Several stationary signals were correlated with global oscillation indices (Table 4.6). Several correlations were not significantly correlated at $p<0.05$, but are presented to show the general relationships among the catchments and the global oscillations. For DOC, the most prominent stationary signals were most often correlated with the AMO, though only one catchment was significantly correlated. For nitrogen species, the predominant stationary signals were most often correlated with the NAO. For TDP, the results are more heterogeneous and complex than those for the other nutrients, with no clear climate oscillation found to be strongest across catchments.

The very short 2.0 to 2.8 year and the long 9.5 to 13.5 year signals were not significantly correlated to any of the tested global climate oscillations (Table 4.6). The short 3.4 to 4.8 year signals were correlated with the MEI (DON and TDP) and NAO (DON and NO_3^--N) indices. The medium 5.7 to 8.0 and 6.7 to 9.5 year signals were correlated with AMO (DOC and TDP), NAO (DON and NO_3^--) and PDO (TDP). Generally, the earlier cycle (5.7 to 8.0 years) was identified in the nitrogen bearing nutrients (i.e., DON, NO_3^--N)), while the later cycle (6.7 to 9.5 years) was identified in the carbon and phosphorus bearing nutrients.

Table 4.6: Results of Pearson correlation tests between isolated stationary signals (short = 3.4 to 4.8 year cycle; medium = 5.7 to 8.0 or 6.7 to 9.5 year cycle) and climate oscillation indices. Several correlations were not significantly correlated at $p<0.05$, but are presented to show the general relationships among the catchments and the global oscillations.

Signal	c35			c38			c47			c50		
	Index	r^2 (Dir)	P	Index	r^2 (Dir)	P	Index	r^2 (Dir)	P	Index	r^2 (Dir)	P
DOC												
Short												
Medium	AMO	0.20 (-)	0.065	AMO	0.28 (-)	0.024				AMO	0.20 (-)	0.065
DON												
Short	MEI	0.16 (-)	0.042	MEI	0.20 (-)	0.024	NAO	0.13 (-)	0.073	NAO	0.15 (-)	0.049
Medium							NAO	0.22 (+)	0.016	NAO	0.18 (+)	0.033
NO_3^--N												
Short				NAO	0.14 (+)	0.056	NAO	0.15 (+)	0.052	NAO	0.14 (+)	0.057
Medium	NAO	0.22 (-)	0.015									
TDP												
Short				MEI	0.12 (-)	0.089	MEI	0.19 (-)	0.025	MEI	0.17 (-)	0.038
Medium	PDO	0.14 (+)	0.063	AMO	0.22 (-)	0.015						

4.4.5 Differential sensitivity of catchments

Catchments did not respond in a homogeneous manner to environmental changes occurring within the region. The two catchments with lower water loading showed greater variability in nutrient export signals. For example, c35 (low water loading, low water storage) generally had the strongest linear trends [i.e., largest magnitude of linear decline in nutrient export flux and largest coefficient of determination values (Table 4.1-4.4)] for nutrients that showed trends. In contrast, c38 (low water loading, high water storage) generally had strongest stationary signals for dissolved organic nutrients [i.e., stationary signals with largest nutrient export amplitudes and largest coefficient of determination value (Table 4.1-4.4)], but the amplitude of the stationary signal was among the smallest for NO_3^--N even though c38 NO_3^--N stationary signals has modest coefficient of determination to explain variability in NO_3^--N export. A combination of catchments is needed to capture climate effects on nutrient export – c35 was the most sensitive to directional climate change, while c38 was most sensitive for detecting climatic oscillations (Table 4.1-4.4).

4.5 Discussion

The effects of climate change on water quality and quantity are not clearly understood (Whitehead *et al.*, 2009). Contributions of non-stationary and stationary climate signals to nutrient export were discriminated in four catchments on a forested landscape. There are few studies that focus on the links between nutrient export from headwater catchments and that discriminate between climate trends vs. multiple climate oscillations, so in this study we highlight the patterns, and suggest processes to explain them (including those that influence nutrient export through changes in hydrological flow partitioning and pathways and/or biogeochemical rates of reactions), which can be tested in future studies.

4.5.1 Climate signals in nutrient export

Both non-stationary and stationary signals were detected in nutrient export in the Turkey Lakes Watershed over a 26-year period. Non-stationary signals were declines in nutrient export (with the exception of DOC which had no directional change), while (multiple) stationary signals had the effect of increasing or decreasing the magnitude of the decline

in nutrient export. Specifically, the combination of signals led to larger declines in nutrient export during the warmer/drier portions of the oscillations (reflected in positive MEI, positive AMO and/or negative NAO), and to smaller declines in export during the cooler/wetter portions of the oscillations. There was one exception, c35, which had low water loading, low water storage, and where warmer, drier conditions lead to further increases in some of the nutrients, NO_3^--N and TDP. This finding is supported by previous studies that show that during cooler, wetter water years, hydrological flow paths may be expanded into new biogeochemical source areas (e.g., vertical (up the soil column) and horizontal (up the contributing hillslopes into the outer extents of the variable source area)) flushing nutrients from near surface and surface soils, while in warmer, drier water years, hydrological flow paths may be contracted (e.g., Creed *et al.*, 1996; Creed and Band, 1998). The consequence is that global climate warming appears to be leading to reduced nutrient export that can be further reduced when oscillations enter a warm, dry period.

The multiple stationary signals occurred at very short (2.0 to 2.8 yr), short (3.4 to 4.8 yr), medium (either 5.7 to 8.0 yr or the overlapping period of 6.7 to 9.5 yr), and/or occasionally at long (9.5 to 13.5 yr) frequencies. The very short signal was observed for all nutrients in all catchments but was not significantly correlated to any of the tested global climate oscillations as the periodicity of these signals was very short compared to the periodicity of the tested climatic oscillations. The short signal was correlated with both the MEI and NAO. This signal falls within the observed MEI periodicity (Huggett, 1997), and the NAO does not have a statistically significant periodicity (Burroughs, 2005). MEI and NAO were also found to be significantly correlated with each other (Mengistu *et al.*, 2012), which may suggest a common climate oscillation influencing the catchments. The medium signal was identified in many catchments, at either 5.7 to 8.0 years or the overlapping period of 6.7 to 9.5 years and was most often correlated with the AMO. The periodicity of the AMO is approximately 60 to 90 years (Knudsen *et al.*, 2011), but previous work has shown that the AMO is strongly correlated with temperature in the Algoma Highlands and may explain about half of the observed temperature increase in the area over the past three decades (Mengistu *et al.*, 2012). The long signal was not significantly correlated to any of the four global climate oscillations.

These findings suggest that multiple oscillations are controlling nutrient export and that some are linked to global climatic oscillations and others are not (and remain unexplained) in part because longer time series are needed.

4.5.2 Non-stationary signals obscure the contributions of stationary signals

Compared to stationary signals, non-stationary signals contribute more to the overall change in nutrient export dynamics due to having higher rates of decline in nutrient export resulting greater cumulative changes over time. For catchments with observed non-stationary signals, the magnitudes of decline associated with the non-stationary signals during the study period were compared with the ranges between the amplitudes of the overall stationary signals (Tables 4.1- 4.4). Non-stationary signals obscure the contributions of stationary signals as non-stationary signals revealed greater over all decline in the magnitude of nutrient export (approximately 572 to 1,248 g/ha for DON; 1,352 to 2,106 g/ha for NO_3^--N; 16 to 23 g/ha for TDP) compared to the ranges explained by the amplitudes of the overall stationary signals (approximately 274 to 672 g/ha for DON: 426 to 1,480 g/ha for NO_3^--N; 6 to 24 g/ha for TDP).

4.5.3 Differential sensitivity of metabolically labile vs. recalcitrant nutrients

Both non-stationary and stationary climate signals were observed to affect nutrient export fluxes. First, for non-stationary signals, Mengistu *et al*. (2012) reported an average decline in water yields of 9.25 mm/yr among these same catchments, but no significant negative linear trends were detected in DOC export flux data (Table 4.1). The fact that water yield declined but DOC in discharge did not suggests that climate has a concentrating effect on DOC export: less water is being exported over time but the amount of DOC being exported is staying the same or even increasing relative to the amount of water being exported. This is supported by reports of trends for increasing DOC concentrations in streams draining forested headwater catchments both in North America (Eimers *et al.*, 2008) and Europe (Worrall and Burt, 2007; Sarkkola *et al.*, 2009). These studies suggest that changes in stream flow have an important role on trends in DOC concentration. In contrast to DOC, significant negative trends were detected in DON, NO_3^--N, and TDP export flux data of most catchments (except c38 and c47 NO_3^--N,

and c47 TDP) (Tables 4.2- 4.4). Dillon and Molot (2005) observed a much greater decrease in total phosphorus and DON compared to DOC in Dorset, Ontario, so mobilization of these nutrients from wetlands is sensitive to changes in water table position and redox levels. It is possible that DON, NO_3^--N and TDP are more labile than DOC (Stepanauskas *et al.,* 2000; Kaushal and Lewis, 2005; Lønborg and Álvarez-Salgado, 2012; Hendrickson *et al.,* 2002), and that with warmer, drier conditions, these more labile nutrients are more preferentially metabolized instead of being exported. If DON, NO_3^--N and TDP are preferentially metabolized, then this finding suggests that there is a shift from more to less labile DOM entering the surface waters as a result of climate warming trends (i.e., shift towards higher C/N ratios).

Second, the overall magnitude of declines in nutrient export associated with the linear trend was compared with the magnitude of the range between the amplitudes of the nutrient export associated with the overall stationary signal model (Tables 4.1- 4.4). For DOC, no significant trends were identified in any catchments and therefore the non-stationary signal was less strong than the overall stationary signal that dominated variability within the DOC nutrient export, which ranged from approximately 5, 174 g/ha to 18,242 g/ha (Table 4.1). For catchments with observed non-stationary signals, the magnitudes of decline associated with the non-stationary signals (approximately 572 to 1,248 g/ha for DON; 1,352 to 2,106 g/ha for NO_3^--N; 16 to 23 g/ha for TDP) were larger than the ranges explained by the amplitudes of the overall stationary signals (approximately 274 to 672 g/ha for DON: 426 to 1,480 g/ha for NO_3^--N; 6 to 24 g/ha for TDP) (Tables 4.2- 4.4). If non-stationary signals are linked to global warming [even if only 50% at most, as was the case for water yield reported in Mengistu *et al*. (2012)], then this suggests that anthropogenic global warming trends have had a greater role in reducing labile (N, P) nutrient loads than natural global warming oscillations at multiple time scales of years to decades. Generally, catchments with high water storage potential (c38 and c50) appeared to show larger amplitudes in the overall stationary signal model of DOC, DON and TDP exports compared to catchments of lower hydrologic storage potential. However, the overll stationary signal from these catchments revealed smaller amplitude for NO_3^--N export.

In general, nitrogen and phosphorus species appear to be more responsive (more labile) than carbon to both climate trends and climate oscillations. This may be due to several reasons: (1) there are greater concentrations of nitrogen and phosphorus in surface and near-surface layers (shoots and roots, litter fall) where climate reactions dominate at the land-surface interface (Devito *et al.*, 2000*;* Liu *et al.*, 2003*;* Marland *et al.*, 2003; Macrae *et al.*, 2005); (2) there could be higher rates of transformation at this land-surface interface due to warmer temperatures; (3) there could be more redox switching from oxidizing to reducing environments due to rising water tables and/or expanding/ contracting surface flows (Creed *et al.*, 2011); and/or (4) nitrogen and phosphorus compounds may have greater mobility along the surface/near-surface hydrologically connected flow pathways (Creed *et al.*, 1996; Devito *et al.*, 2000). These changes have implications for the stoichiometry of exported nutrients and therefore on the productivity and biodiversity of downstream waters *(*Seitzinger *et al., 2005;* Justic *et al., 2005;* Donner and Scavia, 2007). Exported nutrient stochoimetry is also influenced by oscillation linked catchment responses in nutrient transport that results temporally dynamic phase relationships leading to a variable ratio between ecologically important nutrients parameters (Figures 4.13, 4.14). Catchments with lower water loading capacity appeared have extreme stoichiometry, c35 and c38 catchments respectively revealing lowest and highest stoichiometry in both C:N and P:N ratios. Future studies will focus not only on DOM but also on DOM constituents to investigate if there are differences among labile vs. recalcitrant DOC pools. Measuring DOC properties (e.g., SUVA, Fluorescence Index) might reveal a biogeochemical signature that would provide insight into fate of the DOC (e.g., Thurman, 1985; McKnight *et al.*, 2003; Cory *et al.*, 2011).

4.5.4 Differential sensitivity among the catchments

Catchments did not respond in a homogeneous manner to environmental changes occurring within the region. Despite a small range in annual average water loading (up to 10%), climate had a greater effect on nutrient export signals in catchments with lower water loading. The catchment with low water loading and low water storage capacity, c35, generally had the largest declines in nutrient export flux and the most variation explained by non-stationary signals for nutrients that showed trends (Tables 4.2-4.4). The

catchment with low water loading and high water storage, c38, generally had stationary signals with the largest nutrient export amplitudes and the most variation explained, although the magnitude of stationary signal variations were among the smallest for NO_3^--N export (Tables 4.2-4.4).

Water storage capacity has a potentially strong effect on nutrient export by influencing water residence time in the catchment during which biogeochemical transformations can occur that may alter the fate (i.e., storage vs. atmospheric or aquatic export) of nutrients. For example, organic matter decomposes and is metabolized quickly during the snowfree season in catchments with low water storage capacity (Ponnamperuma, 1972; Sahrawat, 2004; Moore *et al*., 2008). In contrast, organic matter can be trapped in catchments with high water storage capacity and decomposition slows down. When the water table drops, oxidation may lead to preferential removal of more labile nutrients, and when the water table rises, the remaining more recalcitrant nutrients will become exported as storage capacity fills and water flows through the catchment (Webster *et al.*, 2008; Creed and Beall, 2009; Creed *et al.*, 2012).

4.5.5 Catchments as sentinels of changing nutrient exports

Are headwater catchments good sentinels of climate change? To answer this question, we consider both the predictability and vulnerability of nutrient export in headwater catchments under changing environmental conditions. For predictability, in most cases, the non-stationary signals explained less variation in nutrient export than stationary signals, suggesting that global climate warming had a smaller (lesser) influence on nutrient export than global climate oscillations. However, in c35, the catchment with low water storage and low water loading, the non-stationary signal explained more variation, suggesting that catchments with few to no wetlands that receive relatively less water may be most sensitive to climate change. On this humid landscape, catchments with less water loading and storage appeared to be more sensitive to changes in climatic conditions. By examining the total variance of the nutrient export explained by stationary and non-stationary signals, it is possible to understand what catchments were most sensitive to climate. Combined signals tended to explain more of the nutrient export variance in catchments with lower water loading potential, a similar pattern to that

observed in water yield (Mengistu *et al.*, 2012). Combined signals for nitrogenous nutrients were strongest in c35, while c38 had the highest amount of variance explained for DOC and TDP. For vulnerability, some catchments showed substantial variation in nutrient export over the observed period. Catchment c35 showed the greatest range in inorganic nutrient export, NO_3^--N, with stationary signals varying by as much as 1480 g NO_3^--N/ha (average annual export for this catchment is 3500 g NO_3^--N/ha/yr, *Creed and Beall*, 2009) and trends showing declines of about 81 g NO_3^--N/ha/yr (for a total of more than 2000 g NO_3^--N/ha over the observed period). This catchment has little accumulation of organic matter because of the steep slopes, shallow soils and minimal water storage capacity. In contrast, c38 showed the greatest range in the export of organic nutrients, DOC, DON and TDP. Minimum and maximum values of the stationary signals ranged by as much as 18,242 g DOC/ha, 672 g DON/ha and 24 g TDP/ha, and linear trends showed declines of 40 g/ha/yr for DON and 0.9 g/ha/yr for TDP (no significant trends for DOC).

Comparing these results with observed stationary and non-stationary signals in water yield (Mengistu *et al.*, 2012), the non-stationary signal explained more variation in magnitude than the overlll stationary signals in c35 for nutrients with observed significant non-stationary signal, showing that there is a link between water yield and nutrient export, but there are also differences. In nearly every case, for catchments where no non-stationary trend was detected, the change in nutrient export related to stationarity was much greater than the variation explained by the non-stationary trends. This suggests that surface water quality is already shifting away from historical ranges controlled by natural fluctuations, and this could be very important for ecosystems adjusted for the levels of the past.

To effectively monitor the effects of both non-stationary and stationary signals of climate on headwater catchments, a combination of catchments is needed to capture climate effects on nutrient export. The catchment with low water loading and low water storage, c35, was the most sensitive to directional climate change, while the catchment with low water loading and high water storage, c38, was most sensitive for detecting climatic oscillations. This suggests that catchments with relatively low water loading and low water storage capacity are good sentinels for detecting the effects of anthropogenic

climate change on nutrient export. In contrast, catchments with relatively low water loading but high water storage are good sentinels for detecting natural climatic oscillations and their effect on nutrient export.

4.6 Conclusions

Climate warming and changes in atmospheric circulation that leads to climatic oscillations have resulted in clear reductions in water and nutrient export from the Turkey Lakes Watershed over the past three decades. Complex links were revealed between non-stationary and stationary changes in climatic conditions *versus* nutrient export to surface waters. More variation was explained in labile nutrients (DON, NO_3^--N, TDP), and these nutrients were also more sensitive to climate signals. Overall, the catchment with low water storage potential and low water loading potential was the most sensitive to non-stationary and stationary climatic conditions, suggesting that it was the most effective sentinel for a dynamic climate. Although we used one of the longest data sets available in Canada, even longer sets would allow the detection of signals with longer periodicities. Applying the framework to other catchments in the Turkey Lakes Watershed and around the world will determine the broad implications of these results.

4.7 References

Adrian R, O'Reilly CM, Zagarese H, Baines SB, Hessen DO, Keller W, Livingstone DM, Sommaruga R, Straile D, Van Donk E, Weyhenmeyer GA, Winder M. 2009. Lakes as sentinels of climate change. *Limnology and Oceanography* **54**. DOI: 10.4319/lo.2009.54.6_part_2.2283.

Bishop K, Buffam I, Erlandsson M, Folster J, Laudon H, Seibert J, Temnerud J. 2008. Aqua Incognita: the unknown headwaters. *Hydrological Processes* **22**. DOI: 10.1002/hyp.7049.

Blenckner T, Adrian R, Livingstone DM, Jennings E, Weyhenmeyer GA, George DG, Jankowski T, Jarvinen M, Aonghusa CN, Noges T, Straile D, Teubner K. 2007. Large-scale climatic signatures in lakes across Europe: a meta-analysis. *Global Change Biology* **13**. DOI: 10.1111/j.1365-2486.2007.01364.x.

Burroughs WJ. 2005. Cycles and periodicities. In Encyclopedia of World Climatology, Oliver JE (ed). Springer-Dordrecht: The Netherlands; 173-177.

Canada Soil Survey Committee. 1978. Canadian system of soil classification. Publ. 1646, 164 pp., Dep. of Agri., Ottawa.

Cory RM, Boyer EW, McKnight DM. 2011. Spectral Methods to Advance Understanding of Dissolved Organic Carbon Dynamics in Forested Catchments. *Forest Hydrology and Biogeochemistry: Synthesis of Past Research and Future Directions* **216**. DOI: 10.1007/978-94-007-1363-5_6.

Creed IF, Band LE. 1998. Export of nitrogen from catchments within a temperate forest: Evidence for a unifying mechanism regulated by variable source area dynamics. *Water Resources Research* **34**. DOI: 10.1029/98WR01924.

Creed IF, Band LE, Foster NW, Morrison IK, Nicolson JA, Semkin RS, Jeffries DS. 1996. Regulation of nitrate-N release from temperate forests: A test of the N flushing hypothesis. *Water Resources Research* **32**. DOI: 10.1029/96WR02399.

Creed IF, Trick CG, Band LE, Morrison IK. 2002. Characterizing the spatial heterogeneity of soil carbon and nitrogen pools in the Turkey Lakes Watershed: A comparison of regression techniques. *Water Air Soil Pollution. Focus* **2**: 81-102.

Creed IF, Beall FD. 2009. Distributed topographic indicators for predicting nitrogen export from headwater catchments. *Water Resources Research* **45**: W10407. DOI: 10.1029/2008WR007285.

Creed IF, Beall FD, Clair TA, Dillon PJ, Hesslein RH. 2008. Predicting export of dissolved organic carbon from forested catchments in glaciated landscapes with shallow soils. *Global Biogeochemical Cycles* **22**: GB4024. DOI: 10.1029/2008GB003294.

Creed IF, Sass GZ, Beall FD, Buttle JM, Moore RD, Donnelly M. 2011a. Hydrological principles for conservation of water resources within a changing forested landscape: A State of Knowledge Report. *Sustainable Forest Management Network*, Edmonton, Alberta.

Creed IF, Enanga EM, Mengistu SG, Beall FD, Hazlett P. 2011b. Role of redox surfaces in explaining catchment nitrogen export across multiple spatial and temporal scales. *American Geophysical Union Fall Meeting*, December 5-9, San Francisco, CA.

Creed IF, Webster KL, Braun GL, Bourbonniere RA, Beall FD. 2012. Topographically regulated traps of dissolved organic carbon create hotspots of carbon dioxide efflux from forest soils. *Biogeochemistry*, In Press.

Devito K, Creed I, Rothwell R, Prepas E. 2000. Landscape controls on phosphorus loading to boreal lakes: implications for the potential impacts of forest harvesting. *Canadian Journal of Fisheries and Aquatic Sciences* **57**: 1977-1984. DOI: 10.1139/cjfas-57-10-1977.

Dillon PJ, Molot LA. 2005. Long-term trends in catchment export and lake retention of dissolved organic carbon, dissolved organic nitrogen, total iron, and total phosphorus: The Dorset, Ontario, study, 1978-1998. *Journal of Geophysical Research-Biogeosciences* **110**: G01002. DOI: 10.1029/2004JG000003.

Giblin PE, Leahy EJ. 1977. Geological compilation of the Batchawana sheet, Districts of Algoma and Sudbury, Ontario. Preliminary Map 302, Geol. Surv. Can., Ontario.

Grinsted A, Moore J, Jevrejeva S. 2002. Cross wavelet and wavelet coherence Matlab Package. Downloaded from http://www.pol.ac.uk/home/research/waveletcoherence/ on October 15, 2011.

Grinsted A, Moore J, Jevrejeva S. 2004. Application of the cross wavelet transform and wavelet coherence to geophysical time series. *Nonlinear Processes in Geophysics* **11**: 561-566.

Hansen J, Sato M, Ruedy R. 2012. Perception of climate change. *Proceedings of the National Academy of Sciences of the United States of America* **109**.

Huggett RJ. 1997. Environmental change. The evolving ecosphere. Routledge: London; 119.

Intergovernmental Panel on Climate Change. 2007. Assessment Report of the Intergovernmental Panel on Climate Change. In Climate Change 2007: Synthesis Report, Pachauri RK, Reisinger

A (eds). Contribution of Working Groups I, II and III to the Fourth Assessment Report of the Intergovernmental Panel on Climate Change, *IPCC: Geneva*.

Jeffries DS, Kelso JRM, Morrison IK. 1988. Physical, Chemical, and Biological Characteristics of the Turkey Lakes Watershed, Central Ontario, Canada. Canadian *Journal of Fisheries and Aquatic Sciences* **45**: 3-13.

Jones JA, Creed IF, Hatcher KL, Warren RJ, Adams MB, Benson MH, Boose E, Brown WA, Campbell JL, Covich A, Clow DW, Clifford CN, Elder K, Ford CR, Grimm NB, Henshaw DL, Larson KL, Miles ES, Miles KM, Sebestyen S, Spargo AT, Stone AT, Vose JM, Williams MW. 2012. Ecosystem Processes and Human Influences Regulate Streamflow Response to Climate Change at Long-Term Ecological Research Sites. BioScience **62**: 390-404.

Kang S, Lin H. 2007. Wavelet analysis of hydrological and water quality signals in an agricultural watershed. *Journal of Hydrology* **338**. DOI: 10.1016/j.jhydrol.2007.01.047.

Kaushal SS, Lewis WM. 2005. Fate and transport of organic nitrogen in minimally disturbed montane streams of Colorado, USA. *Biogeochemistry* **74**: 303-321. DOI: 10.1007/s10533-004-4723-5.

Kiem AS, Franks SW. 2001. On the identification of ENSO-induced rainfall and runoff variability: a comparison of methods and indices. *Hydrological Sciences Journal-Journal Des Sciences Hydrologiques* **46**. DOI: 10.1080/02626660109492866.

Knudsen MF, Seidenkrantz M, Jacobsen BH, Kuijpers A. 2011. Tracking the Atlantic Multidecadal Oscillation through the last 8,000 years. *Nature Communications* **2**: 178. DOI: 10.1038/ncomms1186.

Liu W, Fox JED, Xu Z. 2003. Nutrient budget of a montane evergreen broad-leaved forest at Ailao Mountain National Nature Reserve, Yunnan, southwest China. *Hydrological Processes* **17**: 1119-1134. DOI: 10.1002/hyp.1184.

Marland G, Pielke RA, Apps M, Avissar R, Betts RA, Davis KJ, Frumhoff PC, Jackson ST, Joyce LA, Kauppi P, Katzenberger J, MacDicken KG, Neilson R, Niles JO, Niyogi DS, Norby RJ, Pena N, Sampson N, Xue Y. 2003. The climatic impacts of land surface change and carbon management, and the implications for climate-change mitigation policy. *Climate Policy* **3**: 149-157. DOI: 10.1016/S1469-3062(03)00028-7.

McKnight DM, Hood EW, Klapper L. 2003. Trace organic moieties of dissolved organic material in natural waters. In *Aquatic Ecosystems: Interactivitiy of Dissolved Organic Matter*, Findlay SEG, Sinsabaugh RL (eds). Academic Press: San Diego; 71–96.

Mengistu, SG, Creed IF, Kulperger RJ, Quick CG. 2012. Russian nesting dolls effect – Using wavelet analysis to reveal non-stationary and nested stationary signals in water yield from catchments on a northern forested landscape. Hydrol. Process. In press. doi: 10.1002/hyp.9552

Moore TR, Trofymow JA, Siltanen M, Kozak LM. 2008. Litter decomposition and nitrogen and phosphorus dynamics in peatlands and uplands over 12 years in central Canada. *Oecologia* **157**. DOI: 10.1007/s00442-008-1076-0.

Paerl HW, Paul VJ. 2012. Climate change: Links to global expansion of harmful cyanobacteria. *Water research* **46**. DOI: 10.1016/j.watres.2011.08.002.

Ponnamperuma FN. 1972. The chemistry of submerged soils. *Advances in Agronomy* **24**: 29–96.

Sahrawat K. 2004. Organic matter accumulation in submerged soils. *Advances in Agronomy* **81**: 169-201. DOI: 10.1016/S0065.2113(03)81004-0.

Seitzinger SP, Harrison JA, Dumont E, Beusen AHW, Bouwman AF. 2005. Sources and delivery of carbon, nitrogen, and phosphorus to the coastal zone: An overview of Global Nutrient Export from Watersheds (NEWS) models and their application. *Global Biogeochemical Cycles* **19**: GB4S01. DOI: 10.1029/2005GB002606.

Semkin RG, Jeffries DS, Neureuther R, Lahaie G, Norouzian F, Franklyn J. 2001. Summary of hydrological and meteorological measurements in the Turkey Lakes Watershed, Algoma, Ontario, 1980–1999 National Water Research Institute, Environment Canada, Burlington, Ontario.

Strand LT, Haaland S, Kaste O, Stuanes AO. 2008. Natural variability in soil and runoff from small headwater catchments at Storgama, Norway. *Ambio* **37**: 18-28. DOI: 10.1579/0044 7447(2008)37[18:NVISAR]2.0.CO;2.

Thurman EM. 1985. *Organic geochemistry of natural waters*. Nijoff/Junk Publishers: Boston.

Torrence C, Compo GP. 1998. A practical guide to wavelet analysis. *Bulletin of the American Meteorological Society* **79**: 61-78. DOI: 10.1175/1520-0477(1998)079<0061:APGTWA>2.0.CO;2.

Webster KL, Creed IF, Bourbonniere RA, Beall FD. 2008. Controls on the heterogeneity of soil respiration in a tolerant hardwood forest. *Journal of Geophysical Research-Biogeosciences* **113**: G03018. DOI: 10.1029/2008JG000706.

Whitehead PG, Wilby RL, Battarbee RW, Kernan M, Wade AJ. 2009. A review of the potential impacts of climate change on surface water quality. *Hydrological Sciences Journal-Journal Des Sciences Hydrologiques* **54**. DOI: 10.1623/hysj.54.1.101.

Wickware GM, Cowell DW. 1985. Forest Ecosystem Classification of the Turkey Lake Watershed, Ecol. Classif. Ser. 18, Lands Dir., Environ, Ottawa, Canada.

Williamson CE, Dodds W, Kratz TK, Palmer MA. 2008. Lakes and streams as sentinels of environmental change in terrestrial and atmospheric processes. *Frontiers in Ecology and the Environment* **6**. DOI: 10.1890/070140.

Wolter K, Timlin MS. 1998. Measuring the strength of ENSO events: How does 1997/98 rank? *Weather* **53:** 315-323.

Chapter 5: Conclusion

5.1 Research Findings

This dissertation used a combination of spatial analysis, statistical modeling and wavelet analysis to investigate the relationship between topography and the spatial and temporal controls of water and nutrient export from small headwater catchments in the Turkey Lakes Watershed (TLW) that are dominated by otherwise uniform vegetation and bedrock geology. The major contributions of this thesis are the (1) understanding of the role of various topography related catchment spatial characteristics on the export of nutrients; (2) explanation of the mechanism of topography regulated hydrologic control on the export behaviour dissolved organic carbon (DOC), dissolved organic nitrogen (DON), nitrate-nitrogen (NO_3^--N), and total dissolved phosphorus (TDP); (3) development of an analytical framework to detect non-stationary (linear trends) and nested stationary (non-linear oscillations) signals from catchment yearly water yield and nutrient export responses; (4) understanding of the relative sensitivity of TLW headwater catchments to climatic forcing by quantifying the variability explained by non-stationary and nested stationary components of catchment responses; and (5) identification of the dominant climatic oscillations that have detectable periodic patterns in the yearly time series of water yield and nutrient export parameters.

Chapter 2 tested the hypothesis that topography was the most organizing template for hydrology influenced nutrient export control from thirteen relatively undisturbed headwater catchments in the TLW. Several topography related metrics of hydrological flushing potential (e.g. VSA, *eff*VSA) and hydrological storage potential (e.g. flats, depressions) were derived following the methods outlined in Creed and Beall (2009), which were then statistically assessed for their role in explaining the observed spatial variance in nutrient export behaviours among the studied catchments. Topographic metrics representing hydrological flushing and hydrological storage explained most of the spatial variance in nutrient export. Higher redox potential (oxygenation) in *eff*VSAs when water tables are relatively low favours nitrification (oxidation of NH_3^+-H to NO_3^--N),

making *eff*VSA a net source of NO_3^--N. The strong positive association observed between *eff*VSA and catchment NO_3^--N export suggests flushing of accumulated NO_3^--N from the *eff*VSA as the main mechanism of NO_3^--N export when the water table rises and intersects the soil layer. *Eff*VSA also showed moderately strong but negative association with export of organic forms of nutrients (DOC, DON) and TDP, suggesting continued mineralization of organic matter and adsorption of organic matter by mineral soils before transported to receiving water bodies.

Metrics reflecting hydrological storage, however, showed significant positive relationships with DOC, DON and TDP, suggesting that an increase in the relative proportion of depression and flats in a catchment would increase the export of organic forms of nutrients due to presence of hydrologic features favouring mechanisms of organic matter production in the catchment. There was a significant negative relationship between metrics reflecting hydrologic storage and NO_3^--N export, suggesting that wetlands positioned along the hydrologic pathway can intercept NO_3^--N loaded runoff before reaching streams, becoming sinks of NO_3^--N by facilitating its conversion to organic matter or its alternative route in the form of gas efflux from denitrification.

The focus of Chapter 2 was to investigate the relationship between topography and temporal responses to climate signals in water yield time series from the TLW. The sensitivity of four topographically and hydrologically representative headwater catchments were analyzed to test the hypothesis that annual water yield time series are composed of a complex mixture of non-stationary linear and cyclic stationary climatic trends that are manifested differently in catchments with different topographic organization. An analytical framework was developed to reveal if the selected catchments had differential sensitivity to non-stationary climate change and naturally occurring stationary climate oscillations in water yield time series over 28 years. The variability explained by non-stationary signals from annual water yield time series were independently analyzed, and wavelet analysis was employed to disassociate the remaining stationary component into signals of various periodicities.

The analytical framework detected non-stationary (linear) declines in all catchment water yield data except catchment c47 and three major stationary cycles in the water yields in all the studied catchments. The observed non-stationary catchment

responses may have been linked to the unidirectional global warming of one-degree Celcius per decade rise in temperature in the region. Stationary responses might be linked to climate oscillations, including AMO, NAO, PDO and ENSO. Each of these global climatic oscillation indices showed correlation with catchment water yield, even though the timing, persistence, and direction of correlation varied. Despite the limitation of having only 28 years of water yield data, cross coherence analysis revealed that AMO showed the strongest influence in the regional hydrology, with consistently high negative correlations. AMO also exhibited strong correlations with TLW climatic variables, suggesting it might partially explain the unidirectional global warming experienced in TLW region.

Generally, catchments with different topographic organizations exhibited differential sensitivity to climate change signals. Catchments with lower water loading and lower water storage potential showed a stronger decline in water yield over time compared to catchments with higher water loading and higher water storage potentials. The catchment with the lowest water loading and the lowest water storage potential (c35) was the most sensitive to non-stationary signals, while the catchment with the highest water loading and the lowest water storage potential (c47) was the least sensitive to non-stationary climatic signal, suggesting that non-stationarity is affected more by water loading potential than water storage potential. Catchments with higher water storage potential, however, appeared to buffer fluctuations in water yield associated with shorter-term periods.

The main focus of Chapter 4 was investigating topographic influences on climate related catchment temporal responses in nutrient export. The analytical framework that was developed and tested in Chapter 3 was applied to detect non-stationary and stationary signals in yearly time series of DOC, DON, NO_3^--N, and TDP nutrient export. There was a significant negative non-stationary (linear) trend in all nutrients except DOC. The lack of significant declines in DOC coupled with the significant declines in water yield declines suggest that there is a concentrating effect of climate on DOC. Significant nested stationary signals were also detected in all nutrient export data and in all catchments at very short (2 to 3 year), short (3 to 5 year), medium (5 to 9 year) and long (9 to 13 year) scales. Some of the observed stationary signals were linked to global climatic

oscillations, but others were not, in part because longer time series are needed to detect oscillations of longer periodicities.

In general, the combined stationary and non-stationary signals were able to explain most of the variation in nutrient export, with more variation explained in catchments with low water loading potential. The non-stationary linear trend explained the most variation in the catchment with relatively low water loading and low water storage capacity, suggesting these traits are characteristic of good sentinels for detecting the effects of anthropogenic climate change on nutrient export. In contrast, stationary trends explained the most variation in the catchment with relatively lower water loading but higher water storage potential, suggesting these catchment topographic organizations may be good sentinels for detecting natural climatic oscillations and their effect on nutrient export. More variation was explained in metabolically more active or labile nutrients (DON, NO_3^--N, TDP) than metabolically less active nutrients (DOC), and these nutrients were also more sensitive to climate signals.

While wavelet and wavelet coherence analyses are becoming more widespread when studying hydrological time series and relationships between time series, this chapter takes an interesting and slightly different approach than previous wavelet-based investigations in hydrology by de-convoluting dominant signals in the time series in an attempt to understand the predominant climate forcing. Without applying this framework, these climate signals would not have been identified, discriminated, nor quantified from the original water yield and nutrient time series.

5.2 Recommendations for Future Research

Landscape physical characteristics play important roles in controlling the natural hydrological and biogeochemical dynamics in catchments (Neff *et al.*, 2003; Christopher *et al.*, 2008; Deng *et al.*, 2011), and therefore not only control spatial differences in catchment nutrient export but also influence climate-linked catchment temporal responses in water yield and nutrient export. This thesis examined the role of topography in controlling spatial and climate linked temporal export responses of water and nutrient from relatively pristine headwaters. The following suggestions will continue to improve our understanding of these complex systems:

1. Conduct similar investigations in geographic areas of different climate and/or long term monitoring stations: A 28-year data set is particularly short for time series and wavelet analysis. Trends in the data may be missed or ascribed to non-stationary signals. Longer time series will allow the detection of signals with longer periodicities.
2. Extend the analytical framework to investigate finer time scales (seasonal, monthly and daily data sets): This will allow us to see if signals of stationary responses reveal themselves when short frequency time series are used for both water yield and nutrient export investigations. Multiple stationary signals can be detected in shorter frequency time series, even if non-stationary linear trends could be difficult to detect because of the inherent seasonal variability in finer scale time series. While annual time scale investigations are important to understand yearly nutrient dynamics and long term trends, annual investigation may mask finer scale biogeochemical processes strongly influencing the overall biogeochemical dynamics in catchments (Oczkowski *et al.,* 2006).
3. Explore the effectiveness of the tested topographic metrics in explaining nutrient export at larger scales and in different forested regions: As a catchment scale increases so does the heterogeneity in landscape spatial characteristics, which in turn has implications for associated catchment responses, making scale the most important issue in process based investigations. Different processes become important at different spatial scales and processes that are important at small scales may not be important at large scales as new dominant processes may emerge as the scale gets larger (Meentemeyer and Box, 1987; Bloschl and Sivapalan, 1995). One way of understanding process behavior in large scale catchments is to investigate small-scale process behavior in hopes of extending that behavior to larger scales (Frisbee *et al*., 2012). Catchments also vary in their biogeochemical responses based on forest type (Amiotte-suchet *et al.*, 2007), forest disturbance (Lamontagne *et al.,* 2000; Smith *et al.,* 2012) and deposition regime (Sleutel *et al.,* 2009). Extending this investigation to other catchments of varying scale, physical, environmental and landuse conditions is necessary in

order to have a broader understanding of the controls on catchment nutrient export.

4. Explore the effectiveness of the tested topographic metrics in predicting nutrient export at finer (seasonal, monthly and weekly) time scales: Such exploration would confirm if the tested metrics are capable of capturing finer time scale processes, for example seasonally distinct biogeochemical processes, which are important to larger scale export phenomena. This would further our process based understanding of nutrient export controls.
5. Extend the spatial analysis to evaluate the effectiveness of the tested topographic metrics in predicting other forms of nutrients at various time scales: The extension would enhance our understanding of the underlying linkages between nutrients and the mechanisms of their export control. This would, in turn, have implications for the management of watershed for water protection.

5.3 Anticipated Significance

The research developed a new framework for analysing the role of climate (unidirectional climate change and stationary climatic variations) in catchment responses. The framework employed a novel approach by de-convoluting dominant signals in catchment responses in an attempt to understand the predominant climate forcing. Without applying the proposed framework, these climate signals would not have been identified, discriminated, nor quantified from the original time series of water yields and nutrient export responses. The framework can, therefore, be extended to other environmental studies involving time series analysis. Furthermore, the study introduced new spatial metrics that are robust in terms of modeling nutirent export fluxes from the studied catchments in addition to testing the spatial metrics outlined in Creed and Beall (2009) on a range of nutrients having longer time series.

This research improves the scientific understanding of catchment (hydrological and biogeochemical) responses to various temporal and spatial environmental factors. There is considerable climatic variability and significant unidirectional climate change in the Algoma Highlands region, and this study provided a key insight in revealing the complex links between directional climate change, large scale oscillations of atmospheric

circulation, and water yield and nutrient fluxes from a range of topographically, and thus hydrologically, diverse but relatively pristine forested catchments. In addition, the study increased our understanding of the most important topography-related catchment characteristics on the export of range of different nutrients of organic and inorganic nature. Furthermore, the investigation provides comprehensive information about natural nutrient dynamics and export behaviors against which similar conditions in disturbed situations can be compared.

The Algoma Highlands region is characterized by granite-dominated bedrock geology that makes water bodies and aquatic ecosystems in the region susceptible to the effects of acid rain as a result of low buffering capacity (Scheider *et al.*, 1979; Shrivastava, 2007). Without well-planned land-use management strategies, climate change and increased rates of environmental disturbance in the region from resource extraction threatens not only the quality and quantity but also the ecosystem integrity of water resources in the region. Practically, the knowledge gained from the research can be used to support policies of sustainable development in the region at present and in the future.

5.4 References

Amiotte-suchet P, Linglois N, Leveque J, Andreux F. 2007. ^{13}C composition of dissolved organic carbon in upland forested catchments of the Morvan Mountains (France): Influence of coniferous and deciduous vegetation. *Journal of Hydrology* **335**: 354-363. DOI: 10.1016/j.jhydrol.2006.12.002.

Bloschl G, Sivapalan M. 1995. Scale Issues in Hydrological Modeling - a Review. *Hydrological Processes* **9**: 251-90. DOI: 10.1002/hyp.3360090305.

Christopher SF, Mitchell MJ, McHale MR, Boyer EW, Burns DA, Kendall C. 2008. Factors controlling nitrogen release from two forested catchments with contrasting hydrochemical responses. *Hydrological Processes* **22**: 46-62. DOI: 10.1002/hyp.6632.

Creed IF, Beall FD. 2009. Distributed topographic indicators for predicting nitrogen export from headwater catchments. *Water Resources Research* **45**: W10407. DOI: 10.1029/2008WR007285.

Deng J, Zhou Z, Zhu B, Zheng X, Li C, Wang X, Jian Z. 2011. Modeling nitrogen loading in a small watershed in southwest China using a DNDC model with hydrological enhancements. *Biogeosciences* **8**. DOI: 10.5194/bg-8-2999-2011.

Frisbee MD, Phillips FM, Weissmann GS, Brooks PD, Wilson JL, Campbell AR, Liu F. 2012. Unraveling the mysteries of the large watershed black box: Implications for the

streamflow response to climate and landscape perturbations. *Geophysical Research Letters* **39**: L01404. DOI: 10.1029/2011GL050416.

Lamontagne S, Carignan R, D'Arcy P, Prairie Y, Pare D. 2000. Element export in runoff from eastern Canadian Boreal Shield drainage basins following forest harvesting and wildfires. *Canadian Journal of Fisheries and Aquatic Sciences* **57**: 118-128. DOI: 10.1139/cjfas-57-S2-118.

Meentemeyer V, Box EO. 1987. Scale effects in landscape studies. In *Landscape Heterogeneity and Disturbance*, Turner MG (ed). Springer-Verlag: ; pp. 15-34.

Neff J, Chapin F, Vitousek P. 2003. Breaks in the cycle: dissolved organic nitrogen in terrestrial ecosystems. *Frontiers in Ecology and the Environment* **1**: 205-211. DOI: 10.1890/1540-9295(2003)001[0205:BITCDO]2.0.CO;2.

Oczkowski AJ, Pellerin BA, Hunt CW, Wollheim WM, Vorosmarty CJ, Loder,Theodore CLIII. 2006. The role of snowmelt and spring rainfall in inorganic nutrient fluxes from a large temperate watershed, the Androscoggin River basin (Maine and New Hampshire). *Biogeochemistry* **80**: 191-203. DOI: 10.1007/s10533-006-9017-7.

Scheider WA, Jeffries DS, Dillon PJ. 1979. Effects of Acidic Precipitation on Precambrian Fresh Waters in Southern Ontario Canada. *Journal of Great Lakes Research* **5 (1): 41-51**.

Shrivastava, AK. 2007. Global Warming. APH Publishing Corp.: New Delhi; 48-53.

Sleutel S, Vandenbruwane J, De Schrijver A, Wuyts K, Moeskops B, Verheyen K, De Neve S. 2009. Patterns of dissolved organic carbon and nitrogen fluxes in deciduous and coniferous forests under historic high nitrogen deposition. *Biogeosciences* **6**.

Smith HG, Hopmans P, Sheridan GJ, Lane PNJ, Noske PJ, Bren LJ. 2012. Impacts of wildfire and salvage harvesting on water quality and nutrient exports from radiata pine and eucalypt forest catchments in south-eastern Australia. *Forest Ecology and Management* **263**: 160-169. DOI: 10.1016/j.foreco.2011.09.002.

Appendix 1: Evaluatating the role of topography in nutrient export using two windows of investigation

The appendix investigates the role of topography in explaining the observed spatial variation in nutrient export among the headwater catchments of Turkey Lake Watershed (TLW) using two independent periods of investigation. The first window of investigation run from water year 1981 to 1996 and involved all the 13 headwater catchments. The second window of investigation extended the study period to 2008 water year, but removed all the catchments that experienced disturbance in 1997 forest harvesting experiment (catchment c31, c33 and c34). Topographic metrics discussed in Chapter 2 were regressed against long-term annual average nutrient flux for the two windows of investigation. This analysis confirms the results obtained in chapter 2, which used the annual nutrient fluxes (kg/ha/a) for the water year from 1981 to 2008 (except for the three harvested catchments, c31, c33 and c34, for the period 1981 to 1996 water years).

Regression analyses examining the relationship between topographic metrics and annualized N, P and C export are presented in Table A.1 and Table A.2 for 1981 to 1996 and 1981 to 2008 windows of investigation respectively. The investigation confirms that metrics representing flushing mechanism and flat areas are major players in controlling nutrient export and each of these metrics have completely opposite reactions towards NO_3^--N and DOC, DON or TDP nutrients. NO_3^--N showed a strong positive correlation with metrics of flushing mechanism while a general pattern of direct association was observed between wetlands and DOC, TDP and DOC nutrients. As indicated in Table A.3, most catchment variances in annualized DOC, DON and TDP export were best explained by regression models created using W:*eff*VSA as independent variable. Annualized NO_3^--N exports, however, were well predicted by metrics representing flushing mechanism (as indicated by the multiple regression model involving *NWeff*VSA and d^2*eff*VSA / dTI_n^2).

Table A1.1: Relationships between topography related metrics and annualized nutrient export (1981 to 1996 water years) of the 13 headwater catchments in the Turkey Lakes Watershed (Direction = Directions of relationship, R^2 = coefficient of determination, and NS = not significant, all other relationships $p < 0.05$).

Topographic Metrics	**NO_3^--N**		**DOC**		**DON**		**TDP**	
	Direction	***R^2***	***Direction***	***R^2***	***Direction***	***R^2***	***Direction***	***R^2***
Wetlands (%)	-	0.674	+	0.916	+	0.640	+	0.769
VSA (%)	NS	---	NS	---	NS	---	NS	---
*eff*VSA (%)	+	0.518	-	0.456	-	0.526	-	0.471
*NWeff*VSA (%)	+	0.738	-	0.741	-	0.679	-	0.648
d^2*eff*VSA/dTI_n^2	+		NS	---	NS	---	NS	---
W:VSA	-	0.637	+	0.935	+	0.709	+	0.848
W:*eff*VSA	-	0.626	+	0.937	+	0.729	+	0.869
*NWeff*VSA and d^2*eff*VSA/dTI_n^2	+	0.873	---	---	---	---	---	---

Table A1.2: Relationships between topography related metrics and annualized nutrient export (1981 to 2008 water years) of the 13 headwater catchments in the Turkey Lakes Watershed (r = correlation, R^2 = coefficient of determination, and NS = not significant, all other relationships $p < 0.05$).

Topographic Metrics	**NO_3^--N**		**DOC**		**DON**		**TDP**	
	Direction	***R^2***	***Direction***	***R^2***	***Direction***	***R^2***	***Direction***	***R^2***
Wetlands (%)	-	0.630	+	0.920	+	0.766	+	0.814
VSA (%)	NS	---	NS	---	NS	---	NS	---
*eff*VSA (%)	+	0.710	-	0.496	-	0.552	-	0.497
*NWeff*VSA (%)	+	0.855	-	0.815	-	0.779	-	0.706
d^2*eff*VSA/dTI_n^2	+		NS	---	NS	---	NS	---
W:VSA	-	0.632	+	0.930	+	0.819	+	0.888
W:*eff*VSA	-	0.638	+	0.934	+	0.841	+	0.909
*NWeff*VSA and d^2*eff*VSA/dTI_n^2	+	0.887	---	---	---	---	---	---

Table A1.3: Best regression models for predicting average annual C, N and P export from TLW headwater catchments. Two models, one for each window of investigation, are presented for each parameter.

Response Variable	**R^2, p**	**Equation**
NO_3^--N (kg N ha^{-1} a^{-1})	0.873, <0.001	NO_3-N = 0.966 + (0.241 x *NWeff*VSA) + (49969.886 x d^2*eff*VSA/dTI^2_n)
NO_3^--N (kg N ha^{-1} a^{-1}) *	0.887, <0.001	NO_3-N = 0.892 + (0.274 x *NWeff*VSA) - (25521.513 x d^2*eff*VSA/dTI^2_n)
DOC (kg C ha^{-1} a^{-1})	0.937, <0.001	DOC = 13.519 + (10.541 x W: *eff*VSA)
DOC (kg C ha^{-1} a^{-1}) *	0.934, <0.001	DOC = 13.052 + (10.527 x W: *eff*VSA)
DON (kg N ha^{-1} a^{-1})	0.729, <0.001	DON = 1.113 + (0.328 x W: *eff*VSA)
DON (kg N ha^{-1} a^{-1}) *	0.841, <0.001	DON = 0.895 + (0.352 x W: *eff*VSA)
TDP (kg P ha^{-1} a^{-1})	0.869, <0.001	TDP = 0.0158 + (0.0123 x W: *eff*VSA)
TDP (kg P ha^{-1} a^{-1}) *	0.909, <0.001	TDP = 0.0143 + (0.0118 x W: *eff*VSA)

* Equations for 1981 to 2008 window of investigation.

Appendix 2: John Wiley and Sons license terms and conditions

Dec 19, 2012

This is a License Agreement between Samson G Mengistu ("You") and John Wiley and Sons ("John Wiley and Sons") provided by Copyright Clearance Center ("CCC"). The license consists of your order details, the terms and conditions provided by John Wiley and Sons, and the payment terms and conditions.

All payments must be made in full to CCC. For payment instructions, please see information listed at the bottom of this form.

License Number

3052831462758

License date

Dec 19, 2012

Licensed content publisher

John Wiley and Sons

Licensed content publication

Hydrological Processes

Book title

Licensed content author

Samson G. Mengistu, Irena F. Creed,Reg J. Kulperger,Christopher G. Quick

Licensed content date

Oct 17, 2012

Start page

n/a

End page

n/a

Type of use

Dissertation/Thesis

Requestor type

Author of this Wiley article

Format

Electronic

Portion

Full article

Will you be translating?

No

Order reference number

Total

0.00 USD

Terms and Conditions

TERMS AND CONDITIONS

This copyrighted material is owned by or exclusively licensed to John Wiley & Sons, Inc. or one of its group companies (each a "Wiley Company") or a society for whom a Wiley Company has exclusive publishing rights in relation to a particular journal (collectively WILEY"). By clicking "accept" in connection with completing this licensing transaction, you agree that the following terms and conditions apply to this transaction (along with the billing and payment terms and conditions established by the Copyright Clearance Center Inc., ("CCC's Billing and Payment terms and conditions"), at the time that you opened your Rightslink account (these are available at any time at http://myaccount.copyright.com)

Terms and Conditions

1. The materials you have requested permission to reproduce (the "Materials") are protected by copyright.

2. You are hereby granted a personal, non-exclusive, non-sublicensable, non-transferable, worldwide, limited license to reproduce the Materials for the purpose specified in the licensing process. This license is for a one-time use only with a maximum distribution equal to the number that you identified in the licensing process. Any form of republication granted by this licence must be completed within two years of the date of the grant of this licence (although copies prepared before may be distributed thereafter). The Materials shall not be used in any other manner or for any other purpose. Permission is granted subject to an appropriate acknowledgement given to the author, title of the material/book/journal and the publisher. You shall also duplicate the copyright notice that appears in the Wiley publication in your use of the Material. Permission is also granted on the understanding that nowhere in the text is a previously published source acknowledged for all or part of this Material. Any third party material is expressly excluded from this permission.

3. With respect to the Materials, all rights are reserved. Except as expressly granted by the terms of the license, no part of the Materials may be copied, modified, adapted (except for minor reformatting required by the new Publication), translated, reproduced, transferred or distributed, in any form or by any means, and no derivative works may be made based on the Materials without the prior permission of the respective copyright owner. You may not alter, remove or suppress in any manner any copyright, trademark or other notices displayed by the Materials. You may not license, rent, sell, loan, lease, pledge, offer as security, transfer or assign the Materials, or any of the rights granted to you hereunder to any other person.

4. The Materials and all of the intellectual property rights therein shall at all times remain the exclusive property of John Wiley & Sons Inc or one of its related companies (WILEY) or their respective licensors, and your interest therein is only that of having possession of and the right to reproduce the Materials pursuant to Section 2 herein during the continuance of this Agreement. You agree that you own no right, title or interest in or to the Materials or any of the intellectual property rights therein. You shall have no rights hereunder other than the license as provided for above in Section 2. No right, license or interest to any trademark, trade name, service mark or other branding ("Marks") of WILEY or its licensors is granted hereunder, and you agree that you shall not assert any such right, license or interest with respect thereto.

5. NEITHER WILEY NOR ITS LICENSORS MAKES ANY WARRANTY OR REPRESENTATION OF ANY KIND TO YOU OR ANY THIRD PARTY, EXPRESS, IMPLIED OR STATUTORY, WITH RESPECT TO THE MATERIALS OR THE ACCURACY OF ANY INFORMATION CONTAINED IN THE MATERIALS, INCLUDING, WITHOUT LIMITATION, ANY IMPLIED WARRANTY OF MERCHANTABILITY, ACCURACY, SATISFACTORY QUALITY, FITNESS FOR A PARTICULAR PURPOSE, USABILITY, INTEGRATION OR NON-INFRINGEMENT AND ALL SUCH WARRANTIES ARE HEREBY EXCLUDED BY WILEY AND ITS

LICENSORS AND WAIVED BY YOU.

6. WILEY shall have the right to terminate this Agreement immediately upon breach of this Agreement by you.

7. You shall indemnify, defend and hold harmless WILEY, its Licensors and their respective directors, officers, agents and employees, from and against any actual or threatened claims, demands, causes of action or proceedings arising from any breach of this Agreement by you.

8. IN NO EVENT SHALL WILEY OR ITS LICENSORS BE LIABLE TO YOU OR ANY OTHER PARTY OR ANY OTHER PERSON OR ENTITY FOR ANY SPECIAL, CONSEQUENTIAL, INCIDENTAL, INDIRECT, EXEMPLARY OR PUNITIVE DAMAGES, HOWEVER CAUSED, ARISING OUT OF OR IN CONNECTION WITH THE DOWNLOADING, PROVISIONING, VIEWING OR USE OF THE MATERIALS REGARDLESS OF THE FORM OF ACTION, WHETHER FOR BREACH OF CONTRACT, BREACH OF WARRANTY, TORT, NEGLIGENCE, INFRINGEMENT OR OTHERWISE (INCLUDING, WITHOUT LIMITATION, DAMAGES BASED ON LOSS OF PROFITS, DATA, FILES, USE, BUSINESS OPPORTUNITY OR CLAIMS OF THIRD PARTIES), AND WHETHER OR NOT THE PARTY HAS BEEN ADVISED OF THE POSSIBILITY OF SUCH DAMAGES. THIS LIMITATION SHALL APPLY NOTWITHSTANDING ANY FAILURE OF ESSENTIAL PURPOSE OF ANY LIMITED REMEDY PROVIDED HEREIN.

9. Should any provision of this Agreement be held by a court of competent jurisdiction to be illegal, invalid, or unenforceable, that provision shall be deemed amended to achieve as nearly as possible the same economic effect as the original provision, and the legality, validity and enforceability of the remaining provisions of this Agreement shall not be affected or impaired thereby.

10. The failure of either party to enforce any term or condition of this Agreement shall not constitute a waiver of either party's right to enforce each and every term and condition of this Agreement. No breach under this agreement shall be deemed waived or excused by either party unless such waiver or consent is in writing signed by the party granting such waiver or consent. The waiver by or consent of a party to a breach of any provision of this Agreement shall not operate or be construed as a waiver of or consent to any other or subsequent breach by such other party.

11. This Agreement may not be assigned (including by operation of law or otherwise) by you without WILEY's prior written consent.

12. Any fee required for this permission shall be non-refundable after thirty (30) days from receipt.

13. These terms and conditions together with CCC’s Billing and Payment terms and conditions (which are incorporated herein) form the entire agreement between you and

WILEY concerning this licensing transaction and (in the absence of fraud) supersedes all prior agreements and representations of the parties, oral or written. This Agreement may not be amended except in writing signed by both parties. This Agreement shall be binding upon and inure to the benefit of the parties' successors, legal representatives, and authorized assigns.

14. In the event of any conflict between your obligations established by these terms and conditions and those established by CCC's Billing and Payment terms and conditions, these terms and conditions shall prevail.

15. WILEY expressly reserves all rights not specifically granted in the combination of (i) the license details provided by you and accepted in the course of this licensing transaction, (ii) these terms and conditions and (iii) CCC's Billing and Payment terms and conditions.

16. This Agreement will be void if the Type of Use, Format, Circulation, or Requestor Type was misrepresented during the licensing process.

17. This Agreement shall be governed by and construed in accordance with the laws of the State of New York, USA, without regards to such state's conflict of law rules. Any legal action, suit or proceeding arising out of or relating to these Terms and Conditions or the breach thereof shall be instituted in a court of competent jurisdiction in New York County in the State of New York in the United States of America and each party hereby consents and submits to the personal jurisdiction of such court, waives any objection to venue in such court and consents to service of process by registered or certified mail, return receipt requested, at the last known address of such party.

Wiley Open Access Terms and Conditions

All research articles published in Wiley Open Access journals are fully open access: immediately freely available to read, download and share. Articles are published under the terms of the Creative Commons Attribution Non Commercial License. which permits use, distribution and reproduction in any medium, provided the original work is properly cited and is not used for commercial purposes. The license is subject to the Wiley Open Access terms and conditions:
Wiley Open Access articles are protected by copyright and are posted to repositories and websites in accordance with the terms of the Creative Commons Attribution Non Commercial License. At the time of deposit, Wiley Open Access articles include all changes made during peer review, copyediting, and publishing. Repositories and websites that host the article are responsible for incorporating any publisher-supplied amendments or retractions issued subsequently.
Wiley Open Access articles are also available without charge on Wiley's publishing platform, **Wiley Online Library** or any successor sites.

Use by non-commercial users

For non-commercial and non-promotional purposes individual users may access, download, copy, display and redistribute to colleagues Wiley Open Access articles, as well as adapt, translate, text- and data-mine the content subject to the following conditions:

? The authors' moral rights are not compromised. These rights include the right of "paternity" (also known as "attribution" - the right for the author to be identified as such) and "integrity" (the right for the author not to have the work altered in such a way that the author's reputation or integrity may be impugned).
? Where content in the article is identified as belonging to a third party, it is the obligation of the user to ensure that any reuse complies with the copyright policies of the owner of that content.
? If article content is copied, downloaded or otherwise reused for non-commercial research and education purposes, a link to the appropriate bibliographic citation (authors, journal, article title, volume, issue, page numbers, DOI and the link to the definitive published version on Wiley Online Library) should be maintained. Copyright notices and disclaimers must not be deleted.
? Any translations, for which a prior translation agreement with Wiley has not been agreed, must prominently display the statement: "This is an unofficial translation of an article that appeared in a Wiley publication. The publisher has not endorsed this translation."

Use by commercial "for-profit" organisations

Use of Wiley Open Access articles for commercial, promotional, or marketing purposes requires further explicit permission from Wiley and will be subject to a fee. Commercial purposes include:

? Copying or downloading of articles, or linking to such articles for further redistribution, sale or licensing;
? Copying, downloading or posting by a site or service that incorporates advertising with such content;
? The inclusion or incorporation of article content in other works or services (other than normal quotations with an appropriate citation) that is then available for sale or licensing, for a fee (for example, a compilation produced for marketing purposes, inclusion in a sales pack)
? Use of article content (other than normal quotations with appropriate citation) by for-profit organisations for promotional purposes
? Linking to article content in e-mails redistributed for promotional, marketing or educational purposes;
? Use for the purposes of monetary reward by means of sale, resale, licence, loan, transfer or other form of commercial exploitation such as marketing products
? Print reprints of Wiley Open Access articles can be purchased from:corporatesales@wiley.com

Other Terms and Conditions:

BY CLICKING ON THE "I AGREE..." BOX, YOU ACKNOWLEDGE THAT YOU

HAVE READ AND FULLY UNDERSTAND EACH OF THE SECTIONS OF AND PROVISIONS SET FORTH IN THIS AGREEMENT AND THAT YOU ARE IN AGREEMENT WITH AND ARE WILLING TO ACCEPT ALL OF YOUR OBLIGATIONS AS SET FORTH IN THIS AGREEMENT.

v1.7

If you would like to pay for this license now, please remit this license along with your payment made payable to "COPYRIGHT CLEARANCE CENTER" otherwise you will be invoiced within 48 hours of the license date. Payment should be in the form of a check or money order referencing your account number and this invoice number RLNK500921072.
Once you receive your invoice for this order, you may pay your invoice by credit card. Please follow instructions provided at that time.

Make Payment To:
Copyright Clearance Center
Dept 001
P.O. Box 843006
Boston, MA 02284-3006

For suggestions or comments regarding this order, contact RightsLink Customer Support: customercare@copyright.com or +1-877-622-5543 (toll free in the US) or +1-978-646-2777.

Gratis licenses (referencing $0 in the Total field) are free. Please retain this printable license for your reference. No payment is required.

Curriculum Vitae

Name:	Samson Girma **Mengistu**
Post-secondary Education and Degrees:	The University of Western Ontario London, Ontario, Canada 2007-2012 Ph.D. (Geology and Environmental Science) Anticipated December, 2012
	Free University of Brussels Brussels, Brussels - Capital Region, Belgium 2004-2005 M.Sc. (Water Resources Engineering)
	Catholic University of Leuven Leuven, Flemish Brabant, Belgium 2003-2004 Postgraduate Diploma (Water Resources Engineering)
	Hawassa University Hawassa, SNNPRS, Ethiopia 1996-2000 B.Sc. (Agricultural Engineering)
Honours and Awards:	Western Graduate Research Scholarship University of Western Ontario 2007-2011
	De Vlaamse Interuniversitaire Raad (*VLIR*) Award Scholarship Catholic University of Leuven, University of Brussels 2003-2005
	Japan International Cooperation Agency (JICA) Fellowship Jomo Kenyatta University 2003
Related Work Experience:	Research Assistant, Teaching Assistant The University of Western Ontario 2007-2012, 2007-2011
	Research Assistant University of Guelph 2006-2007
	Lecturer Hawassa University 2005-2006
	Research and Teaching Assistant Free University of Brussels 2004-2005

Research Assistant
Catholic University of Leuven
2003-2004

Assistant Lecturer
Hawassa University
2001-2003

Field Engineer
CoSEARAR
2000-2001

Publications:

Published

1. **Mengistu SG**, Creed IF, Kulperger RJ, Quick C. 2012. Discriminating between non-stationary and stationary responses in water yields from catchments on a northern forested landscape. Hydrological Processes, doi: 10.1002/hyp.9552. **Invited** contribution to Special Issue: "Catchments of the future North: creating science for management in 2050."

Submitted

2. **Mengistu SG**, Creed IF, Webster KL, Enanga E. Searching for similarity in topographic controls on carbon, nitrogen and phosphorus export from forested headwater catchments. Submitted to Hydrological Processes, November 2012
3. **Mengistu SG**, Quick CG, Creed IF. Nutrient export from catchments on forested landscapes reveal complex non-stationary and stationary climate signals. Submitted to Water Resources Research, September 2012.

Presentations:

1. Creed IF, **Mengistu SG**, Quick CG. 2012. Discriminating anthropogenic climate change from natural climate oscillation signals in dissolved organic matter export from headwater catchments. American Geophysical Union Fall Meeting, December 3-7, San Francisco, CA. **Invited Talk.**
2. Creed IF, **Mengistu SG**, Kulperger RJ. 2012. Discriminating between non-stationary and stationary responses in water yields from catchments on a northern forested landscape. Northern Watershed Ecosystem Response to Climate Change, May 21-25, 2012. Potsdam, Germany. **Invited Talk**.
3. Creed IF, Enanga EM, **Mengistu SG**, Beall FD, Hazlett P. 2011. Role of redox surfaces in explaining catchment nitrogen export across multiple spatial and temporal scales. American Geophysical Union Fall Meeting, December 5-9, San Francisco, CA. **Invited Talk.**
4. **Mengistu SG**, Creed IF. 2011. Teleconnections between ENSO and nutrient export from forested catchments. Gordon Research Conference on Catchment

Sciences: Catchments as Sentinels of Global Change, July 10-15, Bates College, Lewiston, Maine, USA.

5. **Mengistu SG**, Creed IF. 2011. Understanding the role of catchment spatial properties in controlling spatial variability of nutrient export from forested Turkey Lakes Watershed (TLW) catchments. Gordon Research Conference on Catchment Sciences: Catchments as Sentinels of Global Change, July 10-15, Bates College, Lewiston, Maine, USA.
6. Beall FD, **Mengistu SG**, Creed IF. 2010. Hydrological consequences of harvesting intensity in forested catchments: The Turkey Lakes Watershed Harvesting Experiment. 44th Annual CMOS congress, 36th Annual Scientific Meeting of CGU and 3rd Joint CMOS-CGU Congress, May 31-June 4, Ottawa, Canada.
7. **Mengistu SG**, Creed IF, Beall FD. 2010. Hydrological consequences of harvesting intensity in forested catchments: Discriminating a harvest signal under different climate scenarios. 44th Annual CMOS congress, 36th Annual Scientific Meeting of CGU and 3rd Joint CMOS-CGU Congress, May 31-June 4, Ottawa, Canada.
8. Rouhani H, Gbadegesin JA, **Mengistu SG**, Feyen J. 2006. Modeling of the water quality of the Medium-Scale River Basin "Grote Nete" (Flanders, Belgium). 7th International Conference on Hydroinformatics (HIC, 2006), September 4-8, Nice, France.